VNIVERSITAT DE VALÈNCIA

DOCTORAL THESIS
May 2018

Doctoral Programme in

Quantitative Finance and Economy

INHERENT INFORMATION IN THE PRICES OF OPTIONS

Maria Magdalena Vich Llompart

Thesis Supervisor:
Antoni Vaello-Sebastià
Universitat de les Illes Balears

Doctor by the Universitat de València

VNIVERSITAT DE VALÈNCIA

DOCTORAL THESIS
2018

INHERENT INFORMATION IN THE PRICES OF OPTIONS

Maria Magdalena Vich Llompart

Acknowledgments

The best thing I have obtained from life is the people I have shared my livings, experiences, hapiness and not-so-happy moments with. During all these years, I have had the opportunity to not only meet a lot of new people, but these people have turned up to be the best people in the world. Fortunately, I could write another thesis expressing my gratitude to all the people who has been, in many different ways, with me during this journey. Unfortunately, I have to keep it brief.

First of all, I would like to thank Dr. Antoni Vaello (my supervisor), who has been with me all this time sharing good moments, sandwiches and teas, mid-afternoon walks, youtube opera and of course for guiding me and sharing Saturday mornings of work. Thank you for all your time and support. He is on regattas now and I know he will be good at it because we have had to race quite a few times without boat, and we are alive. Thank you for eveything and for being my boat!

During all these years I have also had the support of all the team of the Business Department from the University of the Balearic Islands. Thank you for having me there and sharing good moments and laughs with me (specially in Christmas and every July). Not to forget the tupper club, who sometimes wanted to eat my lunch! A special thanks to Dr. Roberto Pascual for being my advisor in many ways and having been willing to help me and support me in everything I have ever needed.

Additionally, a special thanks to Miryam and Paula, who have listened to me while I was complaning, but as well during moments of excitement or decorating the office for Skype meetings. Thank you for all the *pasillo* memories I take with me.

Another special mention is for Tolo who has been supporting me since many years ago all the way to here in the most sincere way. His signature is behind most of the things I have done and many journeys I have taken. Thank you for everything!

I would like to thank also Dr. Luiz Vitiello for hosting me in Essex University during my visiting as well as for all the support and help he has provided me during and after my stay.

Dr. Pedro Serrano is worth a special mention for all his help and support. He has been of great help when I have needed him, thank you for eveything.

A special mention and a big thank you to all my friends, who have been left aside for a while during these last months, thank you for your patience. Specially Antonia and my very special nephew Mateuet. I would also like to thank Xisca Vallespir for all her support and fondness.

I cannot forget my mathematician friends, who have delighted me with mid-morning coffees with laughter and much more (but they never shared their sandwiches with me).

And the best for the end, a very special mention to all my family, who have made this journey smoother and full of support, understanding and love. They have witnessed all the process with its consequences, and they have known how to make it easier. I would like to thank my sister for many many different things and unconditonal help, as well as my mum, husband, grandmother and cousins, to make everyday full of love, laughter and good feelings ... and lunch boxes, thank you mum and grandma!

And last but not least, I would like to thank my cat who has been on my lap while

I was writing this thesis (not helping though, just sleeping). Thank you for your warm support and company!

And last but not least (II), the most important thing I have with me everyday is something I cannot see but I can feel. Even though I cannot see you, I know I am not walking alone, thank you dad for making life and what it comes with it possible. You will always be in all the steps I take forward.

Contents

List of Figures

List of Tables

Resumen amplio

En las últimas décadas los activos financieros derivados, y en concreto las opciones, han recibido mucha atención tanto en el ámbito profesional como en el ámbito académico.

En general, los precios de los activos son vistos como la esperanza de los futuros flujos de caja descontados. En el caso particular de las opciones, teniendo diferentes opciones sobre el mismo subyacente y con la misma fecha de vencimiento, podemos obtener información sobre la forma y los diferentes parámetros de la función de densidad con la cuál los agentes valoran los activos derivados, y en definitiva cómo ponen precio a unidades de consumo en diferentes estados de la naturaleza futuros. Existe una gran corriente en la literatura que se dedica a la extracción de las densidades implícitas en el precio de las opciones, siendo estas densidades neutrales al riesgo (que son las que se utilizan en valoración de activos). Por lo tanto, a partir del precio de las opciones podemos obtener las densidades neutrales al riesgo (RND por sus siglas en inglés *Risk-Neutral Densities*), las que a su vez nos permiten analizar diferentes aspectos de los mercados financieros.

Esta información implícita en el precio de las opciones es considerada información *forward-looking* (con miras al futuro). Diferentes estudios han probado su superioridad en diferentes aplicaciones tales como predicción, modelización y valoración, entre otros; en detrimento del uso de medidas estadísticas tradicionales basadas en el análisis de datos históricos.

Consecuentemente, el conocimiento de las RNDs nos permite analizar diferentes aspectos de los mercados financieros. Uno de los principales objetivos de los inversores es la elaboración de previsiones precisas sobre realizaciones de los precios futuros del subyacente, mejorando así la valoración de activos y gestión de carteras, entre otros. Pero, ¿podemos confiar en la capacidad predictiva de las RNDs implícitas en el precio de las opciones?

Entre toda la información adquirida, uno de los aspectos de más preocupación entre los inversores son los movimientos extremos de los precios, principalmente los movimientos a la baja (que son los que forman la cola izquierda de las RNDs). Una de las técnicas más usadas para evitar pérdidas es mediante la diversificación internacional. Sin embargo, hoy en día los mercados internacionales desarrollados presentan un mayor grado de integración, por lo que es de especial interés para los inversores saber si su exposición a las pérdidas esperadas está siendo bien diversificada, así como conocer su grado de exposición a impactos en mercados extranjeros.

Sin embargo, las distribuciones implícitas en el precio de las opciones son neutrales al riesgo, por lo que difieren de las distribuciones reales o subjetivas (SPD por sus siglas en inglés *Subjective Probability Distributions*), ya que estas últimas incluyen las preferencias de los agentes. Por lo tanto, existe una medida de aversión al riesgo (RA por sus siglas en inglés *Risk Aversion*) que recoge estas diferencias entre las RNDs y las SPDs. Pero, ¿presenta esta aversión al riesgo patrones similares a lo largo del tiempo en diferentes países? ¿Cuáles son las causas de esta heterogeneidad?

En la presente tesis pretendemos abordar estos temas a lo largo de tres capítulos. Cada uno de estos capítulos está enfocado a analizar diferentes aspectos de los mercados financieros y contestar las preguntas anteriores analizando el contenido informacional de los precios de las opciones.

En el capítulo 1 analizamos la capacidad de las RNDs para predecir futuras realizaciones de los precios del subyacente, así como la aproximación de las colas de las RNDs. En el capítulo 2 estudiamos los cuantiles de pérdidas esperadas de las RNDs implícitas en los precios de las opciones y cómo impactos en los cuantiles de un mercado se transmiten a mercados financieros extranjeros. El capítulo 3 extrae la aversión al riesgo para tres mercados internacionales y mide patrones sistemáticos entre ellas, tanto en series temporales como transversales.

Cada uno de los capítulos que componen la tesis están explicados en las diferentes secciones que siguen.

R.1 ¿Podemos descartar la capacidad predictiva de las RNDs implícitas en el precio de las opciones?

El primer capítulo tiene como objetivo esclarecer si las RNDs poseen capacidad predictiva de las realizaciones futuras de los precios del subyacente. Para ello extraemos las RNDs para tres índices de Estados Unidos: S&P 500, Nasdaq 100 y Russell 2000. Analizamos una muestra amplia de series de precios para el periodo que comprende desde el año 1996 hasta el año 2015 abarcando así dos crisis financieras. Los tests tradicionales usados previamente con el propósito de testear dicha capacidad predictiva de las RNDs están basados en supuestos restrictivos: normalidad e independencia, principalmente. Con el fin de relajar estas restricciones, en este trabajo calculamos valores críticos utilizando la técnica de re-muestreo Block-Bootstrap. A diferencia de anteriores estudios, nuestros resultados no proporcionan evidencia contra la hipótesis nula de capacidad predictiva de las RNDs. Además, éstos son consistentes para diferentes métodos, horizontes temporales e índices considerados. En este capítulo también analizamos las colas de las RNDs y encontramos que, por lo general, los diferentes métodos tienden a sobreestimar la frecuencia de

ocurrencia de eventos en la cola izquierda; pero sí proporcionan una buena aproximación de la cola derecha.

Los métodos para extraer las RND se pueden agrupar en 2 categorías: métodos paramétricos y métodos no-paramétricos. Los métodos paramétricos se basan en la aplicación de densidades utilizando una función de probabilidad conocida y a partir de ella se ajustan los parámetros que mejor se ciñen a nuestros datos. Véase Jondeau and Rockinger (2000), Bliss and Panigirtzoglou (2002) o Anagnou et al. (2002), entre otros.

Por otra parte, los métodos no-paramétricos se basan en el método propuesto por Breeden and Litzenberger (1978) el cual nos permite obtener las densidades calculando la segunda derivada de la función de valoración con respecto al precio de ejercicio.

A pesar de esto, no hay consenso en la literatura sobre qué método es el más apropiado para la extracción de las RNDs. Por lo general, la literatura concluye falta de capacidad predictiva de las RNDs, véase Lynch and Panigirtzoglou (2008) y Anagnou et al. (2005). Por otra parte, en su estudio para el mercado financiero español Alonso et al. (2005) rechazan la capacidad predictiva de las RNDs cuando consideran la totalidad de la muestra. Sin embargo, cuando consideran sub-periodos, no presentan evidencia en contra de la hipótesis nula.

A pesar de todo, los diferentes estudios pueden presentar diferencias debido a la utilización de muestras y métodos distintos para la extracción de las RNDs. En nuestro estudio, con el fin de evitar sesgos procedentes del método utilizado, ampliamos el abanico aplicando en nuestro análisis diferentes métodos (paramétricos y no-paramétricos), diferentes índices (S&P 500, Nasdaq 100 y Russell 2000) y para diferentes horizontes temporales (30, 45, 60 y 90 días, los cuales son determinados por la fecha de vencimiento de las opciones).

R.1.1 Metodología

Como método paramétrico aplicamos una mixtura de distribuciones Log-Normales que consiste en realizar una media ponderada de dos distribuciones Log-Normales. Entre sus ventajas destacamos su gran flexibilidad y capacidad de aproximar distribuciones de diferentes formas (incluso bimodalidad), así como la garantía de obtener probabilidades positivas para todo el rango de la muestra.

Referente a los métodos no-paramétricos, éstos están basados en el método de Breeden and Litzenberger (1978). La aplicación de este método requiere un rango continuo de precios que abarque todas las posibles realizaciones futuras. Sin embargo, el número de opciones con diferentes precios de ejercicio que se negocian para un mismo subyacente y un mismo vencimiento es limitado, por lo que éstos tienen que ser interpolados dentro del rango de la muestra. Para la interpolación usamos dos técnicas principales: regresiones no-paramétricas y splines de tercer grado.

Para las regresiones no-paramétricas usamos el estimador propuesto por Nadaraya (1964) y Watson (1964) con el fin de obtener un rango continuo de precios. Sin embargo, con este método estamos limitados a extraer solamente la parte de la RND para aquel rango de precios observados. Por lo tanto, perdemos masa probabilística en los extremos de las densidades, ya que, en tales zonas, las observaciones son escasas o incluso nulas. Para lidiar con este problema, aplicamos el método propuesto por Birru and Figlewski (2012) y aproximamos las colas con una distribución Pareto.

Para el segundo método en el que interpolamos con splines, nos encontramos con el mismo problema con respecto a la falta de observaciones en las colas. En este caso completamos el área de dos maneras distintas: la primera es aproximándolas con distribuciones Pareto (igual que se ha hecho para el caso de las regresiones kernel); y la segunda es extrapolando el rango de puntos observados, siguiendo las líneas de Bliss and Panigirtzoglou

(2004).

En cualquiera de los dos métodos, en lugar de realizar la interpolación sobre un espacio precio-precio de ejercicio, interpolamos sobre un espacio de volatilidad implícita-deltas, propuesto por Malz (1997). La ventaja de este método es que las deltas están acotadas entre 0 y 1, a diferencia de los precios de ejercicio que en principio son ilimitados; a la vez que agrupa las observaciones más alejadas.

Una vez extraídas las RNDs para cada día de la muestra, para los diferentes índices, horizontes temporales y métodos, evaluamos su capacidad predictiva. Para ello, la literatura propone principalmente el test de Berkowitz (2001); sin embargo basándose en este test, la mayoría de ésta literatura rechaza la hipótesis nula de capacidad predictiva. Para nuestras RNDs, el test de Berkowitz también rechaza la hipótesis nula, lo cual es consistente con la literatura previa.

No obstante, el test de Berkowitz asume independencia y normalidad de las observaciones, siendo estos supuestos restrictivos y violados debido a la naturaleza de los precios (los cuales presentan autocorrelación). Para verificar la fiabilidad del test, construimos distribuciones bootstrap de los estadísticos Berkowitz. Con el fin de preservar la estructura de dependencia en los datos, simulamos 5,000 muestras bootstrap en bloques de m observaciones consecutivas (block-bootstrap). Una vez simuladas las muestras, calculamos los estadísticos de interés para cada una de ellas, los cuales a su vez forman una distribución (a la que llamaremos distribución Block-Bootstrap).

Otra manera de evaluar la normalidad e independencia en los datos, es aplicando el test Cramer-von-Mises propuesto por Cramer (1928) y von Mises (1931). Del mismo modo que con el test de Berkowitz, calculamos la distribución Block-Bootstrap de los estadísticos con el propósito de corroborar los resultados de Berkowitz Block-Bootstrap.

En este capítulo también analizamos las colas de las distribuciones y cómo éstas se

ajustan a la realidad. Para ello, y siguiendo las líneas de Anagnou et al. (2005) y Alonso et al. (2006), calculamos el estadístico de Seillier-Moiseiwisch and Dawid (1993) que se basa en el cálculo de Brier Score y mide su diferencia con el valor esperado. A lo largo del capítulo nos referiremos a este test como el test de las colas.

R.1.2 Muestra

Nuestra muestra está formada por opciones europeas para tres índices americanos: el S&P 500, el Nasdaq 100 y el Russell 2000. La batería de datos abarca el periodo comprendido entre Enero 1996 y Octubre 2015, y está formado por opciones con vencimientos a 30, 45, 60 y 90 días.

Se usan opciones out-of-the-money (OTM) y at-the-money (ATM). Para todas las opciones tipo put in-the-money (ITM), se ha calculado su call equivalente mediante la fórmula de la paridad put-call. De esta manera la información implícita en las opciones tipo put es trasladada a su opción call equivalente. Consecuentemente las opciones tipo put son eliminadas de la muestra.

R.1.3 Resultados y conclusiones

En este capítulo valoramos la capacidad predictiva de las RNDs sobre las realizaciones futuras de los precios del subyacente. Las diferentes RNDs han sido extraídas de los precios de las opciones mediante métodos paramétricos (mixtura de distribuciones Log-Normales) y no-paramétricos (Breeden-Litzenberger con regresiones kernel y splines). Se han obtenido RNDs para diferentes índices (S&P 500, Nasdaq 100 y Russell 2000) y horizontes temporales (30, 45, 60 y 90 días). Los resultados muestran RNDs consistentes con lo que se espera en la literatura ya que todas ellas presentan una skewness negativa y kurtosis superior a 3.

Para testear su capacidad predictiva, siguiendo la literatura, calculamos el test de Berkowitz el cual, efectivamente, rechaza la hipótesis nula. Sin embargo, cuando calculamos las distribuciones asintóticas mediante simulaciones Block-Bootstrap, éstas no presentan evidencia en contra de la hipótesis nula. Para reforzar los resultados del test de Berkowitz con Block-Bootstrap, aplicamos el test Cramer-von-Mises, el cual corrobora las conclusiones obtenidas con el primero.

Por otra parte, los resultados del test de colas apuntan que las RNDs tienden a sobreestimar la frecuencia de ocurrencia en la cola izquierda, mientras que para la cola derecha presentan buenas aproximaciones.

Nuestra muestra comprende dos periodos de grandes crisis financieras, la crisis del 2000 y la crisis del 2007. Para evitar que nuestros resultados estén afectados por los movimientos extremos que se dieron durante estos periodos, realizamos nuestro análisis sobre una submuestra en la que hemos eliminado los periodos de grandes turbulencias, esto es el periodo de Marzo 2000 a Octubre 2002, y el periodo de Octubre 2007 a Marzo 2009.

Las conclusiones presentadas para el análisis sobre la totalidad de la muestra se mantienen para el análisis sobre la submuestra, por lo que concluimos que las crisis no son responsables de los resultados obtenidos. Además, los resultados obtenidos son consistentes para los diferentes métodos de extracción de las RNDs usados, para los distintos índices así como también para diferentes horizontes temporales testeados, dando así robustez al análisis.

R.2 Transmisión del riesgo de pérdidas implícito en el precio de las opciones

La conectividad entre los diferentes mercados financieros internacionales es un tema recurrente en la literatura, especialmente en épocas de crisis y periodos turbulentos. Entender los nexos y conexiones de los diferentes mercados financieros internacionales es fundamental para la gestión de carteras y cobertura de riesgos, ya que, de existir una fuerte conexión entre ellos, tendría consecuencias como por ejemplo reducir el beneficio de la diversificación.

En este capítulo se pretende contrastar si existe transmisión de los cambios en los cuantiles de pérdidas esperadas de las RNDs entre diferentes mercados financieros internacionales. Para ello usamos información implícita en el precio de las opciones. Esto nos permite calcular el nivel de pérdidas esperadas para un horizonte temporal determinado, ya que dicha información es considerada *forward-looking* (con miras al futuro). En concreto, analizamos la transmisión entre tres mercados desarrollados principales: Estados Unidos, Eurozona y Japón, representados por los índices S&P 500, EuroStoxx 50 y Nikkei 225, respectivamente. En este estudio tenemos en cuenta la existencia de riesgos globales, los cuales medimos a través del índice VIX de volatilidad. En los resultados hallamos evidencia de trasmisión de shocks en el S&P 500 al resto de mercados; siendo la relación inversa nula.

La transmisión de volatilidad ha sido ampliamente documentada en la literatura, ver Eun and Shim (1989) o Hassan and Malik (2007). Sin embargo estos estudios valoran la transmisión de volatilidad basándose en información histórica de los precios. No obstante, a raíz de los trabajos de Poon and Granger (2003), Poon and Granger (2005) y Bollerslev and Zhou (2006), se evidencia superioridad del contenido de la información implícita (*forward-looking*). Esto supone un giro en la literatura la que, a partir de este

momento, empieza a estudiar la transmisión del riesgo desde el punto de vista de la información implícita, ya no solo en volatilidades sino también en otros momentos de las distribuciones; ver Nikkinen and Sahlstöm (2004) o Siropoulos and Fassas (2013) entre otros.

R.2.1 Metodología

Siguiendo las líneas del capítulo anterior, para la extracción de las RNDs diarias, usamos el método no-paramétrico basado en la técnica propuesta por Breeden and Litzenberger (1978). Esta nos permite extraer las RNDs calculando la segunda derivada de la función de valoración de las opciones con respecto al precio de ejercicio. En este capítulo interpolamos dentro del rango observado usando el método de splines en un espacio volatilidad implícita-delta.

Como en el caso anterior, la falta de observaciones más extremas hace que nos falte área en las colas de las RNDs. Para completar dicha área añadimos dos pseudo-puntos en cada uno de los extremos de la serie de deltas y extrapolamos la spline, como se propone en Bliss and Panigirtzoglou (2004). Una vez extraídas las RNDs, calculamos cuantiles para los niveles 5%, 10%, 15%, 20% y 25%, los cuales son cuantiles de pérdidas esperadas implícitos en el precio de las opciones.

En este análisis consideramos tres principales mercados desarrollados: Estados Unidos, la Eurozona y Japón. Por el hecho de considerar países localizados en diferentes zonas horarias, incurrimos en una desincronización en los cierres de los diferentes mercados. Esto hace que en el momento del cierre del mercado Europeo la información del cierre de Japón ya sea conocida. Lo mismo ocurre en el mercado de Estados Unidos, al ser éste el último en cerrar, toda la información de los otros dos mercados ya está incorporada en su precio de cierre. En cambio, Japón solo podrá reflejar la información de los otros mercados al día

siguiente. Por lo tanto, debemos considerar en nuestro modelo relaciones contemporáneas entre algunos de los mercados considerados según las relaciones anteriores.

Con la finalidad de analizar cómo shocks en un mercado se transmiten a otros mercados, modelizamos cada uno de los cuantiles con un Structural-VAR (S-VAR). Este modelo es muy conveniente porque permite a los cuantiles de cada mercado depender no solo de sus propios retardos y de los retardos del resto de mercados, sino que también permite la incorporación de relaciones contemporáneas entre los mercados.

Con el propósito de aislar el efecto de shocks específicos de esos cambios generales en los cuantiles debido a variaciones en la volatilidad agregada, contemplamos en nuestro modelo como variable exógena series del índice de volatilidad CBOE VIX. Este índice es considerado de referencia para la volatilidad global.

Otra forma de lidiar con el problema de la no sincronización en los mercados, es transformando las series diarias en series de menor frecuencia; véase Yang and Zhou (2017). En el presente estudio, hemos transformado nuestras series diarias en series semanales. De esta manera, los cuantiles ya no son modelizados mediante el modelo S-VAR sino con un modelo VAR, ya que al haber combatido la desincronización de los mercados mediante el cálculo de medias semanales, ya no existen relaciones contemporáneas entre los mercados.

Con el objetivo de analizar los flujos de transmisión de los cuantiles de pérdida entre los diferentes mercados, aplicamos el análisis de impulso-respuesta propuesto por Pesaran and Shin (1998). Este análisis nos permite obtener información de cómo shocks unitarios en uno de los mercados se transmiten a los otros mercados, así como también conocer la duración de tales efectos hasta su absorción. También llevamos a cabo el análisis de la descomposición de la varianza, el cual nos proporciona información sobre la proporción de la varianza de un mercado causada por sus propios shocks y la proporción que se debe a shocks en mercados extranjeros.

R.2.2 Muestra

Para el cálculo de las RNDs, se han tomado datos de la *volatility surface*. Éstas nos proporcionan datos para un rango de deltas de 0.2 a 0.8, junto con sus correspondientes volatilidades implícitas. Los datos han sido obtenidos de IVY OptionMetrics para tres índices: S&P 500, EuroStoxx 50 y el Nikkei 225. Además, se han tomado también series de precios diarios sobre el índice de volatilidad CBOE VIX.

Las *volatility surfaces* proporcionan datos para diferentes horizontes temporales; es decir, para opciones con diferentes vencimientos. En este estudio centramos nuestra atención en horizontes temporales de 30, 60 y 91 días.

R.2.3 Resultado y conclusiones

En el presente capítulo analizamos la transmisión de los cuantiles de pérdidas esperadas implícitos en las RNDs entre tres principales mercados desarrollados: Estados Unidos (S&P 500), Eurozona (EuroStoxx 50) y Japón (Nikkei 225). Para ello consideramos los cuantiles de las RNDs previamente calculadas, para los niveles de 5%, 10%, 15%, 20% y 25%, para diferentes horizontes temporales: 30, 60 y 91 días.

Los resultados empíricos obtenidos del análisis impulso-respuesta revelan que sólo la transmisión de los shocks en los cuantiles de pérdida del S&P 500 al resto de mercados es significativa. Siendo la transmisión de EuroStoxx 50 y Nikkei 225 al resto de mercados no significativa.

Analizamos también las diferencias en la transmisión entre los diferentes cuantiles del S&P 500 a EuroStoxx 50 y Nikkei 225, para un mismo horizonte temporal. Sin embargo, no encontramos diferencias significativas entre éstos. De la misma manera, analizamos posibles diferencias en la transmisión de cuantiles para diferentes horizonte temporales.

Los resultados revelan que la magnitud de la transmisión de shocks en el S&P 500 al resto de mercados es más fuerte para horizontes temporales mayores (60 y 91 días), mientras que la magnitud de la transmisión es más suave para horizontes temporales de 30 días.

Por lo que respeta al análisis de la descomposición de la varianza, los resultados apuntan a que la varianza de cada uno de los mercados viene principalmente explicada por sus propios shocks, lo que revela un comportamiento autoregresivo de los shocks en los cambios de los cuantiles de la cola izquierda.

Cualitativamente los resultados se mantienen para las diferentes metodologías (S-VAR con datos diarios y VAR con datos semanales), para diferentes niveles de pérdida esperada (cuantiles del 5% al 25%) y distintos horizontes temporales (30, 60 y 91 días). Esto nos permite verificar la robustez de nuestros resultados.

R.3 El comportaminento de la aversión al riesgo en economías desarrolladas.

El conocimiento y estudio del comportamiento de la aversión al riesgo es de gran importancia en política macroeconómica y en valoración de activos. Según la teoría económica, la integración de los mercados desarrollados debería dar lugar a patrones similares en el comportamiento de la aversión al riesgo en los diferentes países.

En este capítulo pretendemos adentrarnos en el análisis de las series de aversión al riesgo para diferentes economías desarrolladas: Estados Unidos (S&P 500), Eurozona (EuroStoxx 50) y Japón (Nikkei 225); estudiar las causas de la heterogeneidad entre ellas, así como el comportamineto de las mismas en diferentes momentos de tiempo. Uno de los principales objetivos es determinar si el comportamiento de la aversión al riesgo obedece a factores globales o idiosincráticos. Para ello usamos la información implícita en el precio

de las opciones.

Como hemos visto en los capítulos anteriores, las distribuciones extraídas de los precios de las opciones son distribuciones neutrales al riesgo (RND). Sin embargo, en la realidad los individuos no son indiferentes al riesgo, por lo que existen distribuciones de probabilidad reales o subjetivas (SPD) las cuales incorporan las preferencias de los inversores.

De acuerdo con la literatura, la aversión al riesgo para un determinado mercado se puede obtener directamente de la relación existente entre las RNDs y las SPDs. Ver Jackwerth (2000) y Aït-Sahalia and Lo (2000). En este capítulo las RNDs se extraen de los precios observados de las opciones, mientras que la estimación de las SPDs se hace mediante técnicas econométricas basadas en un modelo GARCH asimétrico, propuesto por Glosten et al. (1993).

Una vez hemos extraído las series de aversión al riesgo, el análisis de componentes principales indica que hay una fuente de comunalidad en las series. Analizamos esta comunalidad proyectando los coeficientes estimados frente a diferentes variables macroeconómicas de carácter global y específico de cada país.

Igualmente, con el objetivo de profundizar en el análisis de las series de aversión al riesgo, regresamos estas series frente a un conjunto de variables macroeconómicas susceptibles de poder explicar las series contemporáneas de la aversión al riesgo. Paralelamente, estudiamos también la aversión al riesgo en series temporales, mediante un análisis VAR.

R.3.1 Metodología

La extracción de las RNDs se hace de acuerdo a la metodología presentada en el capítulo anterior, usando para ello el método no-paramétrico propuesto por Breeden and Litzenberger (1978) junto con el método de ajuste de splines para la interpolación de los

datos observados. Para completar la falta de área en las colas, añadimos dos puntos delta a cada uno de los extremos del rango de observaciones y extrapolamos la spline.

Por otra parte, la estimación de las SPDs se hace mediante observaciones históricas de precios. Sin embargo, al ser las RNDs para un horizonte temporal determinado (*forward-looking*, es decir, con miras al futuro), debemos estimar las SPDs para el mismo horizonte temporal. Para ello usamos el método ARMA-GJR de predicción de volatilidad, seguido de una densidad Kernel. La eficiencia de éstos métodos ha sido probada por diferentes autores, siendo Rosenberg and Engle (2002) un ejemplo.

Una vez extraídas las RNDs y las SPDs, las series de aversión al riesgo son calculadas a partir de la relación existente entre las dos densidades, ver Jackwerth (2000) y Aït-Sahalia and Lo (2000). De esta manera evitamos imponer funciones de utilidad paramétricas.

Una vez tenemos las series de aversión al riesgo para los diferentes mercados, mediante una regresión OLS analizamos la relación de cada serie con variables macroeconómicas. Aplicamos también un análisis de componentes principales, con el que obtenemos información sobre comunalidades entre las series en diferentes países.

Paralelamente, analizamos el comportamiento de las series temporales mediante el estudio de un modelo VAR. Con este modelo pretendemos examinar las dependencias de cada una de las series no solo con sus retardos sino también con los retardos de las otras series. Una vez conocemos las relaciones temporales entre las variables, mediante el análisis impulso-respuesta examinamos cómo shocks unitarios en la aversión al riesgo de un determinado mercado es transmitido al resto de mercados. Así como también el tiempo que tarda el mercado afectado en incorporar tal efecto.

R.3.2 Muestra

Para la extracción de las RNDs, usamos una muestra compuesta por pares de volatilidad-deltas extraídos de la volatility surface proporcionada por la base de datos IVY OptionMetrics. Para la estimación de las SPDs, utilizamos datos de precios de los subyacentes de los diferentes índices: S&P 500, EuroStoxx 50 y Nikkei 225.

Las series de aversion al riesgo son extraídas para el periodo desde Mayo 2004 hasta Septiembre 2015.

Para entender y analizar el comportamiento de las diferentes series de aversión al riesgo, usamos una batería de las principales variables macroeconómicas para cada uno de los mercados, estas variables son: el índice de precios al consumo, el índice de producción industrial, el desempleo, el índice de incertidumbre política, el índice de confianza del consumidor, los tipos de cambio dólar/euro, yen/euro y yen/dólar, y finalmente consideramos los tipos de interés a 5 años de bonos soberanos y el spread calculado como la diferencia entre los tipos de interés a 10 años y 1 año.

R.3.3 Resultados y conclusiones

En general concluimos que las series de aversión al riesgo cambian en el tiempo, llegando a tomar incluso valores negativos durante algunos periodos puntuales. También se aprecian diferencias entre niveles de moneyness. Se han analizado series de aversión al riesgo para moneyness 0.97, 1 y 1.03, y observamos como aumentan los niveles de aversión al riesgo al disminuir el nivel de moneyness (riqueza), esto es, cuando nos adentramos en la cola izquierda de pérdidas.

El análisis de componentes principales, indica la existencia de una fuente de comunalidad entre las series temporales al concluir que un sólo componente explica el 55% de la

variabilidad conjunta. Mediante una regresión de éste con las principales variables macroeconómicas consideradas, concluimos que un componente común a las series de aversión al riesgo podría ser explicado por medidas de incertidumbre global como son el el índice VIX de volatilidad o la pendiente de la curva de tipos de interés.

Con la finalidad de explicar si las series de aversión al riesgo se pueden explicar mediante factores globales o específicos, éstas se han regresado respecto a una batería de variables macroeconómicas. Los resultados muestran como la aversión al riesgo en diferentes países es explicada por diferentes variables, presentando así heterogeneidad entre ellas. Vemos también que son los factores idisincráticos los que lideran las series contemporáneas de aversión al riesgo.

Referente al estudio de su evolución a través del tiempo, éstas son modelizadas con un VAR con el que concluimos que solo los propios retardos son significativos, excepto para el EuroStoxx 50 el cual depende también del retardo del S&P 500, por lo que observamos un componente autoregresivo en las series de aversión al riesgo. Los resultados del análisis de impulso-respuesta concluyen que tan solo shocks en el S&P 500 afectan al EuroStoxx 50, siendo estos resultados corroborados por el test de causalidad de Granger.

R.4 Conclusiones

Como hemos visto, a partir de diferentes opciones sobre el mismo subyacente podemos extraer las densidades neutrales al riesgo (RND) para los diferentes mercados, siendo el conocimiento y el estudio de estas RNDs de gran importancia entre inversores y agentes del mercado.

Entre los principales objetivos de los inversores encontramos la necesidad de realizar predicciones sobre los precios futuros del subyacente, así como analizar las pérdidas esper-

adas y su transmisión entre los diferentes mercados financieros internacionales. Así mismo, al ser estas densidades neutrales al riesgo difieren de las reales (SPD). De la relaci'on existente entre las dos, podemos extraer una medida de aversión al riesgo para los diferentes mercados financieros, la cual es de gran importancia en política macroeconómica y en valoración de activos.

A lo largo de los tres capítulos en los que está dividida esta tesis, hemos contestado a las preguntas anteriores basándonos en información implícita en el precio de las opciones.

En el capítulo 1 hemos analizado la capacidad predictiva de las RNDs. Para ello hemos analizado diferentes índices americanos (S&P 500, Nasdaq 100 y Russell 2000) y hemos usado métodos paramétricos y no-paramétricos para la extracción de las RNDs para diferentes horizontes temporales (30, 45, 60 y 90 días). Analizamos la capacidad predictiva las RNDs basándonos en simulaciones block-bootstrap sobre estadísticos Berkowitz. Los resultados no presentan evidencia en contra de la hipótesis nula, por lo que la capacidad predictiva de las RNDs no puede ser descartada. Los resultados son robustos para todos los métodos analizados así como para los diferentes índices y horizontes temporales. La exclusión de los periodos de crisis en los que se observan movimientos más extremos y puntuales, no tiene efectos sobre los resultados obtenidos.

En este capítulo también se analizan las colas de las distribuciones y se concluye que éstas tienden a sobreestimar la frecuencia de ocurrencia en la cola izquierda, presentando buenas aproximaciones para la cola derecha.

El capítulo 2 analiza la transmisión de las pérdidas esperadas entre los diferentes mercados internacionales. En este estudio consideramos los mercados de Estados Unidos (S&P 500), la Eurozona (EuroStoxx 50) y el mercado japonés (Nikkei 225). Para ello se estiman las RNDs mendiante el método no-paramétrico propuesto por Breeden-Litzenberger junto con interpolaciones spline. Seguidamente, se calculan los quantiles (5%, 10%, 15%, 20% y

25%) para cada uno de los mercados considerados y para horizontes temporales de 30, 60 y 91 días.

Mediante el análisis de impulso-respuesta concluimos que solo shocks en los cuantiles de pérdida del S&P 500 tienen efectos en el resto de mercados estudiados. Éstos efectos son de mayor magnitud para horizontes temporales más largos (60 y 91 días) en comparación con horizontes temporales más cortos (30 días). El análisis de la descomposición de la varianza concluye que la varianza de cada uno de los mercados viene principalmente explicada por los shocks en el propio mercado.

Finalmente, el capítulo 3 estudia la naturaleza de las series de aversión al riesgo en diferentes mercados desarrollados: Estados Unidos (S&P 500), Eurozona (EuroStoxx 50) y Japón (Nikkei 225). Para ello extraemos las RNDs implícitas en el precio de las opciones mediantes el método no-paramétrico propuesto por Breeden-Litzenberger junto con interpolaciones mediante splines. Por otra parte, las SPDs se estiman mediante modelos de predicción de volatiliad ARMA-GJR seguido de una densidad Kernel.

Una vez extraídas las series de aversión al riesgo para los diferentes mercados, el análisis de componentes principales rebela la existencia de un componente común el cuál explica un 55% de la variabilidad conjunta. Este componente viene explicado en parte por factores globales como el VIX y la pendiente de tipos de Estados Unidos. Mediante el cálculo de una regresión de las diferentes series con una batería de variables macroeconómicas, concluimos que las series de aversión al riesgo son heterogéneas ya que en cada mercado y para diferentes periodos considerados (pre- y post-crisis) éstas covarían con diferentes variables. Un análisis VAR indica que tan solo el retardo del S&P 500 es significativo en el mercado europeo; mientras que para el resto de series, solo los propios retardos son significativos. Estos resultados son corroborados con los obtenidos en el análisis de impulso-respuesta y el test de causalidad de Granger.

Introduction

Over the last decades, financial options have received a lot of attention among academics and practitioners. In general, security prices can be seen as discounted future cash flows. In the particular case of the options, by having different options written on the same underlying and with the same time to expiration, we can obtain information about the shape and different parameters of the probability distribution from which investors and market participants take their expectations about future states of the economy. There exists a big strand of the literature which is devoted to extract option-implied distributions from option prices; being these distributions based on a risk-neutral world (which is used for pricing). Therefore, we can obtain information about the whole Risk-Neutral density.

The analysis of the information embedded in option prices is not new and has been highly exploited by the literature due to its convenient forward-looking features to the detriment of traditional statistical measures based on historical data (which are backward-looking). Furthermore, implied measures have been proved to be superior in different applications such as forecasting, modeling, etc.

Therefore, knowledge of Risk-Neutral distributions (heretofore referred as RND) allows us to analyze many different aspects of financial markets. One of the major concerns among investors and market participants is to obtain accurate estimate forecasts about future realizations of the underlying. This is of special interest in order to improve se-

curity valuation and manage their investments, among others. But, can we rely on the forecasting ability of the RNDs about future realizations of the underlying?

Among all the information attained, investors are highly concerned about extreme price movements in the markets, mainly the expected downward movements (which form the left tails of the RNDs). Because investors do not like losses they try to diversify their exposure to them via foreign investment, for instance. But because international developed financial markets are nowadays more integrated across border, it is of special interest and concern to investors to know whether their exposure to expected losses is well-diversified as well as how exposed they are to shocks in foreign markets.

As hereinabove mentioned, distributions extracted from option prices are risk-neutral and therefore different to the actual or real-world ones. The difference between them is mainly due to the preferences of the market agents; thus, the risk aversion is seen as a measure which depicts the deviations between the real and the risk-neutral world. But, does risk aversion in different countries exhibit a similar pattern over time? What are the sources of heterogeneity in its behavior?

This thesis aims to shed some light on the previous concerns along three main chapters. Each of these chapters is devoted to tackle different aspects of the financial markets and answer the previous questions by analyzing the informational content embedded in option prices.

In chapter 1 we aim to answer the question of whether RNDs are indeed good forecasters of future underlying realizations. In order to answer this question we analyze the forecasting ability of option-implied RNDs for three US indexes: S&P 500, Nasdaq 100 and Russell 2000, for a long series (from 1996 to 2015) which encompass two major crisis. Traditional tests rely on restrictive assumptions (mainly normality and independence). In order to overcome these assumptions, we calculate block-bootstrap-based critical val-

ues. Different to existent literature, our results conclude failure to reject their forecasting ability, being these results consistent across different forecast horizons, methodologies and indexes considered. We also analyze the fit of the tails of the RNDs separately, finding that they tend to overestimate the frequency of occurrence of events in the left tail, providing a good fit for the right tail.

Chapter 2 exploits the information embedded in the loss tail of the estimated RNDs by analyzing how shocks in the option-implied risk-neutral loss quantiles are transmitted internationally. Option-implied information has been proved to be more accurate in predicting future volatility, returns and downturns. Moreover, the information embedded in the tails is linked to macroeconomic variables. In this chapter we analyze for the first time the international transmission of option-implied loss quantiles. For this we use data from the S&P 500, the EuroStoxx 50 and the Nikkei 225 index options, we compute the RNDs and calculate impulse-response functions and variance decomposition analyses. Results confirm that shocks in the S&P 500 risk-neutral loss quantile changes have an impact to the quantiles in the other markets, whereas foreign shocks have no effects on the S&P 500 quantiles. These results are robust for different maturities and left-tail quantiles (from 5% to 25%).

Chapter 3 analyses the nature of risk aversion in main developed economic areas. We delve into the systematic patterns describing its time series behavior, disentangling whether risk aversion is driven by global or idiosyncratic forces. Risk aversion series are built using the informational content embedded in option and stock prices from high liquid indexes: S&P 500, EuroStoxx 50 and Nikkei 225. Empirical evidence from a principal component analysis shows an important source of commonality among risk aversion series. OLS estimates also show that risk aversion betas are statistically significant for global uncertainty variables like VIX; however, idiosyncratic covariates like unemployment or interest rates seem not exhibit a clear systematic pattern. A statistically significant lead-

lag relationship from US to Europe is also found.

Finally, chapter 4 presents the main conclusions and gives some guide to open questions for future research.

Chapter 1

Can we really discard forecasting ability of option-implied Risk-Neutral distributions?

It is well known that option-implied Risk-Neutral distributions (RND) are of great use for several purposes: pricing derivatives, hedging, forecasting, inference of preferences, etc. A natural question is whether realized observations are consistent with estimated RNDs. This question arises because on the one hand, RNDs are forward-looking and should be more informative about future prices than statistical methods based on historical data (which is backward-looking). On the other hand, RNDs do not incorporate any risk premium, so they are biased with respect to the distributions under the physical measure. In this study we contribute to this question by assessing the forecasting ability of the RNDs on a larger dataset and, contrary to existent literature, we can not reject the RNDs as the true distributions from where returns are drawn.

Jackwerth and Rubinstein (1996) document that RNDs became skewed and leptokurtic after the crash in 1987. Therefore, different methods have been proposed to infer the RNDs from option prices, which can be classified as parametric and non-parametric. Among the parametric methods, the Log-Normal mixture has been widely used in different fields such as the analysis of the interest rates, see Bahra (1997) and Söderlind and Svensson (1997), among others; Campa et al. (1998) and Jondeau and Rockinger (2000) who use it on exchange rates; as well as Bliss and Panigirtzoglou (2002), Anagnou et al. (2002) and Liu et al. (2007), who apply this technique to equity indexes. Other approaches are the Generalized Beta distribution of the second kind, proposed by Bookstaber and McDonald (1987) and also used by Anagnou et al. (2002) to approximate the RND for options on the S&P 500 and for the GBP/USD exchange rate; or the Variance Gamma Process by Madan et al. (1998).

Non-parametric methods rely on the approach proposed by Breeden and Litzenberger (1978), which needs a continuum of option prices (implied volatilities) with the corresponding strike prices. Representatives include Aït-Sahalia and Lo (1998) and Bliss and Panigirtzoglou (2002) who use either polynomials or splines in order to have a spectrum of strike prices.

Some of the existent literature focuses on deciding which of the above methods approximates the RNDs more accurately. Bliss and Panigirtzoglou (2002) compare the spline method versus a mixture of two Log-Normal distributions, and they find the first technique is better. In the same line, Bu and Hadri (2007) compare the splines method versus a parametric confluent hypergeometric density and conclude that the latter performs better. Alonso et al. (2005) use splines and a mixture of two Log-Normal distributions and find that both methods produce very similar results.

Even though there is no consensus on which method to use, estimation of the RNDs has been practiced for a long time now and one of the main purposes is to test its forecasting

ability, that is, how well they can predict future movements of the underlying. Related literature such as the work of Lynch and Panigirtzoglou (2008) conclude that RNDs are not useful at predicting future realizations but markets do react to events such as crisis. A group of researchers such as Anagnou et al. (2005) for the UK market, Craig et al. (2003) for the German market and Bliss and Panigirtzoglou (2004) for the UK and US market, they all conclude that implied RNDs do not produce accurate forecasts of price realizations. Alonso et al. (2005) study the Spanish market and they can not reject the null hypothesis when they consider the whole sample period, however they do reject it for the sub-periods considered. In general, the different literature advocates that differences between the RND and the actual distribution is due to the presence of risk aversion of the representative agent, and so actual distributions would be more appropriate because they do incorporate investors' beliefs and preferences.

In this study we aim to estimate daily RNDs and assess their forecasting ability. For this, we use option data on three major indexes which are S&P 500, Nasdaq 100 and Russell 2000 and use different time horizons of 15, 30, 45 and 60 days. As previously mentioned, literature is mixed about the method to use to approximate RNDs and no method has been proved to stand out; therefore, we propose to study the forecasting ability of RNDs approximated using different methods: one parametric (mixture of two Log-Normal distributions) and two non-parametric (Breeden-Litzenberger with kernel and with spline techniques). By doing this, we check whether our results hold for different methods.

Previous literature appraise the forecasting ability of the RNDs based on the Berkowitz test; however, we suspect that the hypotheses over which this test is built are not appropriate for this type of data, and so differently from previous works we run block-bootstrap re-sampling to check the forecasting ability of our RNDs. In order to reinforce the results obtained, we also perform Cramer-von-Mises test, which also assesses the forecasting

ability of the densities.

We contribute to the literature by analyzing the longest series of data, ranging from 1996 to 2015, which is of special interest since it embraces two major crisis and increases the size of the test. We compare our results across different existent methods and maturities and prove consistency in the results across all of them. Furthermore, in this analysis we deal with the tail area, whose estimation still remains a challenge in the literature due to the scarcity of data in these regions. Tails are assessed through a tail test based on the Brier Score. Finally, our results prove that, contrary to the common findings on the topic, RNDs can not be rejected as good forecasters of future price realizations.

The chapter is organized as follows: in section 1.1 we present the different methods used to extract the RNDs, section 1.2 contains the tests applied, section 1.3 presents the data, in section 1.4 we find the results and discussion, and finally in section 1.5 we conclude.

1.1 Methodology

There exists a vast literature concerning the extraction of the RNDs. Most of these methods have to do with two techniques: parametric methods, to which major contributors include Banz and Miller (1978) and Rubinstein (1994) among others; and non-parametric methods, being Aït-Sahalia and Lo (1998) and Bliss and Panigirtzoglou (2002) relevant references. In order to provide some robustness to our results we consider three different alternatives to extract the RNDs from option prices, being one parametric and two non-parametric.

Due to its simplicity, the most common method is the parametric approach, which is based on choosing a certain option pricing model built on a flexible parametric return

distribution which allows for thick tails and skewed shapes. Then, RND parameters are set to be those that best fit the observed prices. This approach is fairly easy to implement and yields to well-behaved distributions (non-negative RNDs). For the parametric methods we use the well-known Log-Normal mixture distributions (heretofore LNM).[1]

The non-parametric methods rely on the Breeden and Litzenberger (1978) technique to obtain the RNDs. These methods do not assume any specific form of the probability distribution function and they are based on weaker assumptions. However, they are built on a continuous range of option prices across moneyness, therefore interpolation of the data is needed. Following the works of Aït-Sahalia and Lo (1998) and Bliss and Panigirtzoglou (2002), we use the kernel regression and the spline approaches for interpolating and smoothing the data before applying the Breeden-Litzenberger technique to finally obtain the RNDs.

1.1.1 Parametric RNDs

Mixture of Log-Normal distributions has been widely used in the literature in different fields. This approach consists on a weighted average of Log-Normal distributions. The main advantage of this approach is that non-negativity of the distribution is ensured, as well as being easy to implement and flexible enough to fit a broad range of different shapes, allowing for bimodality.

We derive the estimated RNDs, $f_Q(x)$, as a mixture of two Log-Normal distributions as follows,

$$f_Q(x) = p\,\Psi(x|F_1, \sigma_1, T) + (1-p)\,\Psi(x|F_2, \sigma_2, T) \tag{1.1}$$

where $\Psi(x|F, \sigma, T)$ is a Log-Normal density function with x being the domain of forward

[1] To implement this approach we follow the lines of Taylor (2005). We refer the reader to the book for further details.

prices over which the density is defined, F is the expected forward price of the underlying at maturity T, and σ is the standard deviation. Subscripts 1 and 2 indicate the two different Log-Normal distributions being mixed. The weight placed on each Log-Normal distribution is determined by the parameter p, and consequently $(1-p)$, which takes values between 0 and 1. More details about the derivation of such distributions can be found in the Appendix A.1.

1.1.2 Non-parametric RNDs

As per Breeden and Litzenberger (1978) the whole RND can be extracted by taking the second partial derivative of the option pricing function with respect to the strike price. Hence, the RND of the underlying asset at expiration $f(S_T)$, is given by

$$f\left(S_T\right) = \ e^{r(\tau)} \frac{\partial^2 C\left(S_t, X, T, t\right)}{\partial X^2} \mid_{X=S_T} \tag{1.2}$$

being r the risk-free rate, $C\left(S_t, X, T, t\right)$ the European call price function, S_t the current value of the underlying asset, X the strike price of the option, T the expiration date, t the current date and $\tau = T - t$ the time to expiration. The corresponding cumulative Risk-Neutral distribution function can be obtained as follows,

$$F(X) = e^{r\tau} \frac{\partial C}{\partial X} + 1 \tag{1.3}$$

However, non-parametric methods are challenged with two hurdles due to the nature and availability of the data. To compute numerically equation (1.2) by finite-differences, a thin grid of strike prices encompassing all possible future payoffs is needed. Nevertheless, available data is sparse in the strike domain, hence option prices must be interpolated. The second drawback is that option prices may be noisy, so a smoothing technique needs to be applied. To overcome these drawbacks, we use both the kernel regression and the

spline technique.

For the interpolation of the data, instead of interpolating on prices, Malz (1997) suggests that it is better practice to interpolate on implied volatilities, and instead of interpolating across the strike price domain he also proposes to interpolate across deltas (that is on an implied volatility-delta space). The advantage of this method is twofold: first, it groups away-from-the-money options more closely permitting the data to have a more accurate shape at the center of the distribution where information is more reliable; and second, call option deltas are bounded between $[0; 1]$, in contrast to the strike price domain which is theoretically unbounded. In order to convert option prices into implied volatilities (iv) and exercise prices into deltas, Black-Scholes-Merton (BSM) formula is used. Once the ivs and the deltas are fitted into the corresponding smoothing technique in order to get the continuum of data, they are converted back into option and strike prices using the same formula.[2]

1.1.2.1 Kernel Regression

We propose the kernel regression estimator of Nadaraya (1964) and Watson (1964) as our first non-parametric method to smooth and interpolate the data, namely

$$\hat{m}_h(x) = \frac{n^{-1}\sum_{i=1}^{n} K_h(x - x_i)Y_i}{n^{-1}\sum_{i=1}^{n} K_h(x - x_i)} \qquad ; \qquad K_{h_n}(u) = h_n^{-1} K\left(\frac{u}{h_n}\right)$$

being x and Y_i the delta (Δ) and the implied volatility (iv) of the observed options, respectively; K_{h_n} a kernel function and h the bandwidth (smoothing) parameter.

We choose as K_{h_n} the gaussian kernel, however as mentioned in Aït-Sahalia and Lo

[2]Note that, at this point the use of the BSM pricing formula does not presume that such formula correctly prices the options, it is merely a tool to change from prices to iv and from X to deltas, being reverted back in future steps into exercise price domain. In order to change from exercise price domain to Black-and-Scholes-delta domain we use the same volatility for all observations, which is obtained from a weighted average of the different implied volatilities.

(1998) the choice of the kernel function has not as much influence on the result as the choice of the bandwidth, h, being the outcome very sensitive to this value. A wide range of alternative approaches to calculate h are studied in Silverman (1986) and Härdle (1990). However, there is no consensus in the literature about the optimal h nor the best method to use to calculate it. In this work, we choose among different values calculated using both *leave-one-out cross-validation* and *Silverman's Rule-of-Thumb*. See Appendix A.2 for more details on how h is calculated.

At this point we are faced with the limitation of being able to estimate only the part of the RND corresponding to the observed range of strikes. Extreme strike observations are scarce or even non-existent, being most of them illiquid and therefore the information embedded in such prices may be misleading and unreliable. Not because extreme events, which form the tails of the distribution, are rare means that they cannot occur; but the contrary, the information contained in the tails is of major importance in risk management to carry out value-at-risk analysis, as well as in asset allocation, among others.

We find a scarce literature exploring the issue of the tails which still remains a challenge for researchers. To make estimations beyond the range of observed values, we need to extrapolate somehow the available data. One approach is to assume a parametric probability distribution to approximate the tail zone. Figlewski (2008) states that as per Fisher-Tippett Theorem, a large value drawn from an unknown distribution will converge in distribution to one of the Generalized Extreme Value distributions (GEV) family. Based on this, Birru and Figlewski (2012) propose the use of the Generalized Pareto distribution (GPD), which also belongs to the extreme value distributions family. The attractiveness of this method is that it has only two free parameters, which are η, the scale parameter and ξ, the shape parameter. We follow this approach to complete the tails of the RNDs, and we append GPD tails to our kernel-based RNDs. More details about these procedures are given in the Appendix A.3. An illustrative example is depicted in figure 1.1.

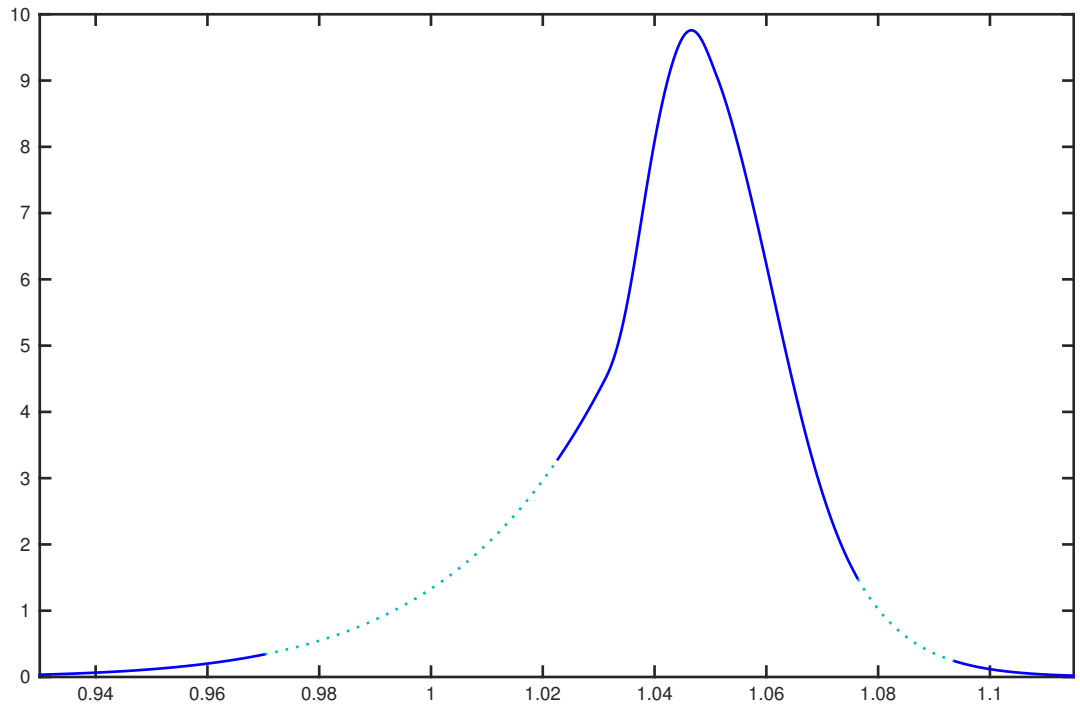

Figure 1.1: **Kernel RND with pareto tails appended.** The figure shows a RND calculated for the S&P 500 for a 30 days time horizon using kernel technique with pareto tails appended. We can distinguish: the central part (solid line) which is the main body of the distribution, which has been calculated using the kernel method; the most extreme regions (also depicted with a solid line) which show the pareto tails appended to the main body of the distribution; and finally the graph depicts the overlapping zone between α_0 and α_1 (dotted line) which has been estimated using a weighting scheme. The RND is for 17 December 2009.

1.1.2.2 Splines

Following Bliss and Panigirtzoglou (2004), we also consider to fit *iv* using cubic smoothing splines (piece-wise polynomials). The smoothing spline is defined by the knots and polynomial coefficients that minimize the following function,

$$S_\lambda = \sum_{i=1}^{n} m_i (Y_i - g(\Delta_i, \theta))^2 + \lambda \int_{-\infty}^{+\infty} p''(x;\theta)^2 dx \tag{1.4}$$

where m_i is a weighting value of the squared error, Y_i is the implied volatility of the ith option observation, $g(\Delta_i, \theta)$ is the fitted iv which is a function of Δ_i and a set of spline parameters, θ; $g(\Delta_i, \theta)$ is any curve which can have any form and whose coefficients are estimated by least-squares. λ is the smoothing parameter, which following Bliss and Panigirtzoglou (2004) takes value 0.99, and $p(x;\theta)^2$ is the smoothing spline.

For the m_i weight in equation (3.2), Bliss and Panigirtzoglou (2004) use the BSM *vegas* of the observed options. However, we slightly modify this weighting scheme using squared *vegas*, which places more weight to those near-to-at-the-money observations and therefore it performs better.

Like in the kernel-based method, we are faced with the limitation of being able to estimate only the part of the RND corresponding to the observed range of strikes, missing some probability at the extremes. For the spline method we deal with the tails using two different approaches. First, we simply extrapolate the spline outside the observed Δ domain; however it can cause implausible or negative ivs, as well as kinks at the ends of the RNDs. Following Bliss and Panigirtzoglou (2004) before extrapolating we add two extra points at both ends of the moneyness domain and assign them the iv value of the corresponding end point. By doing this, we get an extended moneyness range over which we extrapolate the spline. The second approach is to fit pareto tails, the same way as it is done for the kernel method.

To illustrate the different methods used in this work, figure 1.2 exhibits the extracted RNDs calculated for S&P 500 index options with 30 days to maturity for two different days: one RND is from 21 July 2005 (left hand side plots), just before the global financial crisis; while the second RND is from 23 July 2009 (right hand side plots), just after the crisis. The top plots represent the RNDs from parametric method (Log-Normal mixture), while the bottom plots depict the non-parametric ones (kernel with pareto tails appended, splines with extrapolation and splines with pareto tails). From this figure, two facts arise:

first, the different methods used in this work seem capable to capture the main features of option-implied RNDs (skewed shapes, fat tails, etc.); second, comparing the x-axis of the pre and post crisis RNDs, it is clear that the domain (dispersion of futures outcomes) has spread out.

1.2 The tests

In order to verify whether RNDs accurately forecast realized ex-post returns, we rely on three tests. First, we analyze the performance of the Berkowitz (2001) test that jointly tests independence and uniformity, which has been used by Bliss and Panigirtzoglou (2004) and Alonso et al. (2006), among others.[3] Second, we focus on the tails using the Brier Score, which is based on the realized frequency for a certain (extreme) quantile (i.e. 5%, 10%, 90%, 95%). In order to verify the reliability of these tests, we compute the bootstrap distribution of the test statistics. Finally, we re-inforce the findings of the previous with the Cramer-von-Mises test.

Given a set of implied RNDs for each date t_i with a specific τ-horizon, $\hat{f}_{t_i,\tau}\left(S_{t_i+\tau}\right)$, where $S_{t_i+\tau}$ are the values at expiration; the Berkowitz test first transforms $S_{t_i+\tau}$ into a new variable z_{t_i} using the probability integral transform,

$$z_{t_i,\tau} = \Phi^{-1}\left(\int_{-\infty}^{S_{t_i+\tau}} \hat{f}_{t_i,\tau}\left(u\right) du\right) \tag{1.5}$$

where $\Phi^{-1}(\ldots)$ stands for the inverse of the standard Normal distribution function.

Under the null hypothesis that $\hat{f}_{t_i,\tau}\left(\ldots\right) = f_{t_i,\tau}\left(\ldots\right)$ and the assumption that $S_{t_i+\tau}$ are independent, the new variable $z_{t_i,\tau} \sim iid\, N(0,\, 1)$. In this test, independence and normality of $z_{t_i,\tau}$ are tested using a likelihood ratio test by estimating by maximum likelihood

[3] According to Bliss and Panigirtzoglou (2004), this test performs better than several non-parametric tests, such as, Kolmogorov-Smirnov, Chi-squared or Kupier tests.

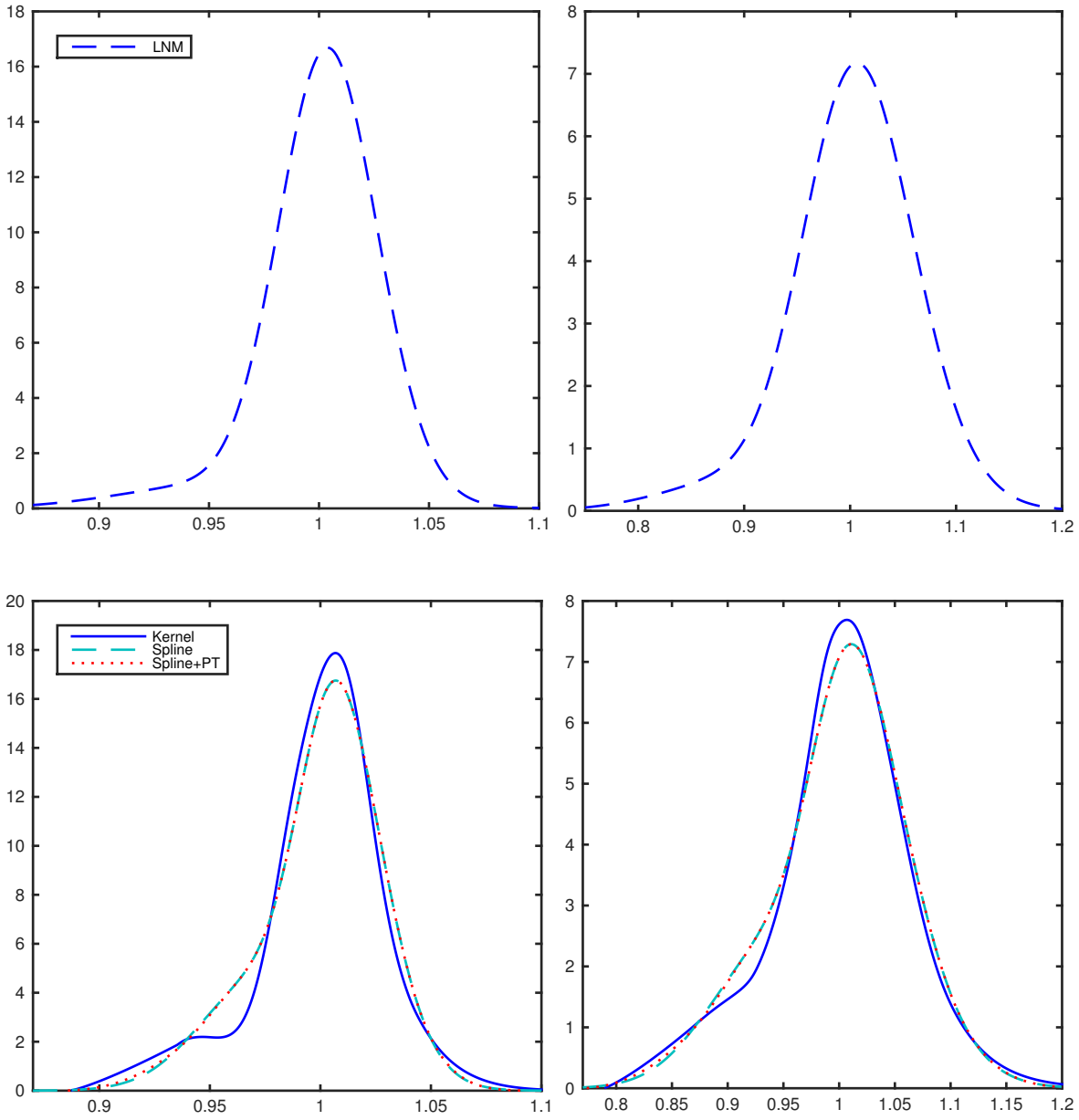

Figure 1.2: **RNDs before and after the crisis.** The figure compares a pre-crisis (21 July 2005) RND (left-hand side plots) and a post-crisis (23 July 2009) RND (right-hand side plots) for the S&P 500 at 30 days maturity for each of the different methods proposed. Both top panels depict parametric RNDs: Log-Normal mixture. The bottom plots show the two non-parametric RNDs: kernel with pareto tails appended (solid line), splines with extrapolation (dashed line) and splines with pareto tails (dotted line).

the following AR(1) model,[4]

$$z_{t_i,\tau} - \mu = \rho\left(z_{t_i-1,\tau} - \mu\right) + \epsilon_{t_i,\tau}, \quad \epsilon_{t_i,\tau}\ iid\, N(0, \sigma_\epsilon^2) \tag{1.6}$$

Under the null hypothesis, the estimated parameters should be $\left[\mu,\ \sigma_\epsilon^2,\ \rho,\right] = [0,\ 1,\ 0]$. Therefore, the likelihood ratio test

$$LR_3 = -2\left[L\left(0, 1, 0\right) - L\left(\hat{\mu}, \hat{\sigma}_\epsilon^2, \hat{\rho}\right)\right] \tag{1.7}$$

is asymptotically distributed as $\chi^2\left(3\right)$ under the null hypothesis.

The presence of overlapping or non-overlapping but serially correlated data may lead to a false rejection of the null hypothesis. For that, Berkowitz (2001) suggests testing the independence assumption separately as follows,

$$LR_1 = -2\left[L\left(\hat{\mu}, \hat{\sigma}^2, 0\right) - L\left(\hat{\mu}, \hat{\sigma}^2, \hat{\rho}\right)\right] \tag{1.8}$$

which under the null hypothesis is asymptotically distributed as $\chi^2\left(1\right)$. As per the previous, LR_3 results will be more reliable when LR_1 fails to reject. Should both LR_3 and LR_1 reject, we cannot ascertain whether the reason is lack of predictability of the RNDs or the presence of serial correlation in the data.[5]

Due to the features of the data (short samples and dependence), the empirical distribution of the statistics in equation (1.7) may differ from the asymptotic ones, yielding to different critical values, and thus wrong decisions about rejection of the null hypothesis may be taken. To overcome this problem, we compute bootstrap-based critical values. Since it is of interest to maintain the structure present in the data, we use block-bootstrap.[6]

[4]Even though dependency can arise from a more complex structure than an AR(1), this dependence structure is the most evident and intuitive, specially in overlapping data.

[5]Note that failure to reject does not necessary imply that the null hypothesis is true.

[6]When re-sampling, note that the outcome will be only as good as the ability of the data generating

This method was first introduced by Künsch (1989) and it divides the sample into different blocks (which may be overlapped) of b consecutive observations. Then, bootstrap samples are built by randomly concatenating blocks to match the original sample size. Künsch (1989) proposes that a reasonable block length would be $n^{1/3}$, where n is the length of the original sample. We have also tried with $n^{1/3}+3$, $n^{1/3}+8$, $n^{1/3}+13$ and $n^{1/3}-1$ observations. These values generate blocks of length 10, 15, 20 and 6 observations, respectively, for the S&P 500 case. In our analysis, results are very similar and lead to the same conclusions regardless the length of the block. Once m bootstrap samples have been generated, the statistics of interest are calculated for each sample.

Another way of assessing whether the estimated densities, $\hat{f}_{t_i,\tau}(\ldots)$, are the true densities, $f_{t_i,\tau}(\ldots)$, is the Cramer-von-Mises test (CM henceforth), which was proposed by Cramer (1928) and von Mises (1931). This test is based on the probability integral transform of the realized prices of the underlying at maturity given our estimated densities,

$$y_{t_i,\tau} = \int_{-\infty}^{S_{t_i+\tau}} \hat{f}_{t_i,\tau}(u)\, du \tag{1.9}$$

Should the null hypothesis that the estimated densities are the true densities hold, the transformed realizations $y_{t_i,\tau}$ should be uniformly distributed. To check that, von Mises (1931) proposes the following statistic,

$$\widehat{CM} = \int_0^1 \left(F_{t_i,\tau} - \hat{F}_{t_i,\tau}(S_{t_i+\tau})\right)^2 (u)\, du \tag{1.10}$$

where $F_{t_i,\tau}$ is the Uniform (0,1) distribution function and $\hat{F}$ is the estimated cumulative RND.

In order to approximate the asymptotic distribution of the CM test, we perform a bootstrap-based test. The same way as it is done for the Berkowitz, we bootstrap m

process (bootstrap samples) to fairly mimic the actual data and their structure.

different samples of series of $y_{t_i,\tau}$ in blocks, over which CM test is calculated, having a series of m CM statistics ($\widehat{CM}_{BB}$) which form a distribution. We reject the null hypothesis in favor to the alternative when the estimated statistic $\widehat{CM}$ is in the upper tail of the series of $\widehat{CM}_{BB}$. Specifically we calculate

$$\widehat{p}_{BB}\left(\widehat{CM}\right) = \frac{1}{m}\sum_{i=1}^{m} \mathbb{1}_{\{\widehat{CM}_{BB_i} > \widehat{CM}\}} \tag{1.11}$$

being $\mathbb{1}_{\{...\}}$ an indicator function which takes value 1 when the expression in brackets is true.

As per the previous, we reject the null hypothesis whenever $\widehat{p}_{BB}\left(\widehat{CM}\right)$ is smaller than some probability level α, which is equivalent to rejecting it when $\widehat{CM}$ exceeds the $1-\alpha$ quantile of the $\widehat{CM}_{BB}$ density.

Following Anagnou et al. (2005) and Alonso et al. (2006), we also test the goodness of fit of the tails separately. They propose the statistic suggested by Seillier-Moiseiwisch and Dawid (1993) to test whether Brier Score departs from its expected value (Tail test henceforth). Brier Score is defined as

$$B = \frac{1}{T}\sum_{t=1}^{T} 2\left(\hat{F}_{t,\tau}^{tail} - R_{t,\tau}\right)^2 \tag{1.12}$$

and measures the accuracy of the probabilistic predictions based on the distance between a selected probability mass in the tail, $\hat{F}_{t,\tau}^{tail}$, and a binary variable, $R_{t,\tau}$, which takes value 1 if the true realization of the underlying falls into the tail being tested, or 0 otherwise.

The statistic is defined as follows,

$$Y = \frac{\sum_{t=1}^{T}\left(1-2\hat{F}_{t,\tau}^{tail}\right)\left(R_{t,\tau}-\hat{F}_{t,\tau}^{tail}\right)}{\left[\sum_{t=1}^{T}\left(1-2\hat{F}_{t,\tau}^{tail}\right)^2 \hat{F}_{t,\tau}^{tail}\left(1-\hat{F}_{t,\tau}^{tail}\right)\right]^{\frac{1}{2}}} \tag{1.13}$$

which is asymptotically distributed as a Standard Normal.

1.3 The Data

We have a set of European call and put options written on three of the major traded indexes, S&P 500, Nasdaq 100 and Russell 2000, from the OptionMetrics database. We have observations ranging from January 1996 until October 2015. We use daily closing prices for all the indexes and calculate the mid-point of the bid and ask price of the options. The risk-free rate used in our analysis is the zero-coupon yield provided by OptionMetrics.[7]

Because extreme observations are considered to be very-far-away-from-the-money and therefore illiquid and fairly unreliable, following Panigirtzoglou and Skiadopoulos (2004) we discard observations with delta values (Δ) beyond the range [0.01; 0.99].

We calculate a RND for those days of the sample with options maturing in 15, 30, 45 and 60 days. Data can present some anomalies, and therefore a filtering is required before the implementation of the different models. Under the assumption of complete markets, those options which do not satisfy the arbitrage conditions are discarded from the sample. Those options which are very-far-away-from-the-money are also dropped from the sample since they are poorly traded and thus illiquid, so the information embedded in their prices can be unreliable and of no use. Therefore, following the literature, we keep only in the sample those observations whose moneyness lies within 0.75 and 1.25. We also require a minimum of 8 observations to perform any estimation.

When working with options we need to deal with the presence of the dividends. Such variables are unobservable and difficult to estimate. We will follow in this study

[7] Bliss and Panigirtzoglou (2004) studied the effect of the risk-free proxy and concluded that a change of 100 basis points in the risk-free rate leads to a two basis points change in the measured implied volatility for a one-month horizon, and this change will be up to 5 basis points for the six-months horizon. Therefore, the proxy used will have little impact on the results.

the approach proposed by Aït-Sahalia and Lo (2000), in which they work with forward quotes of the underlying instead, therefore dividends go out from the formulas. Since the assumption of complete markets holds, we can infer the forward prices, F, for the underlying from the put-call parity formula,

$$F = (C - P)\, e^{r\tau} + X \tag{1.14}$$

where C and P are the prices for the call and put options respectively, r is the risk-free rate, τ is the time left to maturity of the option and X is the strike price

Given a certain day and maturity, there exist a call and a put option for each exercise price. Following Aït-Sahalia and Lo (2000), we remove those call and put contracts that are in-the-money (ITM), which are less liquid. Out-of-the-money put options are translated to their counterpart ITM call options by using the put-call parity, being these put options removed from the sample. By doing this, all the options kept in the sample are OTM. We consider call options to be ITM when their moneyness ratio F/X is higher than 1.03, while puts are ITM when their F/X is below 0.97.

For the non-parametric cases, we consider an additional filter: once RNDs have been estimated and before appending tails, we discard those RNDs which account for less than the 70% of the probability mass. The rational of this filter is to include only those sample days where a large portion of the RNDs have been estimated directly from option prices and not by extrapolating a spline or appending pareto tails.

In case no RND is successful in matching the above criteria, we try to fit the RND on the previous or the following day instead. If the fit at time t is discarded due to the reasons exposed above in this section, we try to fit the RND from the previous day, $t-1$ (in this case the same options will mature in 16, 31, 46 or 61 days). Should this second fit be also discarded, we try to fit data from the following day, $t+1$ (in this case the options

will mature in 14, 29, 44 or 59 days). Should the method fail to obtain a successful distribution, then that specific day is discarded from the sample. As explained before a weak point of the previous research which focuses on the forecasting ability of RNDs is the (short) sample size when running the tests. We proceed in this way in order to get more observations and increase the sample size to run the tests explained in section 1.2.

1.4 Results and discussion

The RNDs have been estimated using different parametric and non-parametric methods from options on three different indexes: S&P 500, Nasdaq 100 and Russell 2000. In figure 1.3 we plot the volatility, skewness and kurtosis implied from the estimated RNDs for the S&P 500 index options with 30 days to maturity. We calculate these moments by numerical integration of the already estimated RNDs.[8] In general, we can appreciate that the implied volatility (top plot) is almost the same for the different techniques. We also see that implied skewness is negative, as expected, but in this case differences across methods are more evident. And finally we can observe a similar pattern for the implied kurtosis: in general it is higher than 3, but with noticeable differences across methods. Regarding the similarities between the different methods they are clearer for spline-based methods. In consequence, to avoid results conditioned by the selected method of extracting the RNDs, it is relevant to check the forecasting ability for RNDs obtained with all different techniques.

Table 1.1 shows the p-values of the LR_3 Berkowitz test statistic for the different methods, maturities and indexes considered in this work, as well as the LR_1 p-values for testing the independence separately. For all cases considered, both tests reject their respective null hypothesis, therefore we can not ascertain the reason of rejection: poor

[8] Similar figures for Nasdaq 100 and Russell 2000 risk-neutral moments are available upon request.

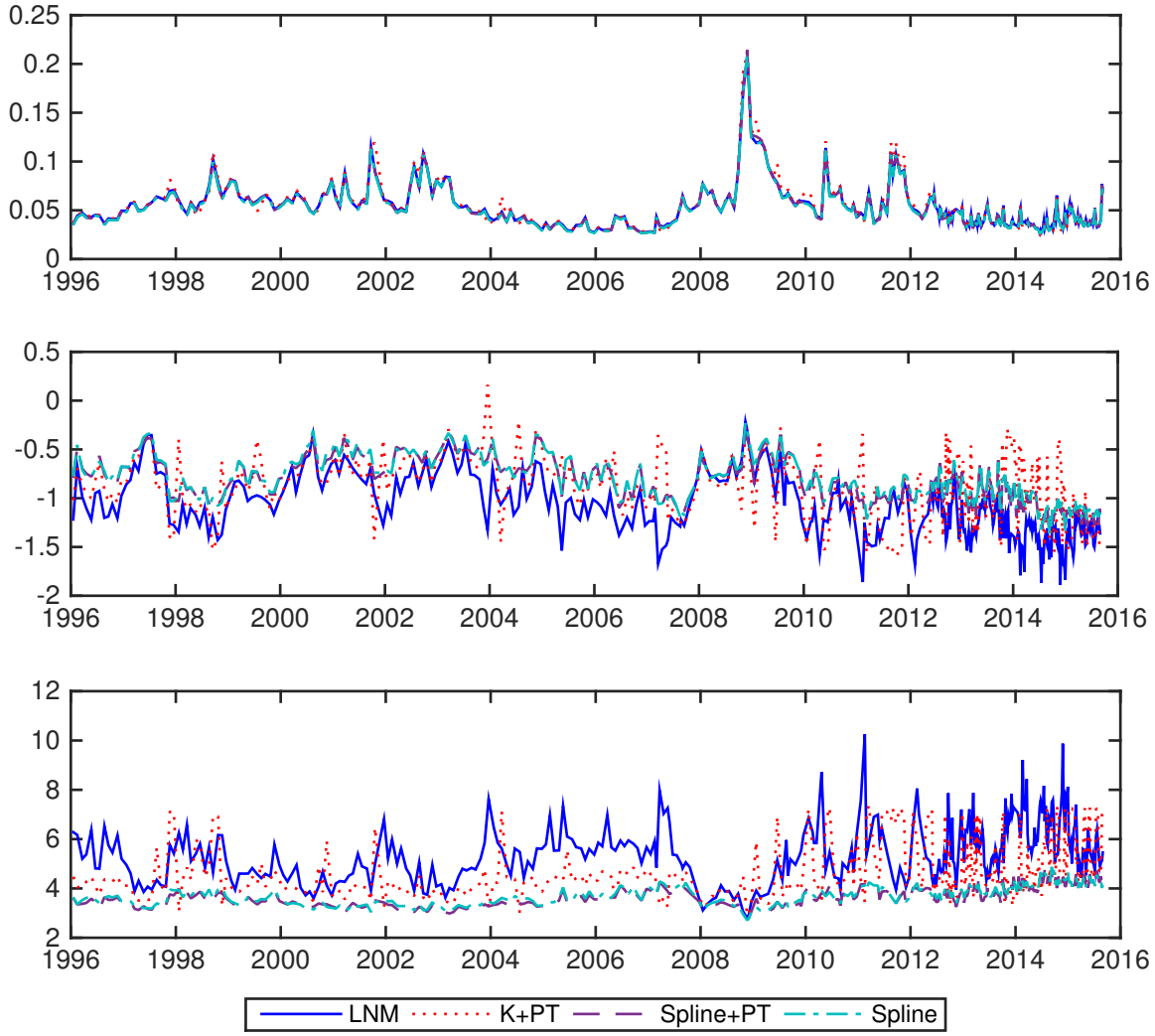

Figure 1.3: **Standard deviation, Skewness and Kurtosis for the RNDs extracted using all different methods.** The figure compares the risk-neutral volatility (30 days), skewness and kurtosis implied in the RNDs calculated for the S&P 500 using all methods used in this study: Log-Normal mixture (LNM), kernel with pareto tails (K+PT), splines with pareto tails (Spline+PT) and splines with extrapolation (Spline). Implied moments are calculated from numerical integration of the obtained RNDs.

forecasting ability or lack of independence of the transformed variables (see equation (1.5)).

Note that during this period financial markets have been hit by two major crisis, one from March 2000 to October 2002; and one from October 2007 until March 2009. The fact that such periods present extreme movements in stock prices might mislead the results of

τ	model	S&P 500		NASDAQ 100		RUSSELL 2000	
		LR_3	LR_1	LR_3	LR_1	LR_3	LR_1
15 days	LNM	0.0000	0.0000	0.0013	0.0007	0.0000	0.0000
	Kernel	0.0000	0.0000	0.0004	0.0003	0.0000	0.0000
	Spline	0.0000	0.0000	0.0004	0.0006	0.0000	0.0000
	Sp+PT	0.0000	0.0000	0.0004	0.0007	0.0000	0.0000
30 days	LNM	0.0000	0.0000	0.0000	0.0000	0.0000	0.0000
	Kernel	0.0000	0.0000	0.0000	0.0000	0.0009	0.0001
	Spline	0.0000	0.0000	0.0000	0.0000	0.0000	0.0000
	Sp+PT	0.0000	0.0000	0.0000	0.0000	0.0013	0.0002
45 days	LNM	0.0000	0.0000	0.0000	0.0000	0.0000	0.0000
	Kernel	0.0000	0.0000	0.0000	0.0000	0.0000	0.0000
	Spline	0.0000	0.0000	0.0000	0.0000	0.0000	0.0000
	Sp+PT	0.0000	0.0000	0.0000	0.0000	0.0000	0.0000
60 days	LNM	0.0000	0.0000	0.0000	0.0000	0.0000	0.0000
	Kernel	0.0000	0.0000	0.0000	0.0000	0.0000	0.0000
	Spline	0.0000	0.0000	0.0000	0.0000	0.0000	0.0000
	Sp+PT	0.0000	0.0000	0.0000	0.0000	0.0000	0.0000

Table 1.1: **Berkowitz test p-values.** The table shows the LR_3 and LR_1 Berkowitz test corresponding p-values. The test is run on the RNDs based on the S&P 500, Nasdaq 100 and Russell 2000 indexes for the different maturities (column τ) and methods used in the work: Log-Normal Mixture (LNM), kernel with pareto tails (Kernel), spline with extrapolation (Spline) and splines with pareto tails (Sp+PT). The analysis is applied to the whole data set which goes from January 1996 until October 2015.

the tests. In order to consider this, both statistics have been calculated on a restricted data set which excludes the above turmoil periods. Results are presented in table 1.2 and they yield to the same conclusion than when testing using the whole sample: rejection of the null hypotheses (both forecasting ability and independence). Thus, we can conclude that observations from the bear markets during the crisis periods are not responsible for those rejections.

τ	model	S&P 500		NASDAQ 100		RUSSELL 2000	
		LR_3	LR_1	LR_3	LR_1	LR_3	LR_1
15 days	LNM	0.0000	0.0000	0.0001	0.0001	0.0000	0.0000
	Kernel	0.0000	0.0000	0.0000	0.0000	0.0000	0.0000
	Spline	0.0000	0.0000	0.0000	0.0001	0.0000	0.0000
	Sp+PT	0.0000	0.0000	0.0000	0.0001	0.0000	0.0000
30 days	LNM	0.0000	0.0000	0.0000	0.0000	0.0000	0.0000
	Kernel	0.0000	0.0000	0.0000	0.0000	0.0000	0.0000
	Spline	0.0000	0.0000	0.0000	0.0000	0.0000	0.0000
	Sp+PT	0.0000	0.0000	0.0000	0.0000	0.0000	0.0000
45 days	LNM	0.0000	0.0000	0.0000	0.0000	0.0000	0.0000
	Kernel	0.0000	0.0000	0.0000	0.0000	0.0000	0.0000
	Spline	0.0000	0.0000	0.0000	0.0000	0.0000	0.0000
	Sp+PT	0.0000	0.0000	0.0000	0.0000	0.0000	0.0000
60 days	LNM	0.0000	0.0000	0.0000	0.0000	0.0000	0.0000
	Kernel	0.0000	0.0000	0.0000	0.0000	0.0000	0.0000
	Spline	0.0000	0.0000	0.0000	0.0000	0.0000	0.0000
	Sp+PT	0.0000	0.0000	0.0000	0.0000	0.0000	0.0000

Table 1.2: **Berkowitz test p-values, excluding crisis.** The table shows the LR_3 and LR_1 Berkowitz test corresponding p-values. The test is run on the RNDs based on the S&P 500, Nasdaq 100 and Russell 2000 indexes for the different maturities (column τ) and methods used in the work: Log-Normal Mixture (LNM), kernel with pareto tails (Kernel), spline with extrapolation (Spline) and splines with pareto tails (Sp+PT). The complete sample contains observations from January 1996 until October 2015. However, in this table periods of crisis (that is the period from March 2000 until October 2002; and the period comprised between October 2007 and March 2009) have been excluded from the analysis.

Due to the nature of the data, one may suspect that the observations indeed present

some kind of auto-correlation structure, specially for longer maturities, where overlapping manifests. Should this be the case, then Berkowitz assumptions would not be accurate. In order to check whether LR_3 statistic is indeed distributed following a χ^2_3, we estimate new p-values by applying the block-bootstrap technique. This estimation is based on $5,000$ different samples. These samples are obtained by re-sampling $z_{t_i,\tau}$ (see equation (1.5)) in blocks with the same length up to reach the original data length. We calculate the LR_3 statistic over each bootstrap sample, obtaining a set of $5,000$ LR_3 values which provide a distribution of the statistic itself.

Tables 1.3 and 1.4 show the 90th and 95th percentile of the block-bootstrap distribution of the statistic. In general, for shorter maturities, these percentiles are higher than the sample Berkowitz LR_3 statistic, suggesting failure to reject the null hypothesis, which states that we can not discard RNDs as good forecasters. However, for longer maturities, we can reject the null hypothesis with confidence level of 90% for S&P 500 and Russell 2000 indexes. Same conclusions are obtained when performing the analysis on the data set without the crisis periods.

Besides Berkowitz test, the Cramer-von-Mises test is also performed in order to assess the forecasting ability of the estimated RNDs for the different methods, indexes and maturities. Results are presented in table 1.5 which shows the CM statistic calculated for all the estimated RNDs (column $\widehat{CM}$), the $95th$ percentile of the series of the block-bootstrapped CM statistics (column $BB_{95\%}$) and the proportion of $\widehat{CM}_{BB}$ statistics which are greater than the $\widehat{CM}$, as per equation (1.11).

Results show that the null hypothesis cannot be rejected, being so for all different methods, indexes and maturities. This confirms the results of the Berkowitz test with block-bootstrap. We also perform the CM test on the restricted data set which excludes the crisis periods, see table 1.6, which also concludes failure to reject the null hypothesis of good forecasters. Figure 1.4 shows the distance of the series of the integral transform

$y_{t_i,\tau}$ and the 45° line for all the different estimated RNDs for the S&P 500 index with 30 days time horizon.[9] In this figure we can appreciate that in general all methods yield to similar results, and the integral transform variables are not significantly different from the 45° line; in particular, the test shows best fit for the right tail observations for all the methods.

Tail tests based on Brier Score (see equations (1.12) and (1.13)) have been performed to test how accurate the tail fitting is based on a given probability mass. In this analysis we focus on the 5% and 10% probability mass levels in both left and right tails. Tables 1.7 to 1.9 show the observed frequency for each percentile, the Tail test statistic and the corresponding p-value for the left and right tails separately, for the different maturities, methods and indexes considered in this work. Tables 1.10 to 1.12 repeat the same analysis excluding the observations from the crisis periods.

For the left tail, which reflects the losses, in general we observe that the RNDs overestimate the frequency in which the observations fall into the extreme tail (5% and 10%), being the observed frequency lower than the predicted one. See for instance the case of the RNDs of the S&P 500 extracted with splines with pareto tails appended (SP+PT) for $\tau = 30$ days in table 1.7. For these, the observed frequency of realizations below the 5% and 10% thresholds are 2.1% and 4.5%, respectively. Similar results are obtained for all methods, indexes and maturities tested. This fact leads to a general rejection of the null hypothesis of good fitting of the left tail. Some exceptions are found to this general rejection, such as those RNDs on the Nasdaq 100 at 30 days. Once we exclude the crisis periods from the sample, the test yields to the same conclusions.

Regarding the fit of the right tail, in contrast to the left tail results, the tests for the 10% threshold conclude no rejection, in general. This result holds across maturities, indexes and methods and also for the restricted sample. For the 5% probability mass for

[9] Results for other indexes and maturities are available from the authors upon request.

the S&P 500 index there is mixed evidence of rejection while for Nasdaq 100 and Russell 2000, in general we cannot reject the null hypothesis, except for those RNDs for the Russell 2000 at 30 days, and those for the Nasdaq 100 at 60 days. These conclusions hold when we exclude observations from the crisis periods.

Regarding the tail fitting results (left tail rejection and right tail failure to reject), they are in line with figure 1.4, where the probability integral transform (PIT) is depicted. We can appreciate that the PIT is more separated from the 45° line in the left tail than in the right tail, where observations are closer to the 45° line.

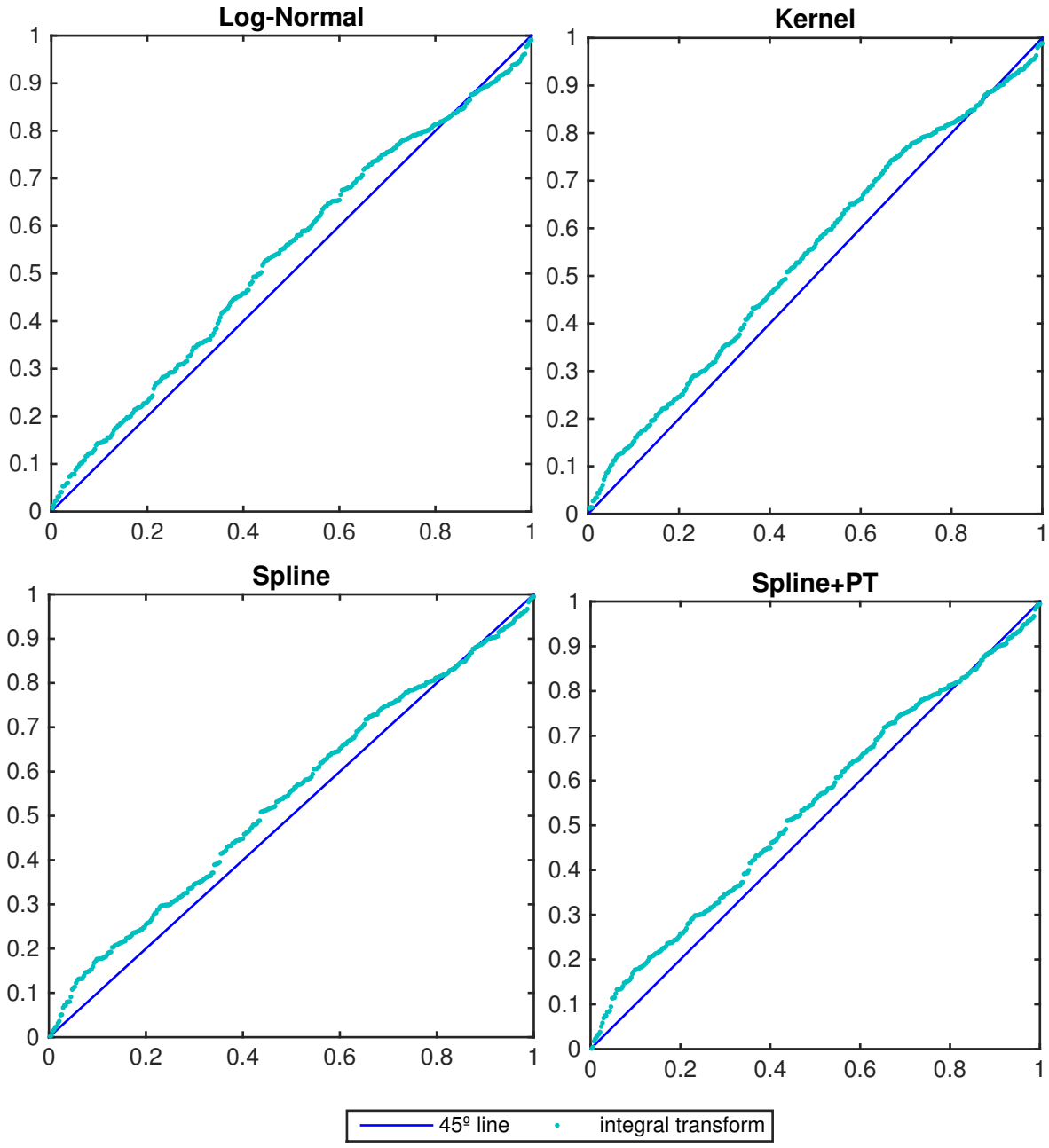

Figure 1.4: **Probability Integral Transform.** The figure compares the 45° line (Uniform(0,1) cumulative distribution) with the probability integral transform of the realized prices of the underlying given the estimated denstities using Log-Normal mixture (top-left plot), kernel with pareto tails (top-right plot), spline with extrapolation (bottom-left plot) and spline with pareto tails (bottom-right plot). Under the null hypothesis, the integral tansform variables should not be statistically different from the 45° line. Plots are for the S&P 500 index with 30 days to maturity.

τ	Model	S&P 500			NASDAQ 100			RUSSELL 2000		
$\chi^2_{3,95\%} = 7.85$		LR_3	$BB_{95\%}$	$BB_{90\%}$	LR_3	$BB_{95\%}$	$BB_{90\%}$	LR_3	$BB_{95\%}$	$BB_{90\%}$
15 days	LMN	37.089	56.791	51.106	15.734	30.353	26.225	46.798	59.388	54.462
	Kernel	40.830	61.197	55.954	18.376	33.637	28.886	48.104	62.778	57.030
	Spline	42.435	62.207	57.062	18.055	33.366	29.355	50.621	66.590	60.923
	Sp+PT	42.610	63.273	57.503	18.275	33.372	29.363	36.592	63.438	56.236
30 days	LMN	58.840	87.300	78.329	26.951	46.834	41.516	27.186	46.592	41.123
	Kernel	63.959	93.908	85.125	30.550	51.410	45.324	16.507	44.535	37.015
	Spline	58.815	90.228	81.248	27.751	49.166	42.889	26.706	47.867	42.218
	Sp+PT	59.706	90.443	82.155	28.253	49.687	43.257	15.686	44.950	36.780
45 days	LMN	74.691	88.563	82.066	47.966	60.312	55.157	33.151	41.623	37.892
	Kernel	63.792	85.459	77.744	49.855	64.174	58.565	34.284	44.908	40.445
	Spline	75.398	89.657	83.564	50.389	65.868	60.164	34.032	43.919	39.874
	Sp+PT	75.361	91.390	84.146	51.376	67.337	61.035	33.878	44.215	40.283
60 days	LMN	112.039	114.398	107.881	73.926	82.252	76.774	71.856	74.598	69.106
	Kernel	114.031	118.013	110.929	74.820	85.662	79.086	70.178	75.586	70.561
	Spline	117.228	120.290	113.944	76.999	88.106	81.938	72.294	77.799	72.927
	Sp+PT	118.137	120.406	114.285	78.316	90.811	83.791	72.180	78.176	72.974

Table 1.3: **Berkowitz test statistic and Block-Bootstrap $95th$ and $90th$ percentiles.** The table shows the LR_3 statistic of the Berkowitz test (column LR_3), as well as the $95th$ and $90th$ block-bootstrap percentiles of the statistic (columns $BB_{95\%}$ and $BB_{90\%}$). The 95% critical value of the χ^2_3 is stated at the second row of the first column. Each block-bootstrap has been computed by re-sampling variable z (equation (1.5)) in blocks over which Berkowitz test LR_3 is calculated. This gives series of 5,000 LR_3 Berkowitz statistics over which the $95th$ and $90th$ percentiles are calculated. The length of the blocks for the re-sampling is $n^{1/3}$. The analysis is calculated for different time horizons (column τ) and for different methodologies: Log-Normal Mixture (LNM), kernel with pareto tails (Kernel), splines with extrapolation (Spline) and splines with pareto tails (Sp+PT). The analysis is applied to the whole data set which goes from January 1996 until October 2015.

τ	Model	S&P 500			NASDAQ 100			RUSSELL 2000		
$\chi^2_{3,95\%} = 7.85$		LR_3	$BB_{95\%}$	$BB_{90\%}$	LR_3	$BB_{95\%}$	$BB_{90\%}$	LR_3	$BB_{95\%}$	$BB_{90\%}$
15 days	LMN	58.728	72.940	66.907	22.274	39.496	35.042	54.467	66.865	61.705
	Kernel	63.196	76.458	70.912	25.361	42.382	37.786	57.626	70.487	65.111
	Spline	64.158	77.117	72.317	24.189	41.926	37.568	58.938	73.456	67.916
	Sp+PT	64.749	78.354	73.457	24.329	43.341	38.305	57.829	73.205	67.418
30 days	LMN	65.347	94.723	85.247	37.419	58.479	51.960	44.097	59.526	54.620
	Kernel	71.704	100.386	91.721	40.078	60.522	54.363	47.158	64.341	57.969
	Spline	67.081	97.828	89.676	38.393	60.599	54.223	45.037	62.686	56.872
	Sp+PT	67.466	100.500	91.147	38.396	61.092	54.459	45.438	62.744	56.94
45 days	LMN	68.997	86.848	80.047	48.223	63.920	58.269	30.899	42.057	37.551
	Kernel	57.365	84.374	76.511	50.545	68.945	62.748	32.024	44.208	40.077
	Spline	71.066	88.472	82.772	52.255	71.565	65.284	32.826	45.046	40.886
	Sp+PT	70.657	90.921	83.505	53.000	72.416	66.267	33.284	46.050	41.673
60 days	LMN	100.802	106.240	100.591	60.959	73.298	67.178	57.443	62.628	57.735
	Kernel	103.383	109.882	103.162	63.768	78.509	72.115	55.901	62.573	57.062
	Spline	106.194	111.730	106.123	65.682	80.561	74.223	58.402	65.406	60.306
	Sp+PT	107.123	113.412	106.820	67.286	83.366	76.998	58.282	66.260	60.931

Table 1.4: **Berkowitz test statistic and Block-Bootstrap $95th$ and $90th$ percentiles, excluding crisis periods.** The table shows the LR_3 statistic of the Berkowitz test (column LR_3), as well as the $95th$ and $90th$ block-bootstrap percentiles of the statistic (columns $BB_{95\%}$ and $BB_{90\%}$). The 95% critical value of the χ^2_3 is stated at the second row of the first column. Each block-bootstrap has been computed by re-sampling variable z (equation (1.5)) in blocks over which Berkowitz test LR_3 is calculated. This gives series of 5,000 LR_3 Berkowitz statistics over which the $95th$ and $90th$ percentiles are calculated. The length of the blocks for the re-sampling is $n^{1/3}$. The analysis is calculated for different time horizons (column τ) and for different methodologies: Log-Normal Mixture (LNM), kernel with pareto tails (Kernel), splines with extrapolation (Spline) and splines with pareto tails (Sp+PT). The complete sample contains observations from January 1996 until October 2015. However, in this table periods of crisis (that is the period from March 2000 until October 2002; and the period comprised between October 2007 and March 2009) have been excluded from the analysis.

51

τ	Model	S&P 500			NASDAQ 100			RUSSELL 2000		
		$\widehat{CM}$	$BB_{95\%}$	freq.	$\widehat{CM}$	$BB_{95\%}$	freq.	$\widehat{CM}$	$BB_{95\%}$	freq.
15 days	LMN	0.272	1.400	0.705	0.243	1.299	0.654	0.135	0.667	0.950
	Kernel	6.082	8.975	0.593	4.875	7.583	0.513	3.615	5.200	0.647
	Spline	0.308	1.325	0.726	0.260	1.342	0.659	0.240	0.759	0.862
	Sp+PT	4.381	7.223	0.453	1.777	3.215	0.549	1.644	3.020	0.485
30 days	LMN	0.812	2.741	0.601	0.806	2.660	0.572	0.374	1.468	0.641
	Kernel	5.165	6.932	0.579	5.884	8.976	0.535	5.270	7.392	0.545
	Spline	0.850	2.797	0.626	0.874	2.773	0.567	0.391	1.537	0.635
	Sp+PT	2.484	5.141	0.475	1.942	3.810	0.551	1.617	2.851	0.589
45 days	LMN	0.271	1.528	0.770	0.686	2.498	0.596	0.079	0.767	0.973
	Kernel	7.625	12.856	0.519	4.405	6.846	0.620	3.597	5.868	0.516
	Spline	0.393	1.548	0.782	0.852	2.819	0.608	0.153	0.928	0.895
	Sp+PT	3.491	7.020	0.507	2.110	4.408	0.562	1.639	2.837	0.565
60 days	LMN	0.290	1.289	0.821	0.673	2.363	0.567	0.200	1.154	0.683
	Kernel	8.887	16.131	0.534	4.503	8.169	0.523	2.823	5.125	0.505
	Spline	0.454	1.504	0.767	0.891	2.628	0.568	0.414	1.539	0.652
	Sp+PT	2.508	5.822	0.563	2.764	5.430	0.532	1.420	3.051	0.543

Table 1.5: **Cramer-von-Mises test statistic and Block-Bootstrap** $95th$ **percentiles.** The table shows the Cramer-von-Mises sample statistic (column $\widehat{CM}$), the $95th$ percentile of the block-bootstrap $\widehat{CM}_{BB}$ statistics (columns $BB_{95\%}$) as well as the percentage of times that the block-bootstrap statistic, $\widehat{CM}_{BB}$, is greater than the $\widehat{CM}$ sample statistic (columns freq.). Each block-bootstrap has been computed by re-sampling variable $y_{t_i,\tau}$ (equation (1.9)) in blocks over which Cramer-von-Mises statistic is calculated. This gives series of 5,000 CM statistics over which the $95th$ percentile is calculated. The length of the blocks for the re-sampling is $n^{1/3}$. The analysis is calculated for different time horizons (column τ) and for different methodologies: Log-Normal Mixture (LNM), kernel with pareto tails (Kernel), splines with extrapolation (Spline) and splines with pareto tails (Sp+PT). The complete sample contains observations from January 1996 until October 2015.

τ	Model	S&P 500			NASDAQ 100			RUSSELL 2000		
		$\widehat{CM}$	$BB_{95\%}$	freq.	$\widehat{CM}$	$BB_{95\%}$	freq.	$\widehat{CM}$	$BB_{95\%}$	freq.
15 days	LMN	0.386	1.766	0.648	0.466	1.818	0.602	1.519	3.537	0.576
	Kernel	4.968	7.780	0.525	3.435	6.661	0.518	2.938	4.856	0.613
	Spline	0.243	0.943	0.854	0.151	0.931	0.932	0.374	1.080	0.638
	Sp+PT	4.181	7.291	0.527	1.551	3.208	0.544	1.557	3.091	0.529
30 days	LMN	1.096	3.221	0.605	1.391	3.757	0.595	0.492	1.832	0.611
	Kernel	4.125	5.970	0.580	3.687	6.349	0.545	3.315	5.103	0.578
	Spline	0.591	1.959	0.683	0.365	1.822	0.638	0.232	1.029	0.831
	Sp+PT	3.509	6.682	0.499	0.725	1.944	0.684	1.358	2.607	0.594
45 days	LMN	0.558	2.108	0.648	1.632	3.914	0.614	0.281	1.324	0.644
	Kernel	6.777	12.251	0.533	2.750	5.070	0.641	2.490	4.565	0.514
	Spline	0.491	1.406	0.779	0.643	2.279	0.616	0.115	0.736	0.940
	Sp+PT	4.600	8.815	0.558	0.613	2.122	0.666	1.564	2.790	0.609
60 days	LMN	0.615	2.018	0.630	1.519	3.539	0.580	0.396	1.599	0.612
	Kernel	8.486	15.980	0.537	3.517	7.354	0.507	2.451	4.511	0.505
	Spline	0.426	1.378	0.830	1.003	2.816	0.583	0.265	1.355	0.724
	Sp+PT	3.464	7.986	0.585	1.735	4.257	0.570	1.626	3.146	0.572

Table 1.6: **Cramer-von-Mises test statistic and Block-Bootstrap $95th$ percentiles, excluding crisis periods.** The table shows the Cramer-von-Mises sample statistic (column $\widehat{CM}$), the $95th$ percentile of the block-bootstrap $\widehat{CM}_{BB}$ statistics (columns $BB_{95\%}$) as well as the percentage of times that the block-bootstrap statistic, $\widehat{CM}_{BB}$, is greater than the $\widehat{CM}$ sample statistic (columns freq.). Each block-bootstrap has been computed by re-sampling variable $y_{t_i,\tau}$ (equation (1.9)) in blocks over which Cramer-von-Mises statistic is calculated. This gives series of 5,000 CM statistics over which the $95th$ percentile is calculated. The length of the blocks for the re-sampling is $n^{1/3}$. The analysis is calculated for different time horizons (column τ) and for different methodologies: Log-Normal Mixture (LNM), kernel with pareto tails (Kernel), splines with extrapolation (Spline) and splines with pareto tails (Sp+PT). The complete sample contains observations from January 1996 until October 2015. However, in this table periods of crisis (that is the period from March 2000 until October 2002; and the period comprised between October 2007 and March 2009) have been excluded from the analysis.

53

			Left tail						Right tail					
			5%			10%			5%			10%		
τ	Model	No. Obs.	Freq.	Stat.	p-value	Freq.	Stat.	p-value	Freq.	Stat.	p-value	Freq.	Stat.	p-value
15 days	LNM	374	0.008	-3.725	0.000	0.072	-1.793	0.073	0.029	-1.827	0.068	0.094	-0.414	0.679
	Kernel	374	0.008	-3.725	0.000	0.045	-3.516	0.000	0.027	-2.064	0.039	0.096	-0.241	0.809
	Spline	374	0.008	-3.725	0.000	0.037	-4.033	0.000	0.037	-1.115	0.265	0.094	-0.414	0.679
	Sp+PT	374	0.008	-3.725	0.000	0.037	-4.033	0.000	0.037	-1.115	0.265	0.094	-0.414	0.679
30 days	LNM	375	0.021	-2.547	0.011	0.056	-2.840	0.005	0.021	-2.547	0.011	0.080	-1.291	0.197
	Kernel	375	0.024	-2.310	0.021	0.048	-3.357	0.001	0.027	-2.073	0.038	0.093	-0.430	0.667
	Spline	375	0.024	-2.310	0.021	0.045	-3.529	0.000	0.032	-1.599	0.110	0.093	-0.430	0.667
	Sp+PT	375	0.021	-2.547	0.011	0.045	-3.529	0.000	0.032	-1.599	0.110	0.093	-0.430	0.667
45 days	LNM	319	0.016	-2.813	0.005	0.063	-2.221	0.026	0.038	-1.015	0.310	0.066	-2.034	0.042
	Kernel	319	0.022	-2.299	0.021	0.041	-3.527	0.000	0.038	-1.015	0.310	0.085	-0.914	0.360
	Spline	319	0.019	-2.556	0.011	0.025	-4.460	0.000	0.041	-0.758	0.449	0.088	-0.728	0.467
	Sp+PT	319	0.019	-2.556	0.011	0.025	-4.460	0.000	0.041	-0.758	0.449	0.088	-0.728	0.467
60 days	LNM	295	0.014	-2.872	0.004	0.047	-3.008	0.003	0.020	-2.337	0.019	0.088	-0.679	0.497
	Kernel	295	0.010	-3.139	0.002	0.041	-3.396	0.001	0.017	-2.605	0.009	0.078	-1.261	0.207
	Spline	295	0.014	-2.872	0.004	0.024	-4.367	0.000	0.027	-1.803	0.071	0.075	-1.456	0.146
	Sp+PT	295	0.010	-3.139	0.002	0.024	-4.367	0.000	0.024	-2.070	0.038	0.075	-1.456	0.146

Table 1.7: **Tail test results for the RNDs on S&P 500.** The table shows the frequency in which the actual value falls into the specific tail area (column Freq.), the statistic for the Tail test (column Stat.) as well as the corresponding p-value for RNDs extracted from the S&P 500 index option prices (column p-value). The Tail test is calculated for different time horizons (column τ) and for different methodologies: Log-Normal Mixture (LNM), kernel with pareto tails (Kernel), splines with extrapolation (Spline) and splines with pareto tails (Sp+PT). The period covered is from January 1996 to October 2015. All information is provided for a 5% and 10% probability mass levels in both tails (left and right tails).

			Left tail						Right tail					
			5%			10%			5%			10%		
τ	Model	No. Obs.	Freq.	Stat.	p-value	Freq.	Stat.	p-value	Freq.	Stat.	p-value	Freq.	Stat.	p-value
15 days	LNM	304	0.013	-2.947	0.003	0.076	-1.415	0.157	0.046	-0.316	0.752	0.115	0.879	0.379
	Kernel	304	0.010	-3.211	0.001	0.063	-2.179	0.029	0.046	-0.316	0.752	0.125	1.453	0.146
	Spline	304	0.013	-2.947	0.003	0.056	-2.562	0.010	0.049	-0.053	0.958	0.115	0.879	0.379
	Sp+PT	304	0.010	-3.211	0.001	0.053	-2.753	0.006	0.049	-0.053	0.958	0.115	0.879	0.379
30 days	LNM	307	0.026	-1.925	0.054	0.081	-1.084	0.278	0.046	-0.354	0.724	0.114	0.818	0.413
	Kernel	307	0.039	-0.877	0.380	0.072	-1.655	0.098	0.046	-0.354	0.724	0.117	1.008	0.313
	Spline	307	0.026	-1.925	0.054	0.068	-1.845	0.065	0.052	0.170	0.865	0.117	1.008	0.313
	Sp+PT	307	0.026	-1.925	0.054	0.068	-1.845	0.065	0.052	0.170	0.865	0.117	1.008	0.313
45 days	LNM	261	0.015	-2.570	0.010	0.057	-2.290	0.022	0.054	0.270	0.787	0.126	1.424	0.155
	Kernel	261	0.015	-2.570	0.010	0.031	-3.735	0.000	0.065	1.122	0.262	0.130	1.630	0.103
	Spline	261	0.015	-2.570	0.010	0.034	-3.528	0.000	0.065	1.122	0.262	0.130	1.630	0.103
	Sp+PT	261	0.015	-2.570	0.010	0.034	-3.528	0.000	0.065	1.122	0.262	0.130	1.630	0.103
60 days	LNM	233	0.009	-2.901	0.004	0.052	-2.468	0.014	0.064	1.007	0.314	0.129	1.463	0.143
	Kernel	233	0.013	-2.600	0.009	0.043	-2.904	0.004	0.077	1.909	0.056	0.146	2.337	0.019
	Spline	233	0.009	-2.901	0.004	0.034	-3.341	0.001	0.082	2.209	0.027	0.142	2.118	0.034
	Sp+PT	233	0.009	-2.901	0.004	0.030	-3.559	0.000	0.082	2.209	0.027	0.142	2.118	0.034

Table 1.8: **Tail test results for the RNDs on Nasdaq 100.** The table shows the frequency in which the actual value falls into the specific tail area (column Freq.), the statistic for the Tail test (column Stat.) as well as the corresponding p-value for RNDs extracted from the Nasdaq 100 index option prices (column p-value). The Tail test is calculated for different time horizons (column τ) and for different methodologies: Log-Normal Mixture (LNM), kernel with pareto tails (Kernel), splines with extrapolation (Spline) and splines with pareto tails (Sp+PT). The period covered is from January 1996 to October 2015. All information is provided for a 5% and 10% probability mass levels in both tails (left and right tails).

55

			Left tail						Right tail					
			5%			10%			5%			10%		
τ	Model	No. Obs.	Freq.	Stat.	p-value	Freq.	Stat.	p-value	Freq.	Stat.	p-value	Freq.	Stat.	p-value
15 days	LNM	335	0.009	-3.447	0.001	0.066	-2.094	0.036	0.015	-2.946	0.003	0.078	-1.366	0.172
	Kernel	335	0.009	-3.447	0.001	0.045	-3.369	0.001	0.015	-2.946	0.003	0.075	-1.548	0.122
	Spline	335	0.009	-3.447	0.001	0.039	-3.733	0.000	0.021	-2.444	0.015	0.078	-1.366	0.172
	Sp+PT	335	0.009	-3.447	0.001	0.039	-3.733	0.000	0.021	-2.444	0.015	0.078	-1.366	0.172
30 days	LNM	327	0.028	-1.865	0.062	0.076	-1.419	0.156	0.034	-1.357	0.175	0.083	-1.051	0.293
	Kernel	327	0.009	-3.387	0.001	0.046	-3.263	0.001	0.028	-1.865	0.062	0.089	-0.682	0.495
	Spline	327	0.018	-2.626	0.009	0.046	-3.263	0.001	0.037	-1.104	0.270	0.092	-0.498	0.619
	Sp+PT	327	0.018	-2.626	0.009	0.046	-3.263	0.001	0.037	-1.104	0.270	0.092	-0.498	0.619
45 days	LNM	262	0.023	-2.013	0.044	0.046	-2.924	0.003	0.034	-1.162	0.245	0.088	-0.659	0.510
	Kernel	262	0.019	-2.296	0.022	0.038	-3.336	0.001	0.034	-1.162	0.245	0.088	-0.659	0.510
	Spline	262	0.023	-2.013	0.044	0.038	-3.336	0.001	0.038	-0.879	0.380	0.092	-0.453	0.651
	Sp+PT	262	0.023	-2.013	0.044	0.038	-3.336	0.001	0.038	-0.879	0.380	0.092	-0.453	0.651
60 days	LNM	237	0.025	-1.744	0.081	0.068	-1.667	0.095	0.038	-0.849	0.396	0.097	-0.152	0.880
	Kernel	235	0.021	-2.020	0.043	0.055	-2.283	0.022	0.047	-0.224	0.822	0.094	-0.326	0.74
	Spline	235	0.026	-1.721	0.085	0.060	-2.066	0.039	0.047	-0.224	0.822	0.106	0.326	0.744
	Sp+PT	235	0.021	-2.020	0.043	0.060	-2.066	0.039	0.047	-0.224	0.822	0.106	0.326	0.744

Table 1.9: **Tail test results for the RNDs on Russell 2000.** The table shows the frequency in which the actual value falls into the specific tail area (column Freq.), the statistic for the Tail test (column Stat.) as well as the corresponding p-value for RNDs extracted from the Russell 2000 index option prices (column p-value). The Tail test is calculated for different time horizons (column τ) and for different methodologies: Log-Normal Mixture (LNM), kernel with pareto tails (Kernel), splines with extrapolation (Spline) and splines with pareto tails (Sp+PT). The period covered is from January 1996 to October 2015. All information is provided for a 5% and 10% probability mass levels in both tails (left and right tails).

			Left tail						Right tail					
			5%			10%			5%			10%		
τ	Model	No. Obs.	Freq.	Stat.	p-value	Freq.	Stat.	p-value	Freq.	Stat.	p-value	Freq.	Stat.	p-value
15 days	LNM	322	0.003	-3.861	0.000	0.065	-2.081	0.037	0.031	-1.560	0.119	0.102	0.149	0.882
	Kernel	322	0.006	-3.605	0.000	0.040	-3.567	0.000	0.028	-1.815	0.069	0.106	0.334	0.738
	Spline	322	0.003	-3.861	0.000	0.034	-3.938	0.000	0.040	-0.793	0.428	0.102	0.149	0.882
	Sp+PT	322	0.003	-3.861	0.000	0.034	-3.938	0.000	0.040	-0.793	0.428	0.102	0.149	0.882
30 days	LNM	326	0.009	-3.380	0.001	0.043	-3.434	0.001	0.025	-2.109	0.035	0.083	-1.034	0.301
	Kernel	326	0.015	-2.872	0.004	0.037	-3.803	0.000	0.031	-1.601	0.109	0.098	-0.111	0.912
	Spline	326	0.012	-3.126	0.002	0.034	-3.988	0.000	0.037	-1.093	0.275	0.098	-0.111	0.912
	Sp+PT	326	0.009	-3.380	0.001	0.034	-3.988	0.000	0.037	-1.093	0.275	0.098	-0.111	0.912
45 days	LNM	267	0.007	-3.187	0.001	0.056	-2.387	0.017	0.041	-0.660	0.509	0.075	-1.367	0.172
	Kernel	267	0.015	-2.625	0.009	0.037	-3.407	0.001	0.041	-0.660	0.509	0.094	-0.347	0.729
	Spline	267	0.011	-2.906	0.004	0.019	-4.427	0.000	0.045	-0.379	0.705	0.097	-0.143	0.886
	Sp+PT	267	0.011	-2.906	0.004	0.019	-4.427	0.000	0.045	-0.379	0.705	0.097	-0.143	0.886
60 days	LNM	240	0.008	-2.962	0.003	0.033	-3.443	0.001	0.025	-1.777	0.076	0.096	-0.215	0.830
	Kernel	240	0.008	-2.962	0.003	0.033	-3.443	0.001	0.021	-2.073	0.038	0.083	-0.861	0.389
	Spline	240	0.008	-2.962	0.003	0.017	-4.303	0.000	0.033	-1.185	0.236	0.083	-0.861	0.389
	Sp+PT	240	0.008	-2.962	0.003	0.017	-4.303	0.000	0.029	-1.481	0.139	0.083	-0.861	0.389

Table 1.10: **Tail test results for the RNDs on S&P 500, excluding crisis periods.** The table shows the frequency in which the actual value falls into the specific tail area (column Freq.), the statistic for the Tail test (column Stat.) as well as the corresponding p-value for RNDs extracted from the S&P 500 index option prices (column p-value). The Tail test is calculated for different time horizons (column τ) and for different methodologies: Log-Normal Mixture (LNM), kernel with pareto tails (Kernel), splines with extrapolation (Spline) and splines with pareto tails (Sp+PT). The period covered is from January 1996 to October 2015, excluding those observations corresponding to the crisis periods (first crisis period from March 2000 to October 2002, and second crisis period going from October 2007 to March 2009). All information is provided for a 5% and 10% probability mass levels in both tails (left and right tails).

57

			Left tail						Right tail					
			5%			10%			5%			10%		
τ	Model	No. Obs.	Freq.	Stat.	p-value	Freq.	Stat.	p-value	Freq.	Stat.	p-value	Freq.	Stat.	p-value
15 days	LNM	255	0.012	-2.801	0.005	0.067	-1.774	0.076	0.047	-0.215	0.829	0.118	0.939	0.348
	Kernel	255	0.012	-2.801	0.005	0.055	-2.401	0.016	0.047	-0.215	0.829	0.133	1.774	0.076
	Spline	255	0.012	-2.801	0.005	0.047	-2.818	0.005	0.051	0.072	0.943	0.122	1.148	0.251
	Sp+PT	255	0.012	-2.801	0.005	0.043	-3.027	0.002	0.051	0.072	0.943	0.122	1.148	0.251
30 days	LNM	259	0.015	-2.552	0.011	0.066	-1.843	0.065	0.050	0.014	0.989	0.124	1.263	0.206
	Kernel	259	0.031	-1.411	0.158	0.058	-2.258	0.024	0.054	0.299	0.765	0.127	1.471	0.141
	Spline	259	0.015	-2.552	0.011	0.050	-2.672	0.008	0.062	0.870	0.385	0.127	1.471	0.141
	Sp+PT	259	0.015	-2.552	0.011	0.050	-2.672	0.008	0.062	0.870	0.385	0.127	1.471	0.141
45 days	LNM	212	0.005	-3.025	0.002	0.042	-2.793	0.005	0.061	0.756	0.449	0.137	1.786	0.074
	Kernel	212	0.005	-3.025	0.002	0.019	-3.938	0.000	0.071	1.387	0.166	0.142	2.015	0.044
	Spline	212	0.005	-3.025	0.002	0.024	-3.709	0.000	0.071	1.387	0.166	0.142	2.015	0.044
	Sp+PT	212	0.005	-3.025	0.002	0.024	-3.709	0.000	0.071	1.387	0.166	0.142	2.015	0.044
60 days	LNM	183	0.011	-2.425	0.015	0.038	-2.784	0.005	0.082	1.984	0.047	0.158	2.637	0.008
	Kernel	183	0.016	-2.086	0.037	0.033	-3.031	0.002	0.098	3.002	0.003	0.180	3.622	0.000
	Spline	183	0.011	-2.425	0.015	0.022	-3.524	0.000	0.104	3.341	0.001	0.175	3.376	0.001
	Sp+PT	183	0.011	-2.425	0.015	0.022	-3.524	0.000	0.104	3.341	0.001	0.175	3.376	0.001

Table 1.11: **Tail test results for the RNDs on Nasdaq 100, excluding crisis periods.** The table shows the frequency in which the actual value falls into the specific tail area (column Freq.), the statistic for the Tail test (solumn Stat.) as well as the corresponding p-value for RNDs extracted from the Nasdaq 100 index option prices (column p-value). The Tail test is calculated for different time horizons (column τ) and for different methodologies: Log-Normal Mixture (LNM), kernel with pareto tails (Kernel), splines with extrapolation (Spline) and splines with pareto tails (Sp+PT). The period covered is from January 1996 to October 2015, excluding those observations corresponding to the crisis periods (first crisis period from March 2000 to October 2002, and second crisis period going from October 2007 to March 2009). All information is provided for a 5% and 10% probability mass levels in both tails (left and right tails).

			Left tail						Right tail					
			5%			10%			5%			10%		
τ	Model	No. Obs.	Freq.	Stat.	p-value	Freq.	Stat.	p-value	Freq.	Stat.	p-value	Freq.	Stat.	p-value
15 days	LNM	286	0.003	-3.608	0.000	0.059	-2.286	0.022	0.017	-2.523	0.012	0.087	-0.710	0.478
	Kernel	286	0.003	-3.608	0.000	0.038	-3.469	0.001	0.017	-2.523	0.012	0.087	-0.710	0.478
	Spline	286	0.003	-3.608	0.000	0.035	-3.666	0.000	0.024	-1.981	0.048	0.087	-0.710	0.478
	Sp+PT	286	0.003	-3.608	0.000	0.035	-3.666	0.000	0.024	-1.981	0.048	0.087	-0.710	0.478
30 days	LNM	279	0.018	-2.459	0.014	0.065	-1.976	0.048	0.039	-0.810	0.418	0.093	-0.379	0.705
	Kernel	279	0.004	-3.557	0.000	0.036	-3.572	0.000	0.032	-1.360	0.174	0.100	0.020	0.984
	Spline	279	0.011	-3.008	0.003	0.032	-3.772	0.000	0.043	-0.536	0.592	0.104	0.220	0.826
	Sp+PT	279	0.011	-3.008	0.003	0.032	-3.772	0.000	0.043	-0.536	0.592	0.104	0.220	0.826
45 days	LNM	213	0.009	-2.719	0.007	0.028	-3.494	0.000	0.042	-0.519	0.604	0.103	0.160	0.873
	Kernel	213	0.009	-2.719	0.007	0.028	-3.494	0.000	0.042	-0.519	0.604	0.099	-0.069	0.94
	Spline	213	0.009	-2.719	0.007	0.028	-3.494	0.000	0.047	-0.204	0.838	0.103	0.160	0.873
	Sp+PT	213	0.009	-2.719	0.007	0.028	-3.494	0.000	0.047	-0.204	0.838	0.103	0.160	0.873
60 days	LNM	187	0.016	-2.131	0.033	0.053	-2.121	0.034	0.048	-0.117	0.907	0.118	0.804	0.421
	Kernel	185	0.016	-2.108	0.035	0.043	-2.573	0.010	0.059	0.590	0.555	0.114	0.613	0.540
	Spline	185	0.016	-2.108	0.035	0.049	-2.328	0.020	0.059	0.590	0.555	0.124	1.103	0.270
	Sp+PT	185	0.016	-2.108	0.035	0.049	-2.328	0.020	0.059	0.590	0.555	0.124	1.103	0.270

Table 1.12: **Tail test results for the RNDs on Russell 2000, excluding crisis periods.** The table shows the frequency in which the actual value falls into the specific tail area (column Freq.), the statistic for the Tail test (column Stat.) as well as the corresponding p-value for RNDs extracted from the Russell 2000 index option prices (column p-value). The Tail test is calculated for different time horizons (column τ) and for different methodologies: Log-Normal Mixture (LNM), kernel with pareto tails (Kernel), splines with extrapolation (Spline) and splines with pareto tails (Sp+PT). The period covered is from January 1996 to October 2015, excluding those observations corresponding to the crisis periods (first crisis period from March 2000 to October 2002, and second crisis period going from October 2007 to March 2009). All information is provided for a 5% and 10% probability mass levels in both tails (left and right tails).

59

1.5 Conclusions

RNDs are of great importance for portfolio and risk managers. Many studies have focused on their ability of forecasting future underlying realizations. In order to check the latter, previous literature has relied on Berkowitz test and concluded that RNDs do lack of such ability. Nevertheless, Berkowitz test is based on the assumption that the probability integral transform is $i.i.d.N(0,1)$. In this work we propose to run block-bootstrap re-sampling in order to check the asymptotic distribution of the Berkowitz LR_3 statistic when the assumptions are violated. In order to reinforce the previous, Cramer-von-Mises test is also performed.

Using a sample from 1996 until 2015 for three US index options (S&P 500, Nasdaq 100 and Russell 2000) and different numerical procedures to extract the RNDs from option prices, Berkowitz test rejects the forecasting ability of RNDs. This result holds when removing observations from crisis periods. However, when we calculate 5,000 block-bootstrap statistics, results suggest that Berkowitz assumptions do not hold for our data set since the statistic is not distributed following a χ^2_3, and what is more, block-bootstrap test fails to reject RNDs as good forecasters. This conclusion is sustained by Cramer-von-Mises test, which yields to the same results.

Regarding the fit of the tails, the Tail test suggests a general rejection for the left tail fit, due to a systematic overweighting of the probability mass (observed frequency in the left tail is lower than the estimated one). On the other hand, the fit of the right tail cannot be rejected. These results hold when excluding those observations from the crisis periods.

Chapter 2

When the (expected) loss quantiles go marching in

Connectedness across international financial markets, specially during turbulent periods, has been a recurrent topic in financial research. In this chapter we propose a novel approach to explore how expected tail risk is transmitted between three international developed financial markets. We analyze the transmission of changes in the (loss) quantiles of the option-implied distributions of three representative indexes of the main developed economic areas: United States, Eurozone and Japan, proxied by the S&P 500, EursoStoxx 50 and Nikkei 225 indexes, respectively.

The main contribution of our work is the use of forward-looking (expected) information implied in option prices, instead of historical returns (backward-looking). After controlling for global risks, measured by the VIX index, our results confirm the existence of transmission from S&P 500 risk-neutral loss quantiles to both EuroStoxx 50 and Nikkei 225 option-implied quantiles, being the transmission in the opposite direction not significant. This result holds for different quantiles in the left tail and different maturities

(horizons).

First studies, such as Eun and Shim (1989), focus on the transmission of shocks in returns from one market to other markets. However, the effects of transmission seemed to be stronger through the second moment. Therefore, literature started studying the transmission effect in volatility which was mainly modeled using the well-known GARCH models, by Bollerslev (1986b). Some representatives are the works of Engle et al. (1990) in monetary markets or Kearney and Patton (2000), Ewing and Malik (2005), and Hassan and Malik (2007) who use the BEKK methodology of Engle and Kroner (1995). Other authors also demonstrate transmission on higher order moments, such as Hong et al. (2009) who use a generalized Student-t, or Hashmi and Tay (2012) who use a skewed-t distribution to analyze the transmission effects in both skewness and kurtosis.

A strand of the literature such as Poon and Granger (2003), Poon and Granger (2005) and Bollerslev and Zhou (2006) show that implied volatility is a better choice in terms of forecasting and is at the same time a better measure of volatility and uncertainty in stock markets. Thus, given the superior informational content of implied volatility, Nikkinen and Sahlstöm (2004), Siropoulos and Fassas (2013), Kenourgios (2014) and Thakolsri et al. (2016) use implied volatilities not only for forecasting purposes, but also to analyze the integration of the markets and the transmission of shocks across countries.

Beyond focusing on implied volatility only, some works confirm the importance of the information embedded in the tails of the option-implied risk-neutral distributions. Works such as Wang and Yen (2017) and Leiss and Nax (2018) show that option-implied risk measures can predict both future returns and large return downturns, respectively. In addition, Almeida et al. (2017) and Massacci (2017) prove the link between the tail risk and macroeconomics.

In consequence, we consider it is worth analyzing the transmission of the option-

implied risk-neutral loss quantiles across international markets. Extraction of the Risk-Neutral distributions (RND) from option prices does not only provide us with a forward-looking measure, but it also allows us to analyze different time horizons. Therefore, by looking at implied measures allows us to have a better understanding of the market expectations and future uncertainty for the desired time horizon. Understanding the linkages of the probability of occurrence of certain level of losses across markets can assist investors, risk managers and policy makers in terms of forecasting, portfolio diversification as well as in managing potential risks and anticipation of adverse shocks.

The rest of the chapter is organized as follows, section 2.1 presents the methodology used to extract the RNDs and the econometric model. Section 2.2 contains a description of the data used. Section 2.3 presents the results and finally section 2.4 concludes.

2.1 Methodology

In order to study the transmission effect in the quantiles of the different markets, this study is based on two main steps. First, we need to obtain the daily RNDs from option prices in order to be able to calculate the different quantiles. Afterwards, the dynamics between the different markets are designed by constructing a Structural-VAR model (S-VAR heretofore). Once this is done, we perform impulse-response and variance decomposition analyses, which will provide us with information about the impact of shocks in one market to the others.

2.1.1 Extraction of the Risk-Neutral Distributions

For the extraction of the RND we use a non-parametric approach based on the technique of Breeden and Litzenberger (1978), which allows us to obtain the whole state

density from observed option prices. This is done by simply taking the second partial derivative of the option pricing function with respect to the strike price. Therefore, we can write the RND of the underlying asset at expiration, $f(S_T)$, as

$$f\left(S_T\right) = \ e^{r(\tau)} \frac{\partial^2 C\left(S_t, X, T, t\right)}{\partial X^2} \mid_{X=S_T} \tag{2.1}$$

where r is the risk-free rate, $C\left(S_t, X, T, t\right)$ is the European call price function, S_t is the current value of the underlying asset, X is the strike price of the option, T is the expiration date, t is the current date and $\tau = T - t$ is the time to expiration of the option.

In order to be able to extract the RND, equation (2.1) requires a continuum of strike prices encompassing all possible future payoffs. However, because options trade at discrete prices, we need to interpolate across strike prices. Malz (1997) proposes to interpolate on an implied volatility (iv) - delta (Δ) space instead of on a price - strike price space. The convenience of this is that away-from-the-money options are brought more closely together. Besides, being Δ bounded between 0 and 1 has some advantages over the strike price space which is theoretically unbounded.

Once the interpolation is done, implied volatilities and Δs are translated back into prices and strike prices in order to extract the RND by applying Breeden-Litzenberger technique.[10] Nevertheless, due to the availability of the data, we are only capable to extract that part of the RND which is within the range of traded strikes (Δs). Extreme observations, which form the tail of the distribution, are scarce or even non-existent, therefore the tail area needs to be approximated. Following the lines of Bliss and Panigirtzoglou (2004), we add two pseudo-points at both ends of the observed range of Δs and their corresponding implied volatility is assumed to be the same as the closest observed Δ. Once these points are added, we interpolate within the range by calculating a cubic smoothing

[10] Black-Scholes and Merton formula (BSM) is used to translate prices into implied volatilities and strike prices into deltas, reverting them back to prices and strike prices after the interpolation is done. Note that BSM formula is used as a mere tool and we are not stating that such formula correctly prices the options.

spline of the form,

$$S_\lambda = \sum_{i=1}^{n} m_i (Y_i - g(\Delta_i, \theta))^2 + \lambda \int_{-\infty}^{+\infty} p''(x;\theta)^2 dx \tag{2.2}$$

where m_i is a weighting value of the squared error, Y_i is the implied volatility (iv) of the ith option observation, $g(\Delta_i, \theta)$ is the fitted iv which is a function of delta, Δ_i, and a set of spline parameters, θ; $g(\Delta_i, \theta)$ is any curve which can have any form and whose coefficients are estimated by least-squares. λ is the smoothing parameter, which takes value 0.9, and $p(x;\theta)^2$ is the smoothing spline.[11]

2.1.2 Econometric Methods

Once the RNDs are fitted, we have information about the whole distribution. Therefore, in order to analyze the transmission in the risk-neutral loss quantiles of the different markets, we compute the 5%, 10%, 15%, 20% and 25% quantiles of these option-implied risk-neutral distributions.

In order to analyze the impact of shocks in the risk-neutral expected loss quantiles of a certain market to the loss quantiles of foreign markets, we model each of the quantiles using a S-VAR(n) model. The use of a S-VAR(n) process is needed because, as we will mention later, we have contemporaneous relationships between some of the markets. In order to isolate specific quantile shocks from general quantile changes due to variations in the aggregate volatility, we add the CBOE VIX volatility index (VIX heretofore) as exogenous variable in our S-VAR(n) model. This index is considered the main driver of global volatility based on options on the S&P 500 index and is at the same time considered as reference of the market volatility.

[11] Bliss and Panigirtzoglou (2004) propose a value of 0.99 for parameter λ; however, in this analysis we assign to this parameter the value 0.9 in order to get a smoother fit.

The analysis has also been performed without considering the VIX index as exogenous variable in our S-VAR(n) model; however, the results show that when the VIX is considered the Hannan-Quinn information criteria (HQIC henceforth), as per Hannan and Quinn (1979), improves. Table 2.1 shows the coefficients and standard errors in parenthesis for the VIX index series included in the S-VAR(n) process as exogenous variable. All coefficients are significant with p-values lower than 0.001 for all cases.

In this particular analysis, we are challenged with the non-synchronicity in trading hours for the different markets due to the time zone difference. That is, on day t the European market closes after the Japanese market does; therefore, the closing prices of the Japanese market may impact the contemporaneous closing prices of the European market, while the reverse is not possible. The same happens for the US market. Since this is the last market to close, closing prices on day t may incorporate the information of the contemporaneous closing prices in Europe and Japan. On the other hand, the Japanese market will only be affected by the lags of the European and the US markets, since at the closing Japanese investors only have information about the closing of the previous day of the European and the US market. Furthermore, not only the trading hours differ between countries, but also the trading days may be different from one country to another due to various reasons such as different national bank holidays or unexpected events, among others.

In order to account for contemporaneous relationships between the different markets, we consider a S-VAR(n) process which accounts for both lagged as well as contemporaneous dynamics between the variables.

$$B_0 \begin{pmatrix} JP_t^\alpha \\ EU_t^\alpha \\ US_t^\alpha \end{pmatrix} = \begin{pmatrix} \gamma_{JP} \\ \gamma_{EU} \\ \gamma_{US} \end{pmatrix} + \sum_{i=1}^{n} B_i \begin{pmatrix} JP_{t-i}^\alpha \\ EU_{t-i}^\alpha \\ US_{t-i}^\alpha \end{pmatrix} + C \cdot VIX_t + \begin{pmatrix} \epsilon_{JP,t} \\ \epsilon_{EU,t} \\ \epsilon_{US,t} \end{pmatrix} \tag{2.3}$$

τ	market	quantile				
		5%	10%	15%	20%	25%
30	JP	-0.034	-0.025	-0.017	-0.011	-0.006
		(0.003)	(0.002)	(0.001)	(0.001)	(0.001)
	EU	-0.070	-0.054	-0.042	-0.031	-0.022
		(0.002)	(0.001)	(0.001)	(0.001)	(0.001)
	US	-0.103	-0.079	-0.059	-0.044	-0.031
		(0.001)	(0.001)	(0.001)	(0.001)	(0.001)
60	JP	-0.031	-0.023	-0.016	-0.010	-0.006
		(0.002)	(0.002)	(0.002)	(0.001)	(0.002)
	EU	-0.073	-0.058	-0.047	-0.037	-0.028
		(0.002)	(0.001)	(0.001)	(0.001)	(0.001)
	US	-0.108	-0.084	-0.065	-0.049	-0.035
		(0.001)	(0.001)	(0.001)	(0.001)	(0.001)
91	JP	-0.029	-0.020	-0.013	-0.008	-0.003
		(0.003)	(0.002)	(0.002)	(0.002)	(0.002)
	EU	-0.073	-0.060	-0.050	-0.039	-0.031
		(0.002)	(0.002)	(0.002)	(0.002)	(0.002)
	US	-0.109	-0.086	-0.067	-0.052	-0.037
		(0.001)	(0.001)	(0.001)	(0.001)	(0.001)

Table 2.1: **Coefficients of the VIX index series included as exogenous variable in the S-VAR(n) analaysis.** The table shows the significant coefficients of the VIX index series included in the S-VAR(n) model as exogenous variable. Results are provided for the different markets under study: Nikkei 225 (JP), EuroStoxx 50 (EU) and S&P 500 (US). Standard errors are shown in parenthesis. Coefficients for the VIX are negative and statistically significant for the different maturities ($\tau = 30,\ 60,\ 91$ days) and different left-tail quantiles (5%, 10%, 15%, 20% and 25%).

being JP^{α}, EU^{α} and US^{α} the series of changes of the α%-quantile being modeled corresponding to the Nikkei 225, the EuroStoxx 50 and the S&P 500 indexes, respectively. The subscript t indicates each day in the sample for the period considered, γ is the constant term, B_0 contains the contemporaneous coefficients and B_i are the matrices of coefficients measuring the effect of the lagged variables $(t-i)$ to the variable being analyzed. VIX is the change in the CBOE VIX index and C its coefficient. Finally, $\epsilon_{i,t}$ is the error term for each market JP, EU and US. In order to determine the optimal number of lags (n) we rely on the HQIC.

The S-VAR(n) model in equation (2.3) can be written as,

$$B_0 y_t = \gamma + B_1 y_{t-1} + \ldots + B_n y_{t-n} + VIX + \epsilon_t \tag{2.4}$$

This expression can be presented in reduced form,

$$y_t = A_\gamma + A_1 y_{t-1} + \ldots + A_n y_{t-n} + V + w_t \tag{2.5}$$

where $A_\gamma = \gamma \cdot B_0^{-1}$, $A_i = B_0^{-1} B_i$, $i = 1, 2..., n$, $V = B_0^{-1} V$ and $w_t = B_0^{-1} \epsilon_t$.

Therefore, knowledge of B_0^{-1} (hence B_0) enables us to recover γ, B_i, V and w_t, but the main issue now is how to recover B_0. One popular way is by using recursively identified models, which is based on an orthogonalization of the reduced-form errors. However, in order to be able to apply this methodology, we need to define a matrix P, such as $PP' = \Sigma_w$, where Σ_w is the covariance matrix of the reduced-form innovations. Matrix P needs to be lower triangular in order to apply Cholesky decomposition of Σ_w. It follows that from $\Sigma_w = B_0^{-1} B_0^{-1'}$ that $B_0^{-1} = P$.

Application of this method will be accurate as long as our data guarantees that matrix

P is lower-triangular.[12] The different closing times of the three markets do support such restrictions. Specifically, our matrix B_0 of contemporaneous effects is lower-triangular as follows,

$$B_0 = \begin{pmatrix} \beta_{JP}^{JP} & 0 & 0 \\ \beta_{EU}^{JP} & \beta_{EU}^{EU} & 0 \\ \beta_{US}^{JP} & \beta_{US}^{EU} & \beta_{US}^{US} \end{pmatrix} \tag{2.6}$$

where β_i^j measures the contemporaneous impact of quantile changes from market j in the quantile changes of market i. β_{EU}^{JP} and β_{US}^{JP} measure the impact of Japan closing prices in the Eurozone and US, respectively; and β_{US}^{EU} collects the impact of the Eurozone closing prices in the US. However, the Japanese market does not have contemporanous information of neither the US nor the European market, and the European market does not know the contemporaneous closing prices from the US market, being the relations between these, zero.

Alternatively to the S-VAR(n), the non-synchronicity problem can be tackled by transforming the daily series to lower-frequency series such as two-days or weekly. See for instance Yang and Zhou (2017) who calculate two-days rolling average series. However, one drawback of using lower-frequency data is the reduction of the sample size. In order to check for robustness, in addition to the S-VAR(n) process we have also fitted a VAR(n) model using weekly series which have been calculated by averaging the daily observations for each week. By doing it this way, we avoid both the issue of contemporaneous effects and the non-matching trading days due to national bank holidays, etc. On the other hand, our sample size reduces from 2,678 to 596 observations. Nonetheless, results for both analyses yield to the same qualitative results. Our VAR(n) model also includes the

[12] A deep analysis of Structural-VAR(n) can be found in Kilian and Lutkepohl (2017).

VIX as exogenous variable and is defined as,

$$\begin{pmatrix} JP_t^\alpha \\ EU_t^\alpha \\ US_t^\alpha \end{pmatrix} = \begin{pmatrix} \gamma_{JP} \\ \gamma_{EU} \\ \gamma_{US} \end{pmatrix} + \sum_{i=1}^{n} B_i \begin{pmatrix} JP_{t-i}^\alpha \\ EU_{t-i}^\alpha \\ US_{t-i}^\alpha \end{pmatrix} + C \cdot VIX_t + \begin{pmatrix} \epsilon_{JP,t} \\ \epsilon_{EU,t} \\ \epsilon_{US,t} \end{pmatrix} \tag{2.7}$$

Hovewer, one recognized problem about fitting a VAR(n) or S-VAR(n) model is that the coefficients have no straightforward identification, as mentioned by Brooks (2008). In order to alleviate this problem, we construct the Granger causality test, see Granger (1969). Nevertheless, as mentioned in Brooks (2008), this test only captures information about the correlation between the current value of one variable and the past values of all the variables, but it does not provide information of whether movements of one variable cause movements to another variable, nor the sign of the effects.

Hence, in order to see the response of the quantile changes in one market due to shocks in quantiles from other markets, we rely on the generalized impulse-response analysis as per Pesaran and Shin (1998).[13] Impulse-response functions trace the effect that one unit shock in one of the foreign markets provokes to the domestic market being analyzed (that is, S-VAR(n)/VAR(n) dependent variable). They also provide information about the sign and significance of the response, as well as the persistence of the effect in time through the dynamics of the S-VAR(n)/VAR(n) model. As per Pesaran and Shin (1998), the generalized impulse-response functions are defined as,

$$IRF_i(n) = \sigma_{jj}^{-1/2} B_n \Sigma e_j \tag{2.8}$$

being σ_{jj} the variance of market j, B_n the coefficient matrices where $n = 0, 1, 2, ...$; Σ the covariances of the innovations term and e_j is the vector of shocks taking value 1 for the

[13]The generalized impulse-response analysis is preferred to orthogonalized impulse-response analysis since its results do not depend on the ordering of the variables, being not the case for the orthogonalized.

variable being shocked and 0 elsewhere.

Additionally, the variance decomposition analysis is used in order to obtain information about the proportion of the variance of a market (i) caused by their own shocks as well as the proportion due to other market's shocks (j). The variance decomposition analysis is defined as,

$$VD_{ij}(n) = \frac{\sigma_{jj}^{-1} \sum_{l=0}^{n} \left(e_i' B_l \Sigma e_j\right)^2}{\sum_{l=0}^{n} e_i' B_l \Sigma B_l' e_i} \tag{2.9}$$

2.2 The Data

The period covered in this analysis is from May 2004 to September 2015. We analyze the S&P 500, the EuroStoxx 50 and the Nikkei 225 indexes as representatives of the US, Eurozone and Japanese markets, respectively. We include a volatility index as exogenous variable represented by the CBOE VIX volatility index, which is constructed on S&P 500 index options. Since it was launched it has been considered the most representative measure for investor sentiment and global market volatility.

To obtain option-implied RNDs for the S&P 500, the EuroStoxx 50 and the Nikkei 225, we use the volatility surface files from IVY OptionMetrics database. These files contain daily information of the implied volatilities for different maturities and deltas (strikes) for calls and puts separately. We use implied volatility surfaces obtained from puts since they are more traded than calls, and the put deltas (domain) are passed to the corresponding call deltas. In this work we focus on the three shortest maturities available in the database: 30, 60 and 91 days. The risk-free rate proxy is considered to be the zero-coupon yield provided by OptionMetrics.[14]

[14]Bliss and Panigirtzoglou (2004) document that the risk-free rate used has little impact on the overall results. They state that for a one-month period, a 100 basis points variation in the risk-free rate is translated in a two basis points change in the measured implied volatility. This variation goes up to 5 basis points change for a six-month period.

As mentioned in section 2.1.1, in order to extract the RNDs we need a continuum of options-implied volatility (iv) - delta (Δ) pairs. The volatility surface files already provide us with these $iv - \Delta$ pairs, in which the Δ domain goes from 0.2 to 0.8 spaced in intervals of 0.05 (13 points) with their corresponding implied volatilities. By restricting the range of Δs we are missing some probability in the tails, which are of special interest in this work. As mentioned before, in order to overcome this issue, we add two pseudo-points at both ends of our delta range spaced also 0.05, which is done following Bliss and Panigirtzoglou (2004). Afterwards, we assign to each pseudo-point the implied volatility of the closest observed delta. This way, we increase the number of Δ/iv points from 13 to 17 and so we are forcing the estimated spline to be flat at the extremes. Once this is done, we interpolate within the range by using a cubic smoothing spline.

In this analysis we use daily data which forms a sample containing 2,678 observations. However, we also use weekly data as an alternative way to deal with the non-synchronicity problem of the daily data. Weekly data is based on the calculation of weekly averages of the daily quantiles and volatility index observations. This leaves us with a sample formed by 596 weeks to perform the analysis. One of the drawbacks about using weekly data is the loss of the sample length; however, in our case we still have a fairly large sample. Anyways, the use of weekly data in this analysis is used to check for robustness only.

2.3 Results

Figure 2.1 exhibits the time series of the daily (top plot) and weekly (bottom plot) 15%-quantiles for a time horizon of 60 days for all markets considered.[15] In general, for both the daily and the weekly series plots, we can observe a common behavior in the three markets, although Nikkei 225 (JP) quantiles reveals more pronounced idiosyncratic

[15]Plots for different quantiles and maturities are not shown because they present a very similar pattern.

spikes. In order to ensure all series are stationary, we apply the augmented Dickey-Fuller test as per Dickey and Fuller (1979). The test concludes stationarity for all series on first differences.

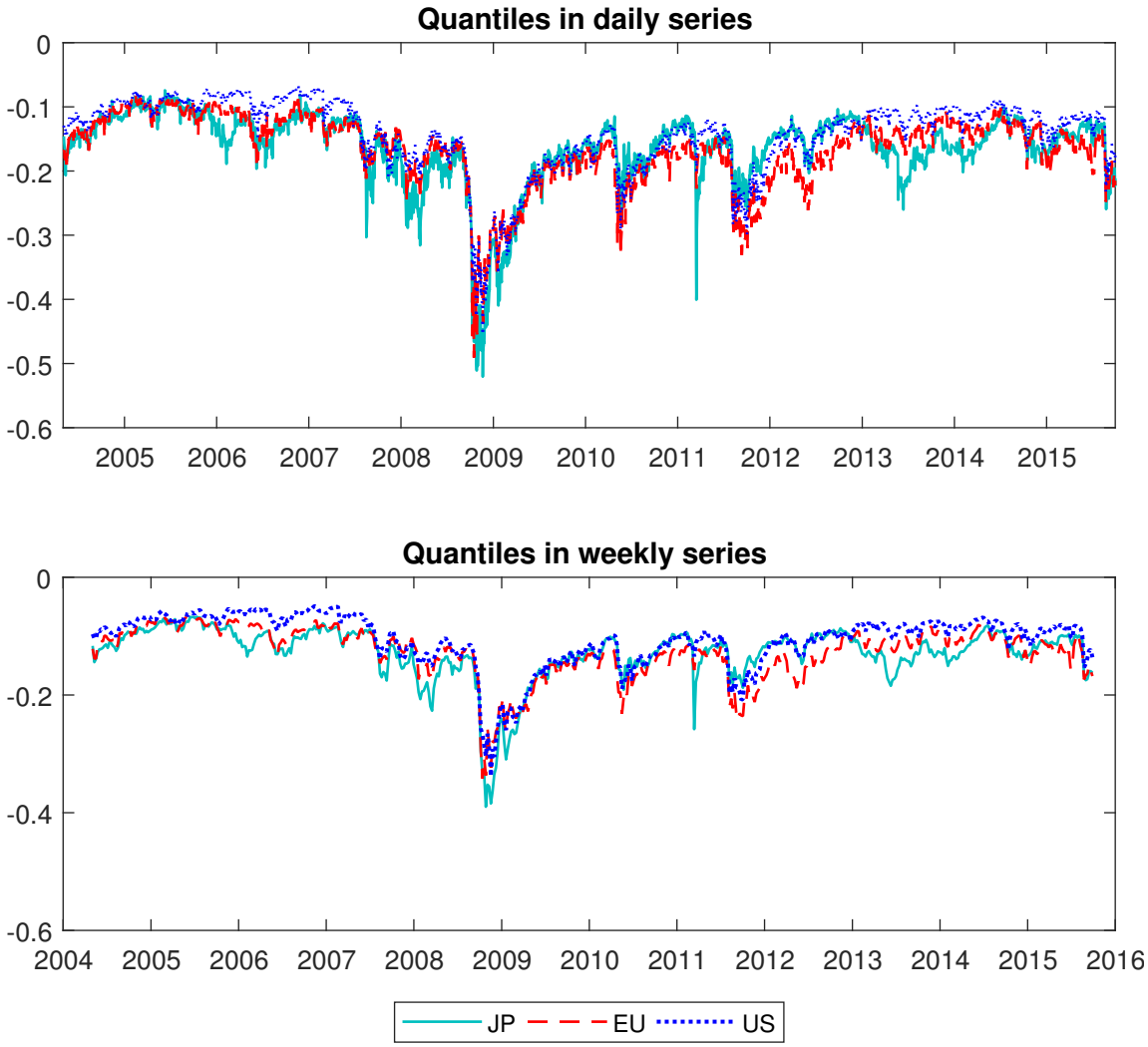

Figure 2.1: **Risk-neutral option-implied 15%-quantile changes for 60 days horizon.** The figure shows the time series of the daily (top plot) and weekly (bottom plot) 15%-quantiles with 60 days maturity for all the markets considered: Nikkei 225 (JP), EuroStoxx 50 (EU) and S&P 500 (US). The weekly quantiles have been calculated as the weekly average of daily observations.

Table 2.2 collects the average correlation between the series of quantile changes of the different underlyings together with the VIX index. In brackets we show the minimum and

	US	EU	JP	VIX
US	1			
EU	0.930 (0.879 ; 0.959)	1		
JP	0.849 (0.807 ; 0.876)	0.794 (0.724 ; 0.845)	1	
VIX	-0.972 (-0.994 ; -0.942)	-0.910 (-0.937 ; -0.850)	-0.862 (-0.894 ; -0.815)	1

Table 2.2: **Average Correlation of Quantile Differences.** The table shows the average correlation of quantile changes between different markets: S&P 500 (US), EuroStoxx 50 (EU) and Nikkei 225 (JP), as well as the VIX index. In parentheses we show the minimum and maximum correlation. The average, minimum and maximum values have been calculated considering different maturities ($\tau = 30,\ 60,\ 91$ days) and different quantiles in the left tail (5%, 10%, 15%, 20% and 25% quantiles).

maximum correlation.[16] In general, we observe that the contemporaneous correlation between S&P 500 and EuroStoxx 50 quantile differences is higher than correlations involving Nikkei 225 quantiles. Nonetheless, the average correlations are fairly high (averages above 0.7). The correlations between the different series and the VIX changes are the highest and negative for all cases, as expected. Among them, the correlation between the VIX and Nikkei 225 quantiles are the weakest.

To choose the optimal number of lags to include in each S-VAR(n) (VAR(n)) model, we rely on HQIC. Optimal lag lengths differ across the different quantiles and maturities considered, as well as for the type of data used (daily or weekly series). Table 2.3 summarizes the optimal number of lags used for each of the quantiles analysis individually using both daily as well as weekly data. We can see that for the case in which daily series are used, the optimal number of lags is 4 for all the model specifications under consideration.

[16] For each pair, the average, minimum and maximum correlations have been calculated using the different maturities and α%- quantiles considered in this work.

	quantile				
daily series	5%	10%	15%	20%	25%
30 days	4	4	4	4	4
60 days	4	4	4	4	4
90 days	4	4	4	4	4
weekly series					
30 days	5	5	5	6	7
60 days	5	5	5	5	6
90 days	5	5	5	5	6

Table 2.3: **Optimal lags as per HQIC.** The table shows the optimal number of lags to include in the VAR(n) systems as per the Hannan and Quinn Information Criterion (HQIC) for each of the quantiles analyzed (5%, 10%, 15%, 20% and 25%).

Granger causality is checked and results are presented on table 2.4. In general, we observe that the S&P 500 option-implied risk-neutral quantile changes Granger cause changes in the same quantile of the Nikkei 225, but it only Granger cause the EuroStoxx 50 risk-neutral loss quantile changes for the most central quantiles. We also see that both the EuroStoxx 50 and the Nikkei 225 loss quantiles Granger cause the S&P 500 ones. Nevertheless, as mentioned before, this test is not the best option to check on the transmission of the effects, nor the strength or the sign.

Information about the propagation of the effects caused by an unit shock in one market to the other markets is provided by the impulse-response analyses. These analyses also provide us with information about the persistence of this effect in time, until it dies away. The analysis has been performed for all different quantiles (5%, 10%, 15%, 20% and 25%) and maturities (30, 60 and 91 days), using both daily and weekly observations. Results are very similar for all of them yielding to the same conclusions.

Figure 2.2 shows the impulse-response results for the 15% risk-neutral quantile changes with 60 days to maturity calculated using daily data (S-VAR(n)), as a representative example. In general, results suggest that changes in the S&P 500 quantiles impact the other

$\tau = 30$ days	5% quantile	10% quantile	15% quantile	20% quantile	25% quantile
JP causes EU	Y	Y	Y	X	X
JP causes US	Y	Y	Y	Y	Y
EU causes JP	Y	Y	Y	Y	Y
EU causes US	Y	Y	Y	Y	Y
US causes EU	Y	X	Y	Y	Y
US causes JP	Y	Y	Y	Y	Y
$\tau = 60$ days					
JP causes EU	Y	X	X	X	Y
JP causes US	Y	Y	Y	Y	Y
EU causes JP	Y	X	X	Y	Y
EU causes US	Y	Y	Y	Y	Y
US causes EU	X	X	X	Y	Y
US causes JP	Y	Y	Y	Y	Y
$\tau = 90$ days					
JP causes EU	X	X	Y	Y	Y
JP causes US	Y	Y	Y	Y	Y
EU causes JP	X	X	Y	Y	Y
EU causes US	Y	Y	Y	Y	Y
US causes EU	Y	X	Y	Y	Y
US causes JP	Y	Y	Y	Y	Y

Table 2.4: **Granger causality test results.** The table shows the Granger causality relations between the different markets for all the quantiles analyzed with maturities 30, 60 and 91 days. Relationships between markets are established in the first column. For each quantile, cells with Y show Granger causality from one market to the other; however, those pairs of markets with an X, Granger causality has been rejected at 5% level. JP represents the Japanese market (Nikkei 225), EU the European (EuroStoxx 50) and US the US market (S&P 500).

markets. One unit shock in the S&P 500 quantiles is transmitted to both Nikkei 225 and EuroStoxx 50 quantiles, being these effects very similar in trend, in both Japanese and European markets but stronger in magnitude for the former. Impulse-response analyses show that the transmission between Nikkei 225 and EuroStoxx 50 quantiles as well as impulses from these two markets to the S&P 500 quantiles are very small and not significant. Results hold for the analysis performed using weekly data (VAR(n)) as we can see in figure 2.3, which shows the corresponding impulse-response function representation for the 15%-quantile changes with 60 days horizon. Since only shocks in the S&P 500 quantiles are significantly transmitted to the other foreign markets considered, only results of the effects caused by shocks in the S&P 500 quantile changes will be reported from here onwards.

Figure 2.4 (for daily data) and 2.5 (for weekly data), show a comparison between the impact of a shock in the S&P 500 risk-neutral implied quantiles to the Nikkei 225 (top plot) and the EuroStoxx 50 (bottom plot) indexes for the different quantiles for a 60 days horizon. Graphs show no significant differences of a unit shock across quantiles, therefore we can conclude that the level of the quantile being checked has no effect on the magnitude of the impact that a shock in the US quantiles has on the Japanese and the European quantiles.

On the other hand, the effects of option maturity in the impulse-response functions can be appreciated in figures 2.6 and 2.7. These figures show how the 15%-quantiles of the Japanese (top plots) and European (bottom plots) quantiles respond to a shock in the US quantiles for different maturities using daily and weekly data, respectively. These figures show a bigger impact in the change of quantiles for the longest horizons (60 and 91 days), being the impact softer for the shortest maturity (30 days). Therefore, there are differences in the magnitude of the impact across different maturities for both the Japanese and the European quantiles.

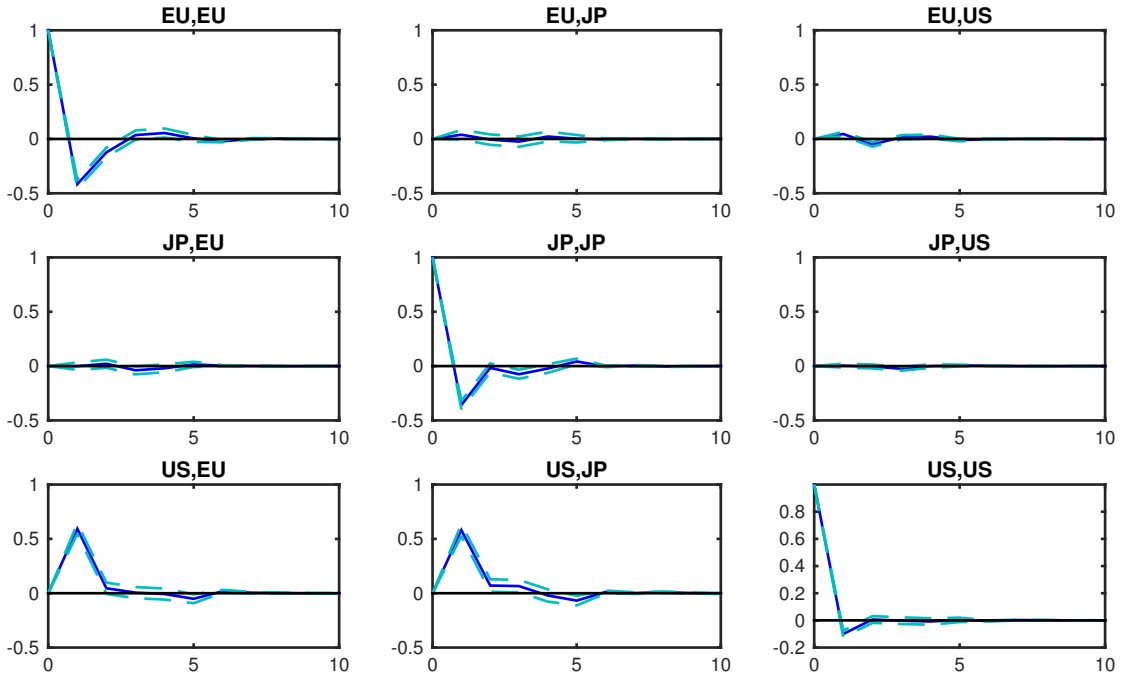

Figure 2.2: **Impulse-response function for the 15%-quantile changes at 60 days time horizon (daily frequency).** The figure shows the impulse-response functions for each pair of markets. First column shows the response of the European market to an unit shock in the European market (top plot), the Japanese market (central plot) and the US market (bottom plot). Second column contains the response of the Japanese market to an unit shock in the European market (top plot), the Japanese market (central plot) and the US market (bottom plot). And finally, the third column shows the response of the US market to an unit shock in the European market (top plot), the Japanese market (central plot) and the US market (bottom plot). Impulse-responses are shown in a solid blue line and confidence intervals are plotted in a dashed light blue line. The analysis is based on daily data.

Regarding the variance decomposition analyses, figure 2.8 shows the portion of the variance of each quantile change that is due to its own shocks and due to shocks in other markets' risk-neutral quantiles. As we can see, for all the markets, almost the whole variance is explained by its own shocks. Results in this figure are based on the analysis performed using daily data. This finding reveals an autoregressive behavior of the changes in the left-tail quantile shocks. In the case for which we use weekly data, figure 2.9 shows the same results except for the S&P 500 quantiles, whose variance is now about $60-70\%$ due to its own shocks, being the rest of the variance equally caused by changes in the

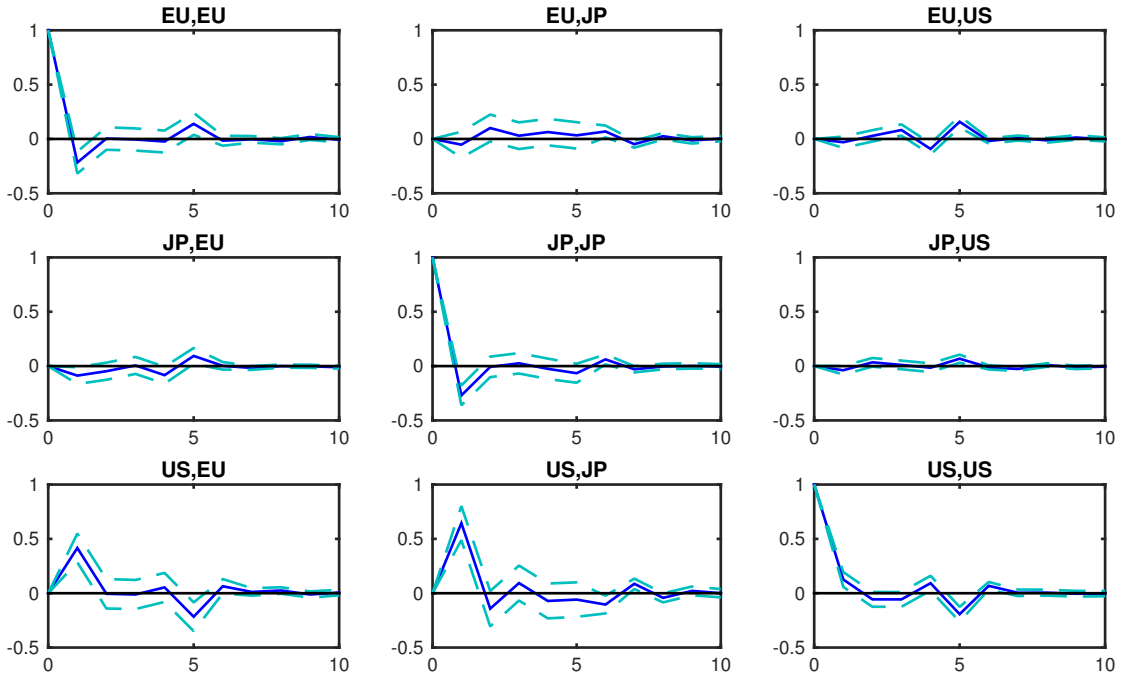

Figure 2.3: **Impulse-response function for the 15%-quantile changes at 60 days time horizon (weekly frequency).** The figure shows the impulse-response functions for each pair of markets. First column shows the response of the European market to an unit shock in the European market (top plot), the Japanese market (central plot) and the US market (bottom plot). Second column contains the response of the Japanese market to an unit shock in the European market (top plot), the Japanese market (central plot) and the US market (bottom plot). And finally, the third column shows the response of the US market to an unit shock in the European market (top plot), the Japanese market (central plot) and the US market (bottom plot). Impulse-responses are shown in a solid blue line and confidence intervals are plotted in a dashed light blue line. The analysis is based on weekly data.

quantiles in the other two foreign markets, the EuroStoxx 50 and the Nikkei 225 indexes.

2.4 Conclusions

Realized and option-implied volatility transmission across international financial markets is a proved stylized fact. In this chapter we analyze the transmission of the option-implied loss quantile changes in three developed markets: US, Eurozone and Japan, represented by the S&P 500, EuroStoxx 50 and the Nikkei 225 indexes, respectively.

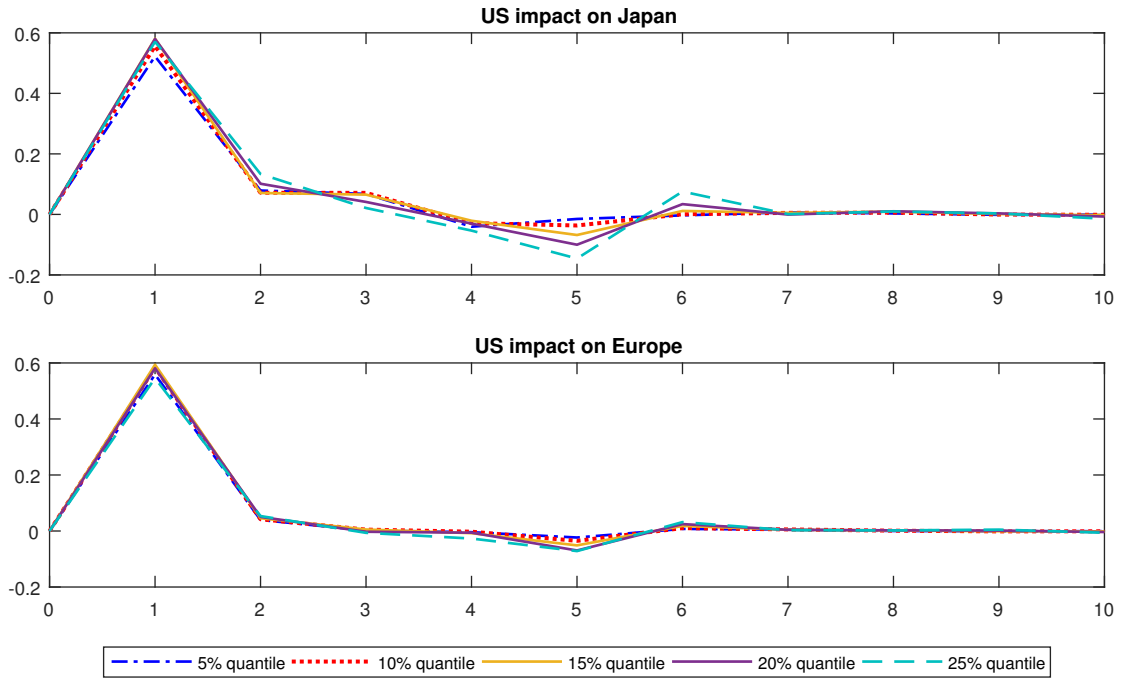

Figure 2.4: **Risk-neutral option-implied daily quantile changes for 60 days horizon.** The top plot shows the impact of a shock in the S&P 500 quantiles to the different daily Nikkei 225 quantiles (5%, 10%, 15%, 20% and 25%) for a 60 days maturity. The bottom plot shows how shocks in the S&P 500 quantiles affect the different EuroStoxx 50 daily quantiles (5%, 10%, 15%, 20% and 25%) for a 60 days maturity.

Different levels of quantiles (5%, 10%, 15%, 20% and 25%) have been obtained from daily option-implied risk-neutral densities, which have been calculated using the Breeden-Litzenberg non-parametric approach. The observed range of data has been extrapolated at the extremes, as per Bliss and Panigirtzoglou (2004), in order to capture more area at the tails. Calculation of the RNDs allows us to analyze different α%-quantiles as well as different time horizons.

However, due to the different time zone of our target markets, we face the problem of non-synchronous data. We use two different approaches to tackle this. In the first approach, the dynamics of the different markets are modeled using a S-VAR(n) process using series of daily risk-neutral quantile changes. The S-VAR(n) model is convenient since

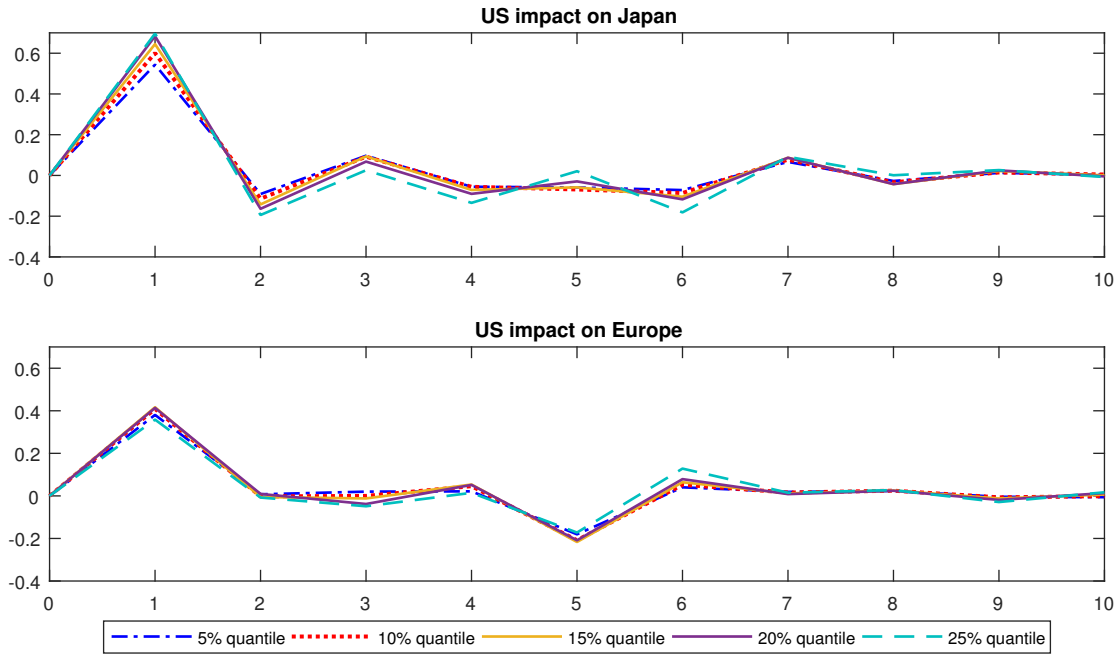

Figure 2.5: **Risk-neutral option-implied weekly quantile changes for 60 days horizon.** The top plot shows the impact of a shock in the S&P 500 quantiles to the different weekly Nikkei 225 quantiles (5%, 10%, 15%, 20% and 25%) for a 60 days maturity. The bottom plot shows how shocks in the S&P 500 quantiles affect the different EuroStoxx 50 weekly quantiles (5%, 10%, 15%, 20% and 25%) for a 60 days maturity. Weekly quantiles are calculated by averaging daily quantile observations for each week.

it allows for both contemporaneous and lagged effects between the markets. The second approach uses a VAR(n) process to design the dynamics of the markets. This approach is based on weekly averages of the daily risk-neutral quantile changes calculated for each week in the sample and it only contemplates lagged effects between markets.

In order to study the transmission effects across markets, their magnitude and persistence in time, we perform the generalized impulse-response analysis as well as the variance decomposition analysis.

By using information from options on the S&P 500, EuroStoxx 50 and Nikkei 225 indexes and controlling the effects of shocks in the VIX index, we find that shocks in the left-tail quantiles of the US index have a response in the left-tail quantiles of the Euro-

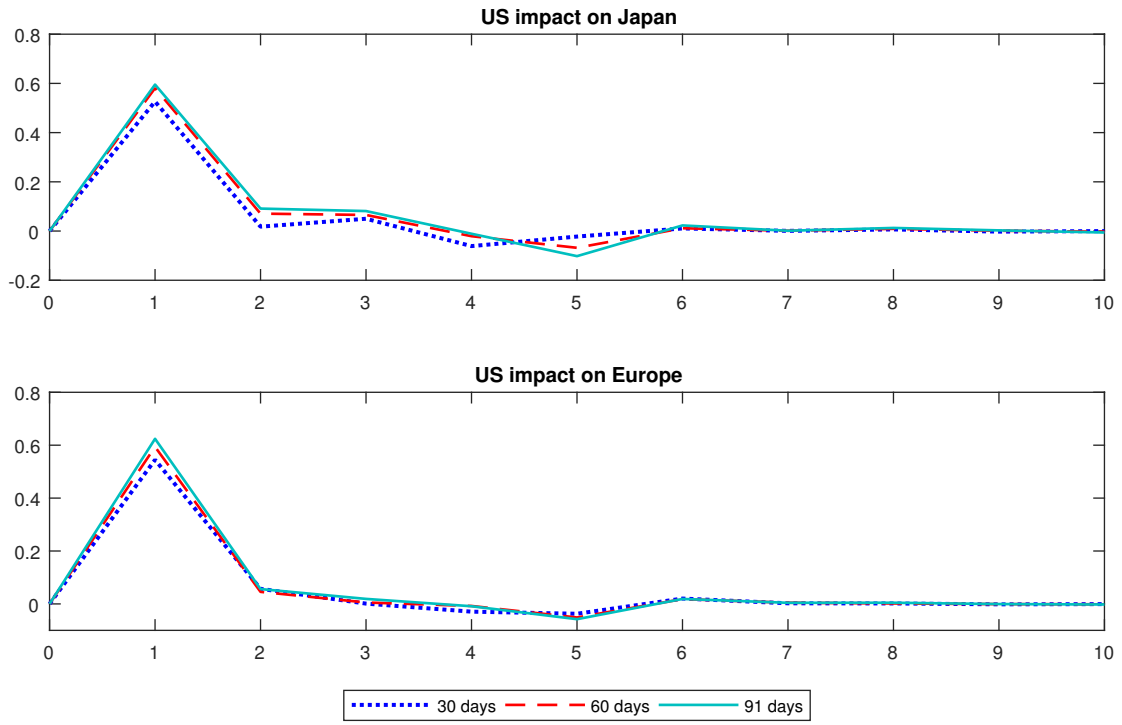

Figure 2.6: **Risk-neutral option-implied daily 15%-quantile changes for different time horizons.** The top plot shows the impact of a shock in the S&P 500 quantiles to the Nikkei 225 daily 15%-quantile for the different maturities considered (30, 60 and 91 days). The bottom plot shows how shocks in the S&P 500 affect the EuroStoxx 50 daily 15%-quantile for the different maturities considered (30, 60 and 91 days).

zone and Japan indexes. These effects hold for different α%-quantiles and different time horizons. Therefore, we can conclude that the S&P 500 quantile changes are transmitted to the EuroStoxx 50 and the Nikkei 225 quantile changes. However, transmissions from both EuroStoxx 50 and Nikkei 225 quantiles to the other markets are non-significant.

We can also appreciate that the responses that a unit shock in the S&P 500 index has to the other foreign indexes are slightly different across maturities, the larger the time horizon, the stronger the impact caused. On the other hand, effects are very similar across different α%-levels of the quantiles, responding all of them in a similar fashion.

Variance decomposition analyses show that for all series the biggest portion of quantile

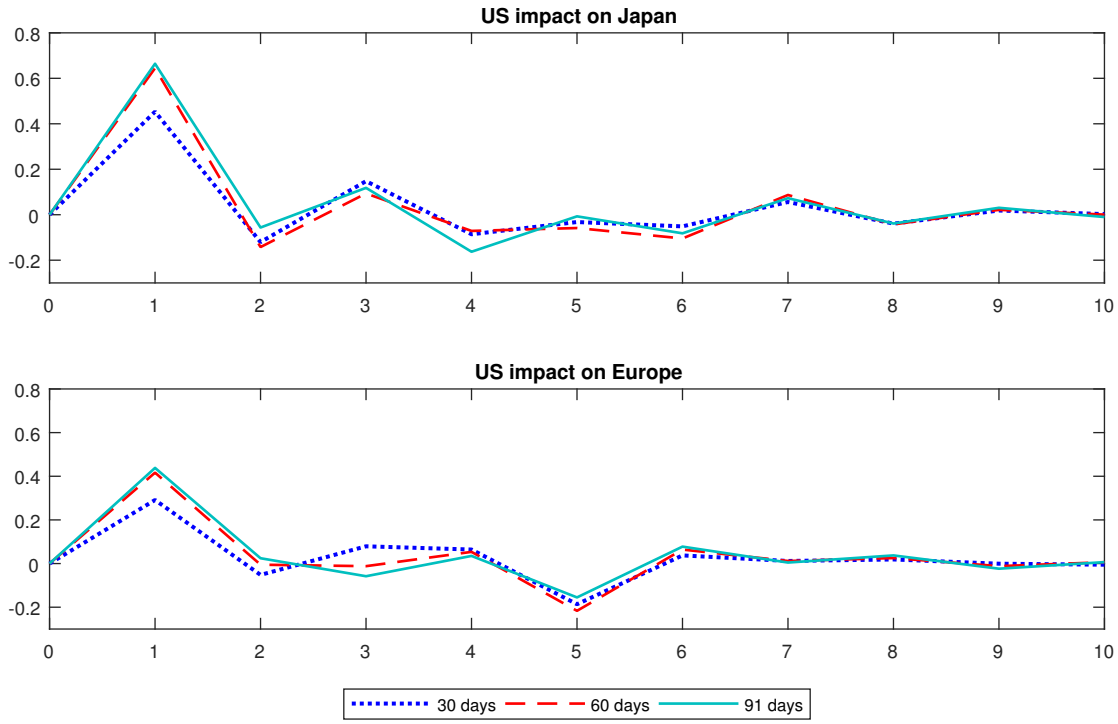

Figure 2.7: **Risk-neutral option-implied weekly 15%-quantile changes for different time horizons.** The top plot shows the impact of a shock in the S&P 500 quantiles to the Nikkei 225 weekly 15%-quantile for the different maturities considered (30, 60 and 91 days). The bottom plot shows how shocks in the S&P 500 affect the EuroStoxx 50 weekly 15%-quantile for the different maturities considered (30, 60 and 91 days). Weekly quantiles are calculated by averaging daily quantile observations for each week.

variance is due to its own quantile shocks (lagged). This finding suggests an autoregressive pattern in the loss quantiles.

The transmission analysis has been performed using both daily and weekly data, using a S-VAR(n) process and a VAR(n) process, respectively, to model the dynamics of the different markets. Qualitative results hold for the different methodologies used, different α%-quantiles and different time horizons targeted, confirming the robustness of the results.

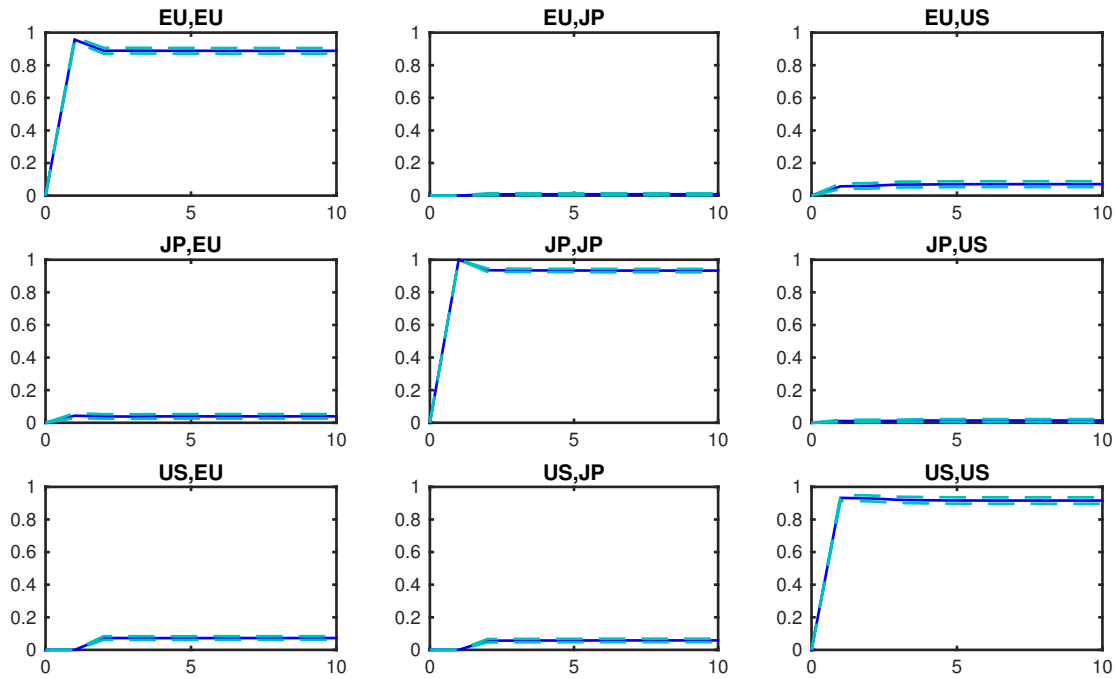

Figure 2.8: **Variance decomposition for the 15%-quantile changes at 60 days horizon (daily frequency).** The figure shows the variance decomposition analysis for each pair of markets. First column shows the response of the European market to an unit shock in the European market (top plot), the Japanese market (central plot) and the US market (bottom plot). Second column contains the response of the Japanese market to an unit shock in the European market (top plot), the Japanese market (central plot) and the US market (bottom plot). And finally, the third column shows the response of the US market to an unit shock in the European market (top plot), the Japanese market (central plot) and the US market (bottom plot). Results for the variance decomposition analysis are shown in a solid blue line and confidence intervals are plotted in a dashed light blue line. The analysis is based on daily data.

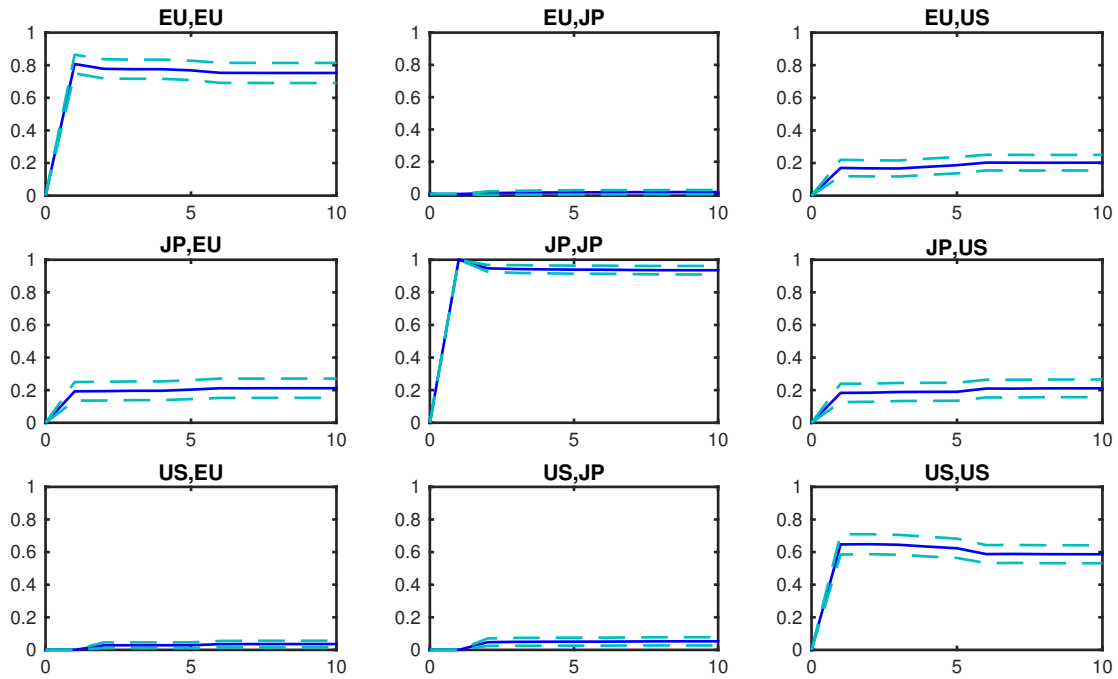

Figure 2.9: **Variance decomposition for the 15%-quantile changes at 60 days horizon (weekly frequency).** The figure shows the variance decomposition analysis for each pair of markets. First column shows the response of the European market to an unit shock in the European market (top plot), the Japanese market (central plot) and the US market (bottom plot). Second column contains the response of the Japanese market to an unit shock in the European market (top plot), the Japanese market (central plot) and the US market (bottom plot). And finally, the third column shows the response of the US market to an unit shock in the European market (top plot), the Japanese market (central plot) and the US market (bottom plot). Results for the variance decomposition analysis are shown in a solid blue line and confidence intervals are plotted in a dashed light blue line. The analysis is based on weekly data.

Chapter 3

Why so different? The behavior of risk aversion in developed economies

According to the economic theory, the integration of developed markets should permit a perfect risk sharing across economies. For instance, mutual funds located in developed Europe are indexed in US stocks, and viceversa. These continuous flows of funds across borders result in an equilibrium between supply and demand, where consumption risk is efficiently shared across countries. Within this context, what is the nature of risk aversion among well-integrated economies? Is this risk aversion driven by global or local forces? Does its time series exhibit a similar pattern over time across economies? If not, what are the sources of heterogeneity in its behavior? Characterizing the behavior of risk aversion is of paramount importance for macroeconomic policy and asset pricing issues.

This chapter analyzes the evolution of risk aversion within main developed economic areas. We delve into the systematic patterns, both in the time-series and cross-section,

that describe its behavior. To infer the evolution over time of the risk aversion, this work exploits the informational content embedded in option and stock prices from a comprehensive database of most liquid market indexes. The main contribution of this study is twofold: first, an important source of commonality in risk aversion series is observed. A principal components analysis (PCA, hereafter) reveals that 55% of variability is explained by one component. The time series of risk aversion change over time, exhibiting negative values occasionally. For a moneyness of 1.00, its magnitude ranges from 0 to 30. Consistent with the economic theory, the higher (lower) the degree of moneyness, the lower (higher) the level of risk aversion.

Interested in explaining the sources of commonality in risk aversion, we project the estimated coefficients onto a set of macroeconomic global and country-specific variables. A second contribution of this study is that country-specific variables have a leading role on explaining contemporaneous values of risk aversion. A dynamic analysis using a vector autoregressive (VAR) model shows a statistically significant lead-lag relationship from the US to Europe. However, alternative linkages among the markets under study are not found.

Since risk aversion represents a fundamental tool in this study, its estimation constitutes a central issue to us. The methodology for estimating the risk aversion series is directly implied from the relationship between risk-neutral (RND) and actual or subjective (SPD) densities. Instead of imposing parametric utility functions, we closely follow the non-parametric approach of Aït-Sahalia and Lo (2000) and Jackwerth (2000).[17] Within the context of this methodology, RNDs are implied from option prices using a non-parametric approach, and SPDs are estimated by forecasting the future volatility using an ARMA-

[17]This novel course gave rise to two different ways to calculate risk aversion. On the one hand, some authors are devoted to parametrize the risk aversion with one of the standard utility functions supported by the literature; see Bartunek and Chowdhury (1997) and Bliss and Panigirtzoglou (2004), among others. However, this approach requires specification of a parametric form of such preferences. Alternatively, the approach adopted in this work requires prior estimation of the RNDs and SPDs.

GJR process followed by the fitting of Kernel densities.[18] RNDs and SPDs are inferred from a comprehensive database of international indexes and their associated options from May 2004 to September 2015, covering more than 10 years of data and the recent financial crisis.

This study attempts to enrich the general understanding of risk aversion when inferred from asset prices. Lucas (1978) already states that in a consumption-based asset pricing model, the pricing kernel can be well approximated by the marginal rate of substitution (MRS). Using option prices, Jackwerth (2000) documents a negative risk aversion around the center of the distribution. This author also documents a pricing kernel puzzle, showing that the risk aversion is positive and monotonically decreasing across wealth for the period prior to the crisis in 1987, a result consistent with the economic theory. However, after the crisis, risk aversion locally increases near to those starting levels of wealth. These findings are still under debate: Rosenberg and Engle (2002) and Perignon and Villa (2002) find evidences agreeing Jackwerth (2000), but Aït-Sahalia and Lo (2000) and Bliss and Panigirtzoglou (2002) seem not to support those results. In recent dates, Bedoui and Hamdi (2015) study the effect of the time to maturity to the risk aversion. To the best of our knowledge, this is the first analysis exploring the commonalities in risk aversion series between developed markets.

In parallel to this literature, this study also belongs to the research interested in the estimation and forecasting of densities from market prices. Because real world investors are not indifferent towards risk –SPDs incorporate investors' preferences, contrary to RNDs, in which investors are risk neutral– the financial literature addresses different approaches for the estimation of price densities.[19] Regarding the risk-neutral world, the extraction of

[18]The subjective densities are unobservable, and their estimation is not an easy task. Financial literature suggests the usage of historical time series of the financial indexes to approximate actual estimates. For instance, Aït-Sahalia and Lo (2000) estimate both RNDs and SPDs using Kernel densities for the S&P 500 index; and Jackwerth (2000) approximates the RNDs using a slightly modified Jackwerth and Rubinstein (1996) approach, using Kernel densities to approximate the SPDs.

[19]Risk-neutral and real worlds are different because investors value differently an extra unit of payoff

RND distributions from option prices has been widely studied by the literature due to its convenient forward-looking features since the seminal paper of Breeden and Litzenberger (1978). Perignon and Villa (2002) use Kernel densities to approximate RNDs on the CAC40 index. Coutant (2000) also studies the CAC40 index using Hermite polynomials. Rosenberg and Engle (2002) use the volatility smile to calculate the RNDs. With respect to SPDs, an extensive literature stresses the usage of historical data to construct SPD forecasts; see, for instance, Perignon and Villa (2002), Coutant (2000) and Rosenberg and Engle (2002), among many others.

This chapter is organized as follows: section 3.1 introduces the methodology to infer RNDs and SPDs. Section 3.2 presents the data, and infers the risk aversion series. A dynamic analysis of risk aversion is presented in section 4. Finally, section 5 concludes.

3.1 Estimation of densities from market prices

This section introduces the foundations for extracting RNDs and SPDs. The methodology for inferring the implied risk aversion is also presented.

3.1.1 Risk-Neutral Distributions

RNDs are daily estimated using the non-parametric approach in Breeden and Litzenberger (1978). This technique permits to infer the whole state price density, $f(S_T)$, from option prices by calculating the second partial derivative of the option pricing function,

$$f\left(S_T\right) = \ e^{r(\tau)} \frac{\partial^2 C\left(S_t, X, T, t\right)}{\partial X^2} \mid_{X=S_T} \tag{3.1}$$

depending on the state (wealth level); they are, in fact, not indifferent to risk. In case that investors were risk neutral, both RND and SPD distributions would match. The pricing kernel captures the risk aversion adjustment to obtain the SPDs.

where r is the risk-free rate, $C(\cdot)$ the European call price function, S_t the current value of the underlying asset, X the strike price of the option, T the expiration date of the option, t the current date, and $\tau = T - t$ the time to expiration of the option.

Expression (3.1) requires a continuum of strike prices encompassing all possible future payoffs. Since options trade at discrete prices, some data interpolation is needed. This technique is implemented following the lines of Malz (1997), who proposes to interpolate on an implied volatility (iv)-delta (Δ) space, instead of on a price-strike price space, as it was common in previous literature. This is a more convenient approach, since it gathers away-from-the-money options closely together. Besides, Δ is bounded between 0 and 1, introducing some advantages over the strike price-space, which is theoretically unbounded. Once the interpolation is done, we use the Black and Scholes (1973) formula to transform implied volatilities and Δs back into prices and strike prices, in order to apply the Breeden and Litzenberger (1978) technique.[20]

An additional challenge in the estimation of RNDs is the limited range of strike prices at which options trade. This circumstance impedes the estimation of the RND mainly in the tails, since extreme observations are scarce. In order to overcome this issue, Bliss and Panigirtzoglou (2004) suggest to add two pseudo-points at both ends of the observed range of Δs, assigning to them the volatility of its closest observed Δ. Once these points are included, we interpolate within the range by calculating a cubic smoothing spline of the form,

$$S_\lambda = \sum_{i=1}^{n} m_i (Y_i - g(\Delta_i, \theta))^2 + \lambda \int_{-\infty}^{+\infty} p''(x;\theta)^2 dx \ , \tag{3.2}$$

where m_i is a weighting value of the squared error, Y_i is the implied volatility (iv) of the ith option observation, and $g(\cdot)$ is the fitted iv, a function of delta (Δ_i) and θ spline

[20] Black and Scholes (1973) formula (BSM) is used to transform prices into implied volatilities and strike prices into deltas, reverting them back to prices and strike prices after the interpolation is done. Note that BSM formula is used as a mere tool; we are not stating that such formula correctly prices the options.

parameters. Finally, λ is the smoothing parameter, and $p(\cdot)$ is the smoothing spline.[21]

3.1.2 Subjective Densities

The estimation of SPDs differs from their risk-neutral counterparts. RNDs are based on implied volatilities from option prices, so they are forward-looking measures for a τ-period ahead by themselves. Instead, SPDs are based on realized index returns and, consequently, the usage of econometric tools is required to forecast the future outcomes of the underlying index τ-periods ahead.

In order to construct our index forecasts, a model that accounts for leptokurtosis, volatility clustering and leverage effects is required. To capture these stylized facts presented in the sample, we propose an ARMA-GJR model, which has also been used by Rosenberg and Engle (2002). ARMA processes are a combination of an autoregressive (AR) and a moving average (MA) process which allow current values of the return series to depend on their own lags and some error term,

$$y_t = \mu + \phi_1 y_{t-1} + \phi_2 y_{t-2} + \ldots + \phi_p y_{t-p} + \theta_1 u_{t-1} + \theta_2 u_{t-2} + \ldots + \theta_q u_{t-q} + u_t \,, \quad (3.3)$$

where y_t are the returns of the index at time t, and u_t is a disturbance assumed to obey standard assumptions. Parameters p and q are the number of lags for the AR(p) and MA(q) processes, respectively.

The conditional variance is modeled using Glosten et al. (1993), who propose an asymmetric GARCH (GJR) model which includes a term to account for asymmetries, besides the volatility clustering presented in the sample. This version has been widely used within the literature in volatility modeling and forecasting; see, for instance, Brooks

[21] Bliss and Panigirtzoglou (2004) propose a value of 0.99 for parameter λ; however, in this analysis we assign to this parameter the value 0.90 in order to get a smoother fit.

(2008) for a more detailed analysis of the different models.[22] The expression of the GJR model is,

$$\sigma_t^2 = \alpha_0 + \alpha_1 u_{t-1}^2 + \beta\sigma_{t-1}^2 + \gamma u_{t-1}^2 \mathbb{1}_{\{y_{t-1}<0\}} \tag{3.4}$$

where, α_1 captures the impact of recent shocks on contemporaneous variance, β reflects the variance persistence and $\gamma > 0$ accounts for the leverage effect. $\mathbb{1}_{\{...\}}$ is an indicator function that equals to 1 if the expression in brackets is true, and 0 otherwise.

Relying on the Bayesian Information Criteria, we set the lags of the mean equation to $p = q = 1$. Thus, the proposed model for the SPD becomes an ARMA(1,1)-GJR, as follows,

$$y_t = \mu + \phi y_{t-1} + \theta u_{t-1} + u_t \tag{3.5}$$

$$u_t \sim N(0, \sigma_t^2) \tag{3.6}$$

$$\sigma_t^2 = \alpha_0 + \alpha_1 u_{t-1}^2 + \beta\sigma_{t-1}^2 + \gamma u_{t-1}^2 I_{\{y_{t-1}<0\}} \tag{3.7}$$

Regarding the model estimation, some articles analyze the *leverage effect puzzle*, which consists on some estimations yielding an inverse leverage effect (negative γ estimates in our case).[23] This anomaly can be explained, in part, by the existence of extreme observations in the sample, that bias the coefficient estimation. In order to prevent this issue, we carry out a robust estimation of the ARMA-GJR model assuming Student-t innovations.[24]

Some details about the model estimation follow. The ARMA-GJR model is fitted

[22]The Generalized Autoregressive Conditionally Heteroscedastic (GARCH) models have been widely used for volatility modeling and forecasting purposes, as a more accurate alternative to simply calculating the variance of historical observations; see, for instance, Bollerslev (1986a) and Taylor (1986). These models allow to fit conditional variances dependent upon their own past information. A common critique shared by standard GARCH models is that they do not capture leverage effects –empirical volatility does not respond similarly to both positive and negative shocks–. This work employs Glosten et al. (1993), an extension of the standard GARCH models which overcome this issue.

[23]The main reference about the *leverage effect puzzle* is Aït-Sahalia et al. (2013).

[24]The assumption of Student-t innovations is done in order to get a robust estimation, and not because we believe that the true distribution of innovations is a Student-t. More details about this technique can be found in Carnero et al. (2007) and Carnero et al. (2012).

using three years of index return data. We then employ the estimated model to construct forecasts with different τ horizons, being $\tau = 30$, 60 and 91 days. Similarly to Aït-Sahalia and Lo (2000) and Jackwerth (2000), forecasts are built using 1,000 Monte Carlo simulations, which are then used to fit the density of the data by means of a non-parametric Kernel estimator,

$$\hat{f}_h(x) = \frac{1}{n}\sum_{i=1}^{n} K_h(x - x_i) = \frac{1}{nh} K\left(\frac{x - x_i}{h}\right) , \tag{3.8}$$

with K a kernel smoothing function, and h the bandwidth parameter. In line with the literature, we choose a Gaussian kernel for K, and bandwidth parameter h is calculated according to *Silverman's* rule-of-thumb. A detailed review of the different methods to calculate K and h can be found in Silverman (1986) and Härdle (1990).

3.1.3 Implied Risk Aversion

Risk aversion is implied from the RNDs and the SPDs following the approach in Aït-Sahalia and Lo (2000) and Jackwerth (2000). Under the assumption of complete markets and in equilibrium, there exists a representative investor with a utility function U such that (Constantinides, 1982),

$$S_t = E_t[\psi(C_T) M_{t,T}], \qquad M_{t,T} \equiv \frac{U'(C_T)}{U'(C_t)} , \tag{3.9}$$

with S_t the security price at the current date t, $\psi(C_T)$ the payoff at terminal date T, and $M_{t,T}$ the stochastic discount factor, or pricing kernel, approximated by the MRS of consumption.

In equilibrium, the investor optimally invests all her wealth W_T at final date T in the market portfolio. Thus, the security price, her wealth and consumption at T coincides

($S_T = W_T = C_T$). The investor maximization problem is,

$$\max \int_0^\infty f_P(S_T)U(S_T)dS_T \ , \tag{3.10}$$

with $f_P(S_T)$ the SPD, the initial endowment is normalized to one,

$$\frac{1}{r}\int_0^\infty f_Q(S_T)S_T dS_T = 1 \tag{3.11}$$

and $f_Q(S_T)$ is the RND.

All things considered, the Lagrange function becomes,

$$L = \int_0^\infty f_P(S_T)U(S_T)dS_T - \lambda\left[\frac{1}{r}\int_0^\infty f_Q(S_T)S_T dS_T - 1\right] \tag{3.12}$$

with λ the shadow price, $f_Q(S_T)$ the RND, $f_P(S_T)$ the SPD and r the risk-free rate. It derives,

$$U'(S_T) = \frac{\lambda}{r}\frac{f_Q(S_T)}{f_P(S_T)} \tag{3.13}$$

$$U''(S_T) = \frac{\lambda}{r}\frac{f'_Q(S_T)f_P(S_T) - f'_P(S_T)f_Q(S_T)}{f^2_P(S_T)} \tag{3.14}$$

and the absolute risk aversion function is,

$$A(S_T) = -\frac{U''(S_T)}{U'(S_T)} = \frac{f'_P(S_T)}{f_P(S_T)} - \frac{f'_Q(S_T)}{f_Q(S_T)} \tag{3.15}$$

As long as RNDs ($f_Q(S_T)$) and SPDs ($f_P(S_T)$) are good approximations of the risk-neutral and subjective density functions, respectively, accurate estimates of the risk aversion can be implied from expression (3.15) without imposing any parametric utility function.

3.2 Empirical results

3.2.1 The Data

A comprehensive dataset for estimating RNDs and SPDs is at our disposal. In this study, we focus on three main economic areas: US, proxied by the S&P 500 index; the Eurozone, proxied by the EuroStoxx 50 index; and Japan, where the Nikkei 225 index is used. The analysis covers the period ranging from May 2004 to September 2015, and captures the subprime mortgage crisis 2007-2010, and the European sovereign crisis 2010-2012. Data frequency is daily.

RNDs are daily inferred from option prices, and are downloaded from the IvyDB Global Indexes of OptionMetrics. This database provides information of historical prices and implied volatilities for listed index options markets worldwide. Data about pairs of implied volatilities and deltas is obtained from the volatility surfaces files also provided in our dataset. We use the information of put options because they are more traded than calls. This information is passed to their corresponding iv-Δs call counterparts to be employed in the calculations. The volatility surfaces are given for a range of Δs from 0.2 to 0.8, constituting a range with 13 equidistant observations in increments of 0.05. As previously mentioned, the area in the tails is computed by adding two Δ pseudo-points beyond each end, assigning to each of the new Δs the implied volatility of the closest observed Δ. Once obtained, a cubic smoothing spline is used to interpolate within the extended range (17 points). The risk-free rate proxy is considered to be the zero-coupon yield provided by OptionMetrics. Lastly, our analysis is based on options with 30, 60 and 91 days to expiration, which form the time horizon of the densities. Concerning the estimation of the SPDs, daily closing prices for the S&P 500, EuroStoxx 50 and Nikkei 225 indexes are employed. This information is extracted from Datastream Thomson Reuters.

3.2.2 Estimated RND and Subjective Densities

From previous data, daily RNDs and SPDs have been calculated for a period of time from May 2004 to September 2015. For the ease of explanation, the reported densities correspond to the 91-days time horizon. The remainder outlooks provide quite similar results, and they are available upon request.

Figure 3.1 compares the RNDs (blue line) and SPDs (red line) for the indexes under study. First to third columns are densities for the S&P 500, the EuroStoxx 50 and the Nikkei 225, respectively. As shown, this figure provides an accurate snapshot of the situation of the financial markets at different periods: before the financial crisis (upper graphs), which depict the densities in 20 March 2006; Lehman Brothers' collapse (central graphs), which represent densities of 15 September 2008; and the European sovereign crisis (bottom graphs), showing densities for 28 September 2011. Lastly, x-axes represent the moneyness.

Some interesting conclusions arise from inspection of figure 3.1. First, we observe that during calmed periods (upper graphs) the RNDs and SPDs differ, having both of them significantly different means. We observe that the SPD is shifted to the right with respect to the RND for the 3 underlyings considered, which is consistent with the economic theory and the existence of a risk premium in the markets. Moreover, as one would expect, the volatility is higher during the crisis periods (central and bottom graphs) in which the moneyness range spreads out significantly. Furthermore, by looking at the plots, it seems that during the crisis the mode of the RNDs and SPDs are fairly similar; however, when looking at the left tail of the densities, we can appreciate that this tail is thicker for the RNDs. This result shows how in crisis periods agents overprice assets with positive payoffs on bad states (left tails).

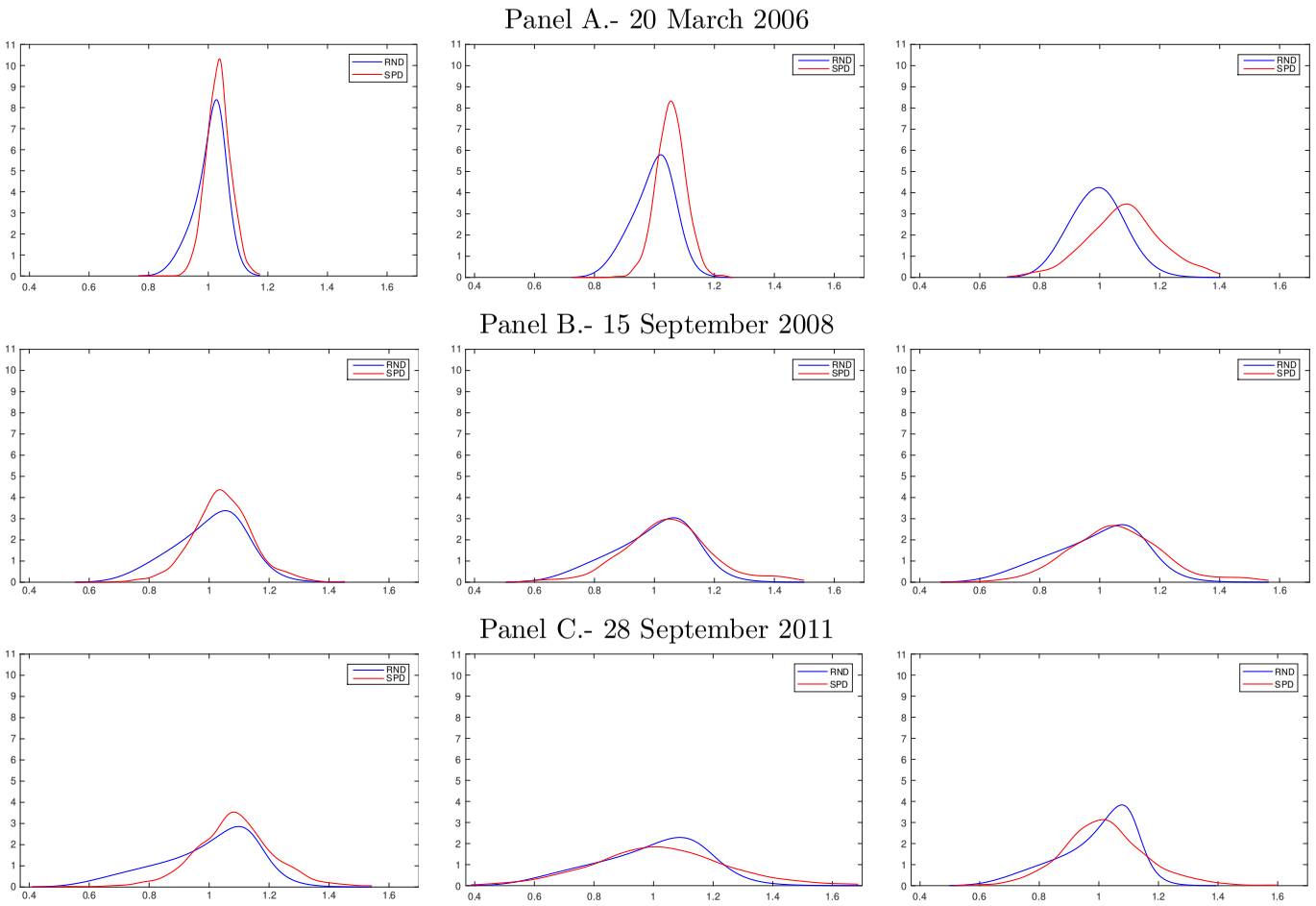

Figure 3.1: **Risk-neutral and subjective densities of S&P 500, EuroStoxx 50 and Nikkei 225 for different dates.** The figure compares Risk-neutral densities (blue line) and subjective densities (red line) for the indexes under study: the S&P 500 (first column), the EuroStoxx 50 (second column) and the Nikkei 225 (third column). Panel A shows comparisons between RNDs and SPDs for one representative day prior to the crisis (20 March 2006), panel B shows the densities on the Lehman Brothers' collapse (15 September 2008) and panel C represents densities for a day during the European sovereign crisis (28 September 2011). Densities are for a 91-days time horizon. The x-axis of the plots depicts the moneyness level.

3.2.3 The time series of risk aversion

The RNDs and SPDs computed in previous section 3.1 permits to obtain daily series of the risk aversion using equation (3.15). Within each month we average the daily risk aversion estimates, therefore, we get a monthly series of risk aversion. We proceed this way for two reasons: first, daily series of risk aversion have outliers, then averaging on a monthly basis we mitigate this problem. Second, our interest is to analyze domestic and foreign macro determinants of risk aversion; therefore we need risk aversion series with the same frequency than the macro variables. The estimated time series are provided in figure 3.2, which depicts the evolution of risk aversion for S&P 500 (dark blue line), EuroStoxx50 (red line), and Nikkei 225 (light blue line) indexes. The graphs show the risk aversion coefficients for different degrees of moneyness: 0.97 (upper graph), 1.00 (middle graph) and 1.03 (lower graph).

We can see that the level of risk aversion drops as the level of moneyness increases; that is, market participants exhibit higher (lower) risk aversion for those expected levels of wealth for which they are worse-off (better-off). From these series we can also appreciate that for some periods the risk aversion takes negative values (being these more frequent for higher levels of moneyness). Additionally, the figure also depicts the existence of some commonalities across series over time, which are explained by different components.

Another perspective about these results is provided in table 3.1. This table provides the descriptive statistics sample mean, median and standard deviation for the monthly risk aversion series for the three underlyings and three different degrees of moneyness.

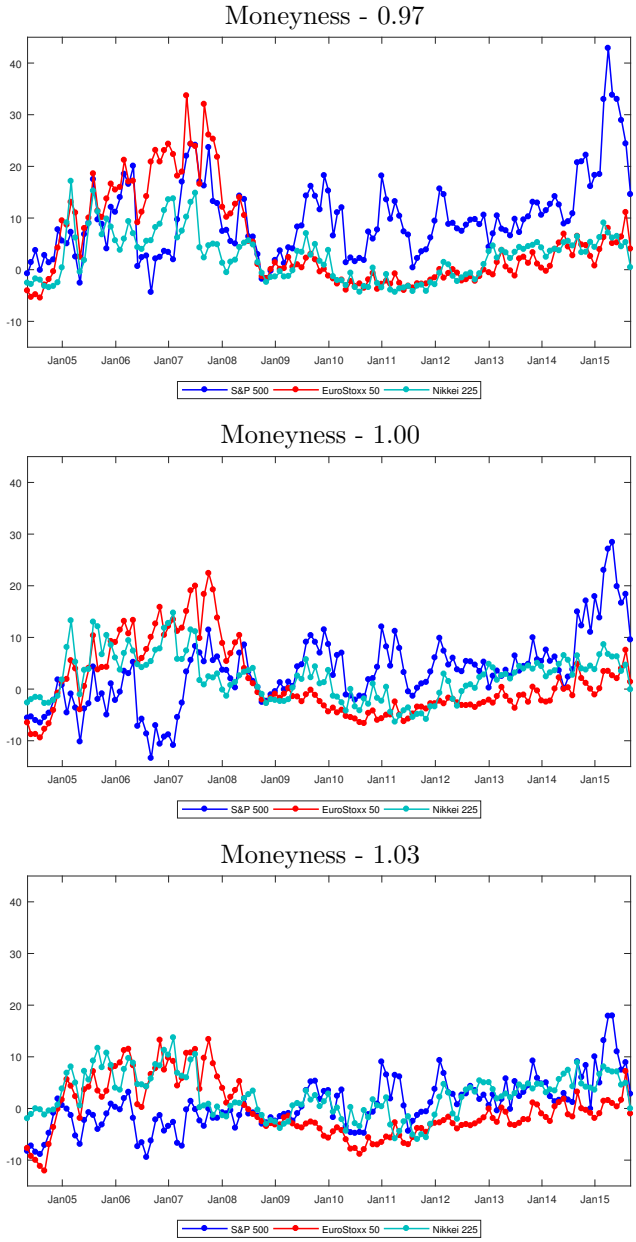

Figure 3.2: **Time series of risk aversion for different markets and moneyness.** The figure shows the evolution over time of the time series of the risk aversion for the S&P 500 (depicted in a dark blue line), the EuroStoxx 50 (red line) and the Nikkei 225 (light blue line). Top plot depicts risk aversion series for a moneyness level of 0.97, central plot is for moneyness 1 and bottom plot represents moneyness 1.03. These plots depict monthly risk aversion series based on a 91-days time horizon.

		Moneyness: 0.97			Moneyness: 1			Moneyness: 1.03		
τ		S&P 500	EuroStoxx 50	Nikkei 225	S&P 500	EuroStoxx 50	Nikkei 225	S&P 500	EuroStoxx 50	Nikkei 225
30 days	Mean	19.6025	9.4964	3.4112	-2.7481	-3.6909	0.0932	7.6795	-1.6910	1.9163
	Median	19.4012	4.5826	2.2251	-2.3036	-5.3077	-0.4640	3.1245	-3.8941	1.8639
	St. Dev.	11.4394	12.6933	7.0006	9.1081	6.9363	5.6362	18.9212	7.9052	5.8610
60 days	Mean	12.1056	6.2023	2.5293	1.5411	-0.3359	1.5003	-0.6011	-1.5897	1.9655
	Median	11.0830	2.1817	2.2647	1.3747	-2.3392	1.4511	-1.1132	-2.7526	1.9724
	St. Dev.	8.4114	10.0219	5.4561	7.7778	6.5351	4.9930	5.2384	5.2039	4.6651
91 days	Mean	9.9357	5.3127	2.6602	3.2462	1.3346	2.2957	0.6332	-0.3158	2.5638
	Median	8.7744	2.0882	3.2942	3.3635	-1.1014	2.5201	-0.1179	-1.6996	2.7788
	St. Dev.	7.8853	8.8541	4.7121	7.1005	6.7845	4.4885	4.8797	5.3696	4.1687

Table 3.1: **Descriptive Statistics of the monthly risk aversion estimates.** This table shows the descriptive statistics sample mean, median and standard deviation for the monthly risk aversion estimates for the S&P 500, the EuroStoxx 50 and the Nikkei 225 indexes. Statistics are provided for different time horizons (30, 60 and 91 days) and for different levels of moneyness (0.97, 1 and 1.03).

101

At first glance, it is striking the negative values of the mean and median risk aversion for various series. Specifically, these negative values are concentrated on at-the-money and in-the-money EuroStoxx 50 risk aversion series. However, for out-of-the-money (OTM hereafter) risk aversion series, all cases exhibit positive means and medians, ranging from 2.0082 to 19.6025, which are *normal* values. Moreover, for moneyness 0.97, we also observe an inverse relationship between risk aversion and time horizon: the larger the time to maturity, the lower the average risk aversion. This result means that agents are prone to pay a higher (risk) premia in order to hedge the immediate (30 days) negative wealth shocks with respect to the premia paid to hedge intermediate term (91 days) wealth shocks.

As previously mentioned, figure 3.2 suggests the existence of commonalities among the estimated series. To provide further insights about this issue, we run a principal component analysis (PCA) on the risk aversion series. Principal components and their corresponding loading factors for different degrees of moneyness are provided in table 3.2. In addition, the explained variance of each component is also shown. The main conclusion of this table is the existence of a notable source of commonality among the risk aversion series. Independently of the moneyness, a first principal component (PC) accounts for more than 50% of the joint variability observed in the data. This magnitude increases a 30% when a second PC is considered.

An interesting aspect of table 3.2 is that loadings seem to be sensible to the degree of moneyness. The more distant to moneyness 1.00 we are, the more even the PC loading coefficients are. See, for instance, the case of the first PC: its loading coefficients for moneyness 1.00 rely on EuroStoxx 50 and Nikkei 225 indexes, and no weight for S&P 500. Surprisingly enough, a lower moneyness of 0.97 results in an (almost) equally-weighted contribution of these three indexes to the first PC – a similar result is found for moneyness 1.03 –. A possible economic interpretation of these results is that risk aversion tends to be higher in more extreme scenarios, leading to a common systematic pattern among the

risk aversion series.

	PC 1	PC 2	PC 3
Panel A.- Moneyness: 0.97			
S&P 500	0.4362	0.8897	0.1346
EuroStoxx 50	0.6213	-0.4059	0.6730
Nikkei 225	0.6510	-0.2088	-0.7298
Expl. variance (%)	65.44	26.19	8.37
Panel B.- Moneyness: 1.00			
S&P 500	0.0091	0.9985	0.0544
EuroStoxx 50	0.7069	-0.0449	0.7059
Nikkei 225	0.7073	0.0320	-0.7062
Expl. variance (%)	54.80	33.40	11.73
Panel C.- Moneyness: 1.03			
S&P 500	0.2161	0.9613	0.1706
EuroStoxx 50	0.6773	-0.2735	0.6830
Nikkei 225	0.7032	-0.0321	-0.7102
Expl. variance (%)	55.85	32.89	11.26

Table 3.2: **Principal Component Analysis.** The table shows the loading factors resulting from the principal component analysis. Panel A provides results for the risk aversion estimates for a moneyness level of 0.97, panel B contains results for moneyness level of 1 and panel C for levels of moneyness 1.03. The first three rows of each panel contain the loading factors for the S&P 500, the EuroStoxx 50 and the Nikkei 225, respectively; and the last row contains the amount of variance explained by each of the components. The different components are shown in columns PC1 (for the first component), PC2 (for the second component) and PC3 (for the third component). Information is based on monthly averages of the risk aversions series for a 91–days time horizon.

Intrigued by the possible sources of covariance of this first principal component, we project the scores of the first PC onto a set of global variables that include the implied volatility index VIX; the exchange rates US dollar to Euro (US/EUR) and Yen to US dollar (Yen/US); and the slope of the US Treasury curve, an estimate of future growth; see Pan and Singleton (2008) for a similar exercise with CDS risk premia. The OLS estimates and their standard errors are provided in table 3.3. Notably, global variables like VIX and the slope of the US Treasury curve are economically relevant and statistically significant

at standard confidence levels. The performance of the regression model is not bad, and adjusted-R^2 coefficients are close to 18% when all variables are considered. According to these results, it seems that a common component of risk aversion is driven by proxies of global uncertainty like VIX or the US Treasury slope.

	Principal Component 1				
vix	-0.0551***				-0.0571***
	(-4.78)				(-4.49)
us_eur		4.753			1.988
		(1.38)			(0.58)
y_us			0.0833		0.0184
			(1.83)		(0.39)
slope_sp				0.996*	1.309**
				(2.02)	(2.87)
cons	1.084***	0.0146	0.00703	0.0197	1.146***
	(4.36)	(0.13)	(0.06)	(0.18)	(4.24)
N	137	136	136	136	136
adj. R-sq	0.139	0.007	0.017	0.022	0.179

t statistics in parentheses

* $p < 0.05$, ** $p < 0.01$, *** $p < 0.001$

Table 3.3: **OLS regression on the first component (PC1).** The table shows coefficient estimates from the regression of the first principal component against a set of macroeconomic variables. Column 1 shows the macroeconomic variables considered: implied volatility index (vix), the exchange rates US dollar to Euro (us_eur) and Yen to US dollar (y_us) and the slope of the term structure for the US market (slope_sp). We find also the constant term (cons). The last two rows show the number of variables used in the regression (N) and the Adjusted–R^2 (adj. R-sq). Columns 2-5 contain the coefficient estimates obtained by regressing the first principal component against each of the variables individually and the last column presents the coefficient estimates from the regression against all the variables contained in column 1. Results are for monthly risk aversion estimates for a moneyness level of 1 and for a 91-days time horizon.

3.3 The dynamics of risk aversion

Previous results exhibit a strong source of commonality between Eurozone and Japan economic areas, and an orthogonal behavior for US. Interested in exploring the global or local nature of risk aversion, we analyze the sources of covariance of our risk aversion estimates with some global and local macroeconomics variables. To this end, we project our monthly series of risk aversion onto a comprehensive pool of variables that capture different characteristics of these economic regions. Additionally, the possible lead-lag relationships between series are explored using a vector autoregressive (VAR) model.

3.3.1 Variable descriptions

We study to which extent risk aversion can be explained by systematic or idiosyncratic macroeconomic variables, in a similar way that Longstaff et al. (2011) for credit spreads. Since there is an unlimited amount of variables which could potentially be linked to the time series behavior of risk aversion, we follow Rosenberg and Engle (2002) and Schwert (1989) to build a set of variables that capture some major features of the economy.

The economic variables are structured in two groups: global and local. With regard to global variables, we consider the CBOE VIX volatility index, or *VIX*. This index is based on the S&P 500 index options, and it is considered as the reference of the global market volatility and, more generally, an index of global uncertainty; see, for instance, Whaley (2009). Data about VIX is downloaded from Datastream.

A second global variable is the Economic Political Uncertainty Index (*EPUI*) of Baker et al. (2016), a novel variable based on textual analysis that captures the political uncertainty on media. This index is built on three different components: one is based on the news about uncertainty collected from 10 largest newspapers, another component is the

federal tax code provisions and the last one is a measure of disagreement among economic forecasters. This index is directly obtained from the web page of the authors.[25] Furthermore, we include the Consumer Confidence Index (*CCI*) in the analysis, which is based on the households' plans for major purchases as well as their economic situation. Data about the Consumer Confidence Interval is provided by the OECD (2018).

The set of local variables seek to capture the idiosyncratic component of risk aversion. Along these lines, we consider the inflation index (*INFL*), proxied by the Consumer Price Index which is computed as a monthly average price changes of goods and services. Similarly, unemployment (*UNEMP*) and the industrial production index (*IPI*) are included as potential local variables that could covariate with risk aversion. Information about previous series for US and Japan have been retrieved from the Federal Reserve Bank of St. Louis. Data concerning the Eurozone has been provided by the European Central Bank (ECB).

The analysis is completed by including information about currency and interests rates. For the exchange rates, we use the US Dollar to Euro (*US/EUR*), the Yen to Euro (*Y/EUR*) and the Yen to US Dollar (*Y/US*). For the interest rates, the 5-year constant maturity government yield (*IR*) is employed as a proxy of the level of interest rates. Additionally, the spread between 10- and 1-year government bonds yields (*Slope*) is our proxy for the slope of the term structure. Data about interest rates has been provided by Thomson Reuters. As standard in research, Germany has been taken as benchmark for the Eurozone yields.

The correlation matrix among regressors is computed to avoid collinearity issues. Correlations are reported in Appendix B.1, where we observe that correlations are relatively low, therefore rejecting the inclusion of redundant variables. Finally, the existence of a unit root is rejected for the increments of all regressors considered, with the exception of

[25] See http://www.policyuncertainty.com/

the VIX series, which is stationary in levels.

3.3.2 OLS estimates

Based on the previous set of explanatory variables, we consider the following OLS regression specification for each of the risk aversion series, i, under study,

$$\begin{aligned} RA_{i,t} &= \alpha_i + \beta_{1,i} VIX_t + \beta_{2,i} EPUI_{i,t} + \beta_{3,i} CCI_{i,t} \\ &+ \beta_{4,i} INFL_{i,t} + \beta_{5,i} UNEMP_{i,t} + \beta_{6,i} IPI_{i,t} \\ &+ \beta_{7,i} US/EUR_t + \beta_{8,i} Y/EUR_t + \beta_{9,i} Y/US_t \\ &+ \beta_{10,i} IR_{i,t} + \beta_{11,i} SLOPE_{i,t} + \epsilon_{i,t},\ i = 1,2,3,\ t = 1,...,T \end{aligned} \tag{3.16}$$

with $RA_{i,t}$ the monthly risk aversion time series, and $\beta_{j,t}$ is the vector of coefficients for the set of global and local variables described in section 3.3.1. Lastly, ϵ_i denotes the random disturbances.

Table 3.4 shows the OLS estimates from expression (3.16) for at-the-money risk aversion series. Three sets of regressions are performed: first, the whole period considering from May 2004 to September 2015. To isolate the effect of the financial crisis, the sample is then split into a pre-crisis (observations prior to August 2008) and a post-crisis period (after August 2008). Some relevant conclusions arise from table 3.4. First, the covariance of risk aversion with economic variables disagree across economic areas. OLS estimates show that, for the whole sample period, there is no statistically significant variable that explains the risk aversion of the S&P 500 index. By contrast, EuroStoxx 50 and Nikkei 225 exhibit statistically significant betas for unemployment ($UNEMP$) and Consumer Confidence Index (CCI), for the former index; and the VIX, for the latter. The sign of the CCI coefficient is negative, as expected: the higher the consumer confidence, the lower the risk aversion. However the sign for the unemployment and the VIX are not the expected ones.

These variables seem to capture an important proportion of variability in sample, with adjusted-R^2 coefficients of 15.3% (EuroStoxx 50) and 19.0% (Nikkei 225).

The comparison by subperiods provides additional insights about the nature of risk aversion. An interesting conclusion is that covariates of risk aversion change over time: within the pre-crisis period, both the implied volatility index (VIX) and the level of interest rates (IR) are statistically significant for the S&P 500 risk aversion series, being both coefficients positive and significant. These results are consistent with those of Rosenberg and Engle (2002), who find that the implied volatility is statistically significant and positive for their sample which covers the period from 1991 to 1995. Nevertheless, no estimates seem to covariate with EuroStoxx 50 and Nikkei 225 risk aversion series for this period.

This situation changes after the crisis. For the S&P 500 index, just the VIX remains significant whose sign changes with the crisis, becoming this coefficient negative. Regarding the Eurozone and Japan, results are the same as for the whole period, that is, unemployment ($UNEMP$) and the Consumer Confidence Index (CCI) are statistically significant for the EuroStoxx 50; and only the implied volatility index (VIX) appears as being statistically significant for the Nikkei 225. Their signs remain unchanged for this period.[26]

These results yield to the conclusion that the risk aversion series do not respond to the same macroeconomic variables in the different markets considered, or even for different periods of time for which economic conditions differ. This suggests that risk aversion series are heterogeneous across markets and in time periods in which the economic reality changes.

[26]These results are for monthly risk aversion series for a level of moneyness 1; however, results hold for a moneyness value of 0.97.

3.3.3 VAR analysis

Interested in the existence of lead-lag relationships among the risk aversion series, we jointly model the monthly behavior of these series with a Vector AutoRegressive process (VAR). This model choice allows us to not only permit each of the variables to depend on their own lags, but also on the others' series lags. The number of lags relies on the Bayesian Information Criteria. The VAR model is designed as follows,

$$\begin{pmatrix} RA_t^{SP} \\ RA_t^{EU} \\ RA_t^{JP} \end{pmatrix} = \begin{pmatrix} \alpha_{SP} \\ \alpha_{EU} \\ \alpha_{JP} \end{pmatrix} + \Gamma \cdot \begin{pmatrix} RA_{t-1}^{SP} \\ RA_{t-1}^{EU} \\ RA_{t-1}^{JP} \end{pmatrix} + \begin{pmatrix} \epsilon_{SP,t} \\ \epsilon_{EU,t} \\ \epsilon_{JP,t} \end{pmatrix}, \tag{3.17}$$

with RA_t^{SP}, RA_t^{EU} and RA_t^{JP} stand for the risk aversion series at time t of S&P 500, EuroStoxx 50 and the Nikkei 225 indexes, respectively; α is a column vector of constants; Γ is a 3x3 matrix for the coefficient estimates of the lagged risk aversion terms, and ϵ is the vector of error terms.

Table 3.5 reports the maximum likelihood estimates of the Γ matrix. In general, risk aversion series just depend on their own lags. These coefficients are positive and statistically significant, being their magnitude comparable and higher than 0.75. This result manifests the high persistence in risk aversion series. Interestingly enough, the lagged term of S&P 500 is statistically significant and negative for the equation of the contemporaneous risk aversion value of EuroStoxx 50 index. It seems that European investors keep an eye on the US events to construct their risk aversion.

Previous results seem to establish a linkage between the US and European risk aversion. Deepening on this observation, our modeling choice in (3.17) permits to explore the responses in the risk aversion of one certain area to shocks in other areas. This is the well-known generalized impulse-response (IRF) analysis, defined by Pesaran and Shin

(1998) as,

$$IRF_i(n) = \sigma_{jj}^{-1/2} B_n \Sigma e_j \tag{3.18}$$

with σ_{jj} the variance of market j, B_n the coefficient matrices of the different periods, where $n = 0, 1, 2, ...$; Σ the covariances of the innovations term, and e_j is the vector of shocks taking value 1 for the variable being shocked and 0 elsewhere.

The results of IRF analysis are presented in figure 3.3. This figure shows, in rows, the impulse of one standard deviation in the risk aversion series of S&P 500 (first row), EuroStoxx 50 (second row) and Nikkei 225 (third row), and the response provoked in other indexes. The main result is that shocks in the risk aversion series from S&P 500 seem to exhibit a significant effect in the EuroStoxx 50 ones. Contrarily, the remainder series do not present significant responses to shocks in foreign markets. These results are in line with those obtained for the VAR model.

Interested on a causality pattern between US and Eurozone risk aversion series, we perform a Granger causality test (Granger, 1969). Table 3.6 provides the results. In line with previous findings, the null hypothesis that S&P 500 risk aversion series Granger causes the risk aversion of EuroStoxx 50 cannot be rejected. Nevertheless, the existence of causality in the sense of Granger is rejected for the rest of cases under study.

3.4 Conclusions

The behavior of the risk aversion is of major importance in macroeconomic policy as well as in asset pricing. This chapter is devoted to study the risk aversion inferred from option prices in three main developed economic areas: United States (S&P 500 index), the Eurozone (EuroStoxx 50 index) and Japan (Nikkei 225 index) and their patterns and relationships across the different markets.

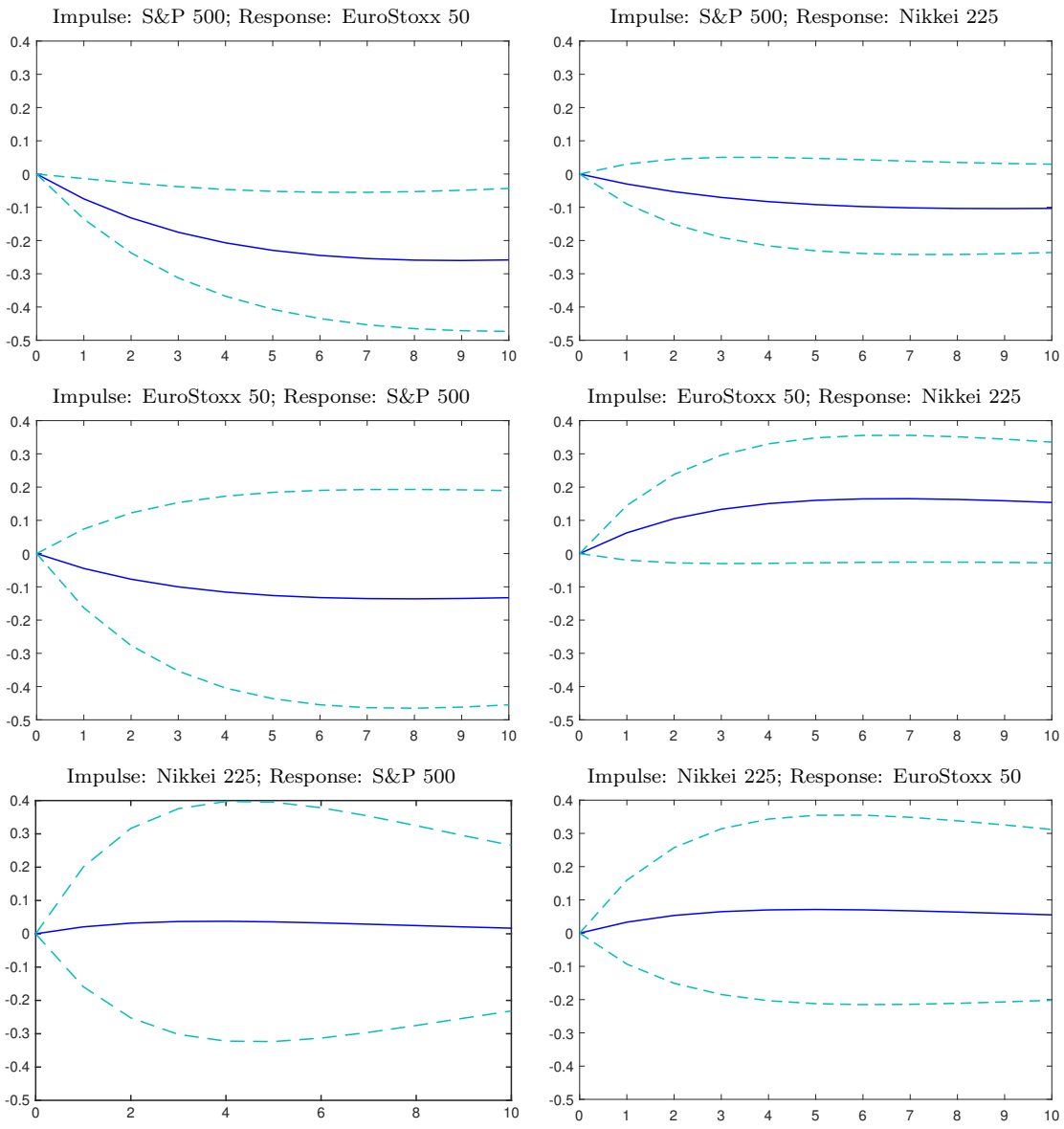

Figure 3.3: **Impulse-response analysis of the risk aversion series.** This figure shows the impulse-response function for the different markets under study. Top row shows impulses (shocks) in the S&P 500 index and their response in the EuroStoxx 50 index (left plot) and in the Nikkei 225 index (right plot). Second row represents impulses in the EuroStoxx 50 index and the effect provoked in the S&P 500 market (left plot) and in the Nikkei 225 market (right plot). Finally, the last row contains the plots of impulses in the Nikkei 225 and how they are transmitted to the S&P 500 index (left plot) and to the EuroStoxx 50 index (right plot). The impulse-response function is depited in a solid blue line and confidence intervals are represented in a dashed light blue line.

Risk aversion series have been obtained directly from the existent relationship between RNDs and SPDs. By doing this, we escape from making assumptions about the correct parametric form of the utility function in the different markets under study. Our RNDs are embedded from observed option prices (forward-looking) using a non-parametric technique. On the other hand, SPDs are estimated using observed prices of the underlying together with GJR methods to make predictions which are then fitted using a Kernel Density.

As one would expect, risk aversion time series exhibit different behavior across different levels of moneyness. In this study we consider moneyness levels of 0.97, 1 and 1.03, and we can see that the level of risk aversion lessens as the moneyness increases. Likewise, and only for the lowest moneyness levels (0.97), the longer the time horizon considered, the lower the risk aversion is. This is consistent with the fact that investors are willing to assume a higher risk premia to avoid negative wealth shocks in the short term (30 days).

We can see that risk aversion time series manifest negative values during some specific periods. Furthermore, comparing the series across markets, we can recognize a common pattern suggesting the existence of commonalities which are further explored by performing a PCA. Indeed, this analysis concludes the existence of a first principal component which explains more than the 50% of the joint variability by itself. This result is consistent across different moneyness levels. For moneyness of 1, this component is mainly represented by the EuroStoxx 50 and the Nikkei 225, whereas for more extreme moneyness values the load of each market is more evenly distributed. In order to dig deeper in such commonalities, we regress this component against some macroeconomic variables to find out that global uncertainty variables such as the VIX index and the US Treasury slope could well drive this common component of the risk aversions.

An OLS regression of the risk aversion series against a pool of macroeconomic variables is performed and concludes that, the risk aversion series from each market covariate

with different macroeconomic variables. We also find differences in the covariates across different periods. When we consider the whole period of observations, no macroeconomic variable seems to explain the series of the S&P 500 index. However, for the subperiod prior to the crisis, both VIX and the interest rate appear as statistically significant and positive. For the post-crisis period, only the VIX index is significant, being its sign now negative. Regarding the EuroStoxx 50 both the unemployment and the Consumer Confidence Index are statistically significant and negative; and for the Nikkei 225 we find negative statistically significance of the VIX index. These results for both markets hold for the post-crisis period as well. However, for the pre-crisis period, none of these two markets seems to be explained by any of the macroeconomic variables considered. These results suggest heterogeneity in the risk aversion series of the different economic areas under study.

A lead-lag relationship between the different series is explored by performing a VAR analysis. Results show how the different series depend on their own lags only, except for the EuroStoxx 50 which also depends upon the S&P 500 lagged series. These results are in line with the findings of the impulse-response analysis, which shows that, among all the markets considered, only a unit shock in the S&P 500 index has some significant impact in the EuroStoxx 50. Likewise, the Granger causality test concludes that only the S&P 500 index Granger causes the risk aversion of the EuroStoxx 50.

	Whole sample period			Pre-crisis period			Post-crisis period		
	sp	eu	jp	sp	eu	jp	sp	eu	jp
vix	0.063	0.039	-0.22***	0.84*	0.793	-0.085	-0.291**	0.058	-0.166***
	(0.67)	(0.39)	(-4.64)	(2.08)	(1.28)	(-0.21)	(-3.37)	(0.67)	(-3.88)
infl	0.211	-0.177	0.263	1.625	-0.327	1.598	0.122	2.181	-0.058
	(0.14)	(-0.08)	(0.27)	(0.80)	(-0.04)	(0.55)	(0.08)	(1.13)	(-0.07)
ipi	-0.755	0.153	0.010	0.0152	0.908	1.098	-0.817	-0.105	-0.029
	(-0.85)	(0.27)	(0.06)	(0.01)	(0.63)	(1.24)	(-1.03)	(-0.20)	(-0.22)
unemp	-6.610	-31.31***	0.496	-1.640	-37.62	-0.045	-0.236	-19.12**	0.280
	(-1.58)	(-3.74)	(0.19)	(-0.18)	(-1.22)	(-0.01)	(-0.06)	(-2.64)	(0.12)
epui	0.005	-0.005	0.007	0.009	0.028	0.065	-0.001	-0.011	0.005
	(0.26)	(-0.28)	(0.51)	(0.16)	(0.50)	(0.93)	(-0.09)	(-0.69)	(0.44)
cci	-0.429	-9.687**	0.013	-2.414	28.66	-6.640	0.436	-9.077**	0.950
	(-0.16)	(-2.81)	(0.01)	(-0.68)	(1.21)	(-0.86)	(0.16)	(-3.21)	(0.65)
us_eur	10.10	18.07		11.23	-25.21		-13.39	18.44	
	(0.45)	(0.81)		(0.20)	(-0.40)		(-0.68)	(0.93)	
y_us	0.385		0.215	-0.248		0.447	0.123		0.308
	(1.15)		(1.13)	(-0.35)		(0.96)	(0.37)		(1.64)
y_eur		0.236	-0.025		0.735	0.537		0.228	-0.084
		(1.04)	(-0.20)		(0.93)	(1.03)		(1.16)	(-0.79)
ir	1.234	2.369	3.075	9.695*	10.85	9.503	2.068	-1.275	-3.163
	(0.40)	(0.67)	(0.63)	(2.17)	(0.91)	(0.84)	(0.68)	(-0.41)	(-0.63)
slope	4.578	1.805	1.341	6.033	-0.822	-2.687	0.285	1.360	4.167
	(1.51)	(0.59)	(0.28)	(0.99)	(-0.06)	(-0.24)	(0.11)	(0.54)	(0.91)
cons	2.121	1.083	6.700***	-14.54*	-8.912	5.760	12.25***	-1.098	4.625***
	(1.07)	(0.54)	(6.63)	(-2.52)	(-0.97)	(1.01)	(6.21)	(-0.60)	(4.65)
N	136	136	136	38	38	38	97	97	97
adj. R^2	-0.015	0.153	0.190	0.174	0.114	-0.026	0.131	0.145	0.165

t statistics in parentheses

* $p < 0.05$, ** $p < 0.01$, *** $p < 0.001$

Table 3.4: **OLS estimates for the risk aversion series against macroeconomic variables.** This table shows the coefficient estimates from the OLS regression performed on each of the risk aversion series against a pool of macroeconomic variables shown in column 1. The regression is performed on three different periods. Columns 2-4 contains the estimates when the whole period of data is considered (from May 2004 to September 2015), columns 5-7 for the pre-crisis period (prior to August 2008) and columns 8-10 for the post-crisis period (after August 2008). All these regresssions are performed for the three markets under study: S&P 500 (sp), the EuroStoxx 50 (eu) and the Nikkei 225 (jp). The regression is performed on monthly series of risk aversion for a moneyness level of 1 and 91-days time horizon.

	SP Risk Aversion	EU Risk Aversion	JP Risk Aversion
Lag sp	0.852***	-0.0747*	-0.0301
	(19.25)	(-2.40)	(-0.98)
Lag eu	-0.0447	0.901***	0.0625
	(-0.74)	(21.19)	(1.49)
Lag jp	0.0208	0.0330	0.757***
	(0.23)	(0.51)	(11.92)
cons	0.597	0.352	0.594*
	(1.57)	(1.32)	(2.25)
adj. R^2	0.7332	0.8559	0.6797

t statistics in parentheses

* $p < 0.05$, ** $p < 0.01$, *** $p < 0.001$

Table 3.5: **VAR estimation coeficients.** The table shows estimates of the VAR model for the risk aversion series of the S&P 500 index (SP Risk Aversion), the EuroStoxx 50 (EU Risk Aversion) and the Nikkei 225 (JP Risk Aversion). Second row shows the coefficient estimates corresponding to the effect of one lag in the S&P 500 (Lag sp), third row contains the effect of one lag in the EuroStoxx 50 (Lag eu) and the fourth row is for a lag in the Nikkei 225 (Lag jp) and fifth row is for the constant term (cons). Information about the adjusted-R^2 for each of the series is provided in the last row (adj. R^2). The analysis is based on monthly series of risk aversion for a moneyness of 1 and 91 days time horizon.

Equation	Excluded	chi2	df	Prob > chi2
S&P 500	EuroStoxx 50	0.54609	1	0.460
S&P 500	Nikkei 225	0.05145	1	0.821
S&P 500	ALL	0.65569	2	0.720
EuroStoxx 50	S&P 500	5.7754	1	0.016
EuroStoxx 50	Nikkei 22 5	0.2628	1	0.608
EuroStoxx 50	ALL	5.9103	2	0.052
Nikkei 225	S&P 500	0.96123	1	0.327
Nikkei 225	EuroStoxx 50	2.2192	1	0.136
Nikkei 225	ALL	3.352	2	0.187

Table 3.6: **Granger causality.** The table shows the Granger causality test results for the risk aversion series of the different indexes (S&P 500, EuroStoxx 50 and Nikkei 225). First column shows the market for which the Granger causality is being tested. Second column shows the variable which is excluded from the chi-squared test of jointly significance; this is, the market assumed by the null hypothesis to not Granger cause the risk aversion series for the market in column 1. Third column (chi2) contains the χ^2 statistic, column (df) shows the number of lags of the dependent variables, and the last column (Prob > chi2) contains the p-value of the test. The analysis is based on monthly series of risk aversion for a moneyness of 1 and 91-days time horizon.

Chapter 4

Conclusions and future work

By having a spectrum of option prices written on the same underlying we can obtain information about the whole Risk-Neutral Distribution (RND). Such RNDs are of great importance for portfolio and risk managers, thus being their analysis of major interest.

Among all investors' concerns, we spot mainly the forecasting ability of the embedded RNDs, as well as the transmission effects of the risk-neutral implied expected losses and how this affects the diversification and exposure of their portfolios. Concurrently, the patterns and changes over time of the risk aversion measure – which depicts the deviations from the risk-neutral and the real-world (investors' preferences) – is of paramount interest in macroeconomic policy and asset pricing.

Throughout these chapters and based on the information embedded in the option prices, we answered the previous questions by implementing different analyses and methodologies.

In chapter 1 we learned about the ability of the RNDs to predict future realizations of the underlying. Results showed that the conclusions reached so far by the literature,

which were based on the Berkowitz test results, are not accurate for this type of data, since the assumptions over which the test is built (normality and independence) are too restrictive and continuously violated. To overcome these issues, we performed block-bootstrap distribution of the Berkowitz statistics. Likewise, in order to double check on the forecasting ability of the RNDs, we also calculated the block-bootstrap distribution of the Cramer-von-Misses statistics. Furthermore, the fit of the tails of the RNDs was also studied.

The analysis was performed on three major US index options: S&P 500, Nasdaq 100 and Russell 2000 for a range of data from 1996 to 2015. In order to avoid biases due to the techniques used to extract the RNDs, both parametric and non-parametric methods were used for different markets and for RNDs with different time horizons (30, 45, 60 and 90 days).

Contrary to the literature, Berkowitz block-bootstrap results could not reject the forecasting ability of any of the estimated RNDs. This conclusion was reinforced by the Cramer-von-Mises block-bootstrap findings. Regarding the fit of the tails, the test suggested that the RNDs tended to overestimate the frequency of occurrence of the left tail, providing a good fit for the right tail.

Additionally, when we removed from the sample those turbulent periods from the crises, results still held. Therefore, results also claimed that the crisis periods were not responsible for such conclusions.

Analysis in chapter 2 helped us to gain some knowledge about the connectedness of different markets and how shocks in the expected (loss) quantiles of the option-implied distributions are transmitted across borders. We considered three main developed financial markets: United States, Eurozone and Japan, represented by the S&P 500, EuroStoxx 50 and Nikkei 225 indexes, respectively.

We calculated the RNDs non-parametrically for each day in the sample for different time horizons (30, 60 and 91 days) and for different indexes. The period covered by this analysis is from May 2004 until September 2015. In order to obtain the implied expected losses, we calculated different quantiles (5%, 10%, 15%, 20% and 25%) of the extracted RNDs. Furthermore, to deal with the non-synchronicity of the data due to the time-zone difference of the markets, we modeled the dynamics of the markets using an S-VAR process (which accounts for contemporaneous relationships) as well as a VAR model by computing weekly averages of the observations. Global risk effects were considered by including series of the VIX index as exogenous variable in both of the previous approaches.

Impulse-response analyses concluded transmission only of shocks in the S&P 500 expected loss quantiles to the rest of the markets; however, there was no significant evidence of the transmission of shocks from the other markets. Results also showed that the effects provoked by shocks in the S&P 500 index to other markets were the same regardless of the level of the quantile considered (5% to 25%). However, differences did exist depending on the time horizon considered, being the effects of the transmission softer for shorter horizons (30 days) and stronger for longer horizons (60 and 91 days).

Finally, variance decomposition analyses concluded that most of the variance was explained by shocks in its own quantile (lagged), suggesting an autoregressive pattern in the loss quantiles. Empirical results qualitatively held for the different methodologies, quantile levels and time horizons, proving robustness of the results.

Chapter 3 enriched our knowledge about risk aversion series in different developed markets: US (S&P 500), Eurozone (EuroStoxx 50) and Japan (Nikkei 225). This chapter studied the patterns and evolution of risk aversions over time and within different markets. Time series showed an inverse relationship between the risk aversion and the level of moneyness tested, presenting occasionally negative values. A principal component analysis confirmed the existence of a source of commonality which explained more than the 50%

of the joint variability (being so for different levels of moneyness tested). After an OLS regression, we concluded that this could be well explained by global factors such as the VIX index and the US Treasury slope.

In order to gain insight into the relationship between risk aversion series and some major macroeconomic variables, an OLS regression is run for each of the market series. Results concluded heterogeneity since each of them covariate with different factors. Besides this difference was also notable not only across markets, but also between different periods considered (pre- and post-crisis). The analysis concluded that country-specific forces led the contemporaneous risk aversion series. We also found a lead-lag relationship between US and Europe, where lags of the S&P 500 risk averion series had significant effects in the EuroStoxx 50 series. These results were further confirmed by the impulse-response analysis and the Granger causality test.

4.1 Future research

The analyses done in this thesis have enriched our knowledge about important questions such as the forecasting ability of the RND and expected loss transmission across different countries. Furthermore, it has also provided us with a broader vision about the nature and evolution of the risk aversion series in different markets.

Nevertheless, there is still room for further improvement, and while doing this thesis we have spotted some interesting issues which will set the course of forthcoming research during these years to come.

First of all, even though the analysis of the implied expected loss transmission in chapter 2 gives some guides on the transmission effects across markets, further analyses are required in order to determine whether there is in fact a driving market. Moreover, by

replicating the analysis of the transmission effects for longer maturities, we will be able to recognize whether option-implied risk-neutral quantile shocks are permanent or transitory.

Furthermore, from the results in chapter 3, interesting features are captured in the left tails of the RNDs and SPDs; therefore, lower levels of moneyness are worth to study so to gain knowledge about the risk premia and bad states fear.

Moving a step forward, the previous sets the foundations for a new line of research using information retrieved from option prices (forward-looking) to the study of portfolio choice.

Appendix A

Can we really discard forecasting ability of option-implied Risk-Neutral distributions?

A.1 Derivation of Mixture of Two Log-Normal Distributions

A mixture of two Log-Normal distributions is equivalent to a weighted average of two Log-Normal distributions. Therefore, being $\Psi(x|F,\, \sigma,\, T)$ a Log-Normal density function, the estimated Risk-Neutral distribution $f_Q(x)$ is of the form,

$$f_Q(x) = p\,\Psi(x|F_1, \sigma_1, T) + (1-p)\,\Psi(x|F_2, \sigma_2, T) \tag{A.1}$$

where x is the domain of forward prices over which the density is defined, F_1 (F_2) is the expected forward price of the underlying at a specific time T for the first (second)

Log-Normal distribution and σ_1 (σ_2) is the standard deviation for the first (second) Log-Normal distribution in the mixture. Parameters p and $(1-p)$ are the weights placed on each of the two Log-Normal distributions being mixed and are defined within $0 \leq p \leq 1$.

In order to fit the mixture of two Log-Normal distributions to estimate the RNDs, five parameters need to be calibrated, $\theta = \{F_1,\, F_2,\, \sigma_1,\, \sigma_2,\, p\}$. However, as it is explained in Taylor (2005), for equation (A.1) to be a Risk-Neutral distribution (RND) we must ensure that,

$$F = p\, F_1 + (1-p)\, F_2$$

At this point, there is no need to estimate F_2 any longer since it can be inferred from the previous as follows,

$$F_2 = \frac{F - p\, F_1}{(1-p)}$$

therefore, we carry out the calibration on the remaining four parameters, $\theta = \{F_1,\, \sigma_1,\, \sigma_2,\, p\}$.

The theoretical price for a call option whose underlying distribution is a LNM is given by,

$$c(X|\theta, r, T) = p \cdot C_{BS}(F_1, T, X, r, r, \sigma_1) + (1-p) \cdot C_{BS}(F_2, T, X, r, r, \sigma_2) \tag{A.2}$$

where $C_{BS}(F_i, T, X, r, r, \sigma_i)$ is the theoretical price for a call option using Black-Scholes formula, F_i the forward price at time T, X the exercise price, r the risk-free rate and σ_i its standard deviation, for $i = 1, 2$.

The value of the unknown parameters $\theta = \{p, F_1, \sigma_1, \sigma_2\}$, can be fairly easily estimated by minimizing the sum of the squared pricing errors,

$$\theta^* = \arg\min \sum_{i=1}^{n_j} \left(C_{i,j}^m - \widehat{C}_{i,j}(\theta) \right)^2 \tag{A.3}$$

where n_j is the number of observations on day j, $C^m_{i,j}$ are the observed market option prices on day j and $\widehat{C}_{i,j}(\theta)$ stands for the corresponding theoretical option prices estimated under the selected model (LNM in this case).

A.2 Chossing the bandwidth

RNDs are very sensitive to the choice of the bandwidth parameter (h). Therefore, setting parameter h is crucial in order to obtain good estimates of the RNDs. If we set a small bandwidth we will get a rough estimation, reflecting all the noise of the data and yielding to inconsistent densities (densities with negative portions). On the other hand, choosing a large value for the bandwidth will result in the data being oversmoothed. Since our goal is the second derivative of the smoothed function, in general we will need to oversmooth the fit using values of h slightly higher than usual.

In order to obtain the bandwidth parameter h, the most common approaches are the *Silverman's Rule-of-Thumb* (h_{RoT}) and *leave-one-out cross-validation* (h_{cv}). For a given day in our sample, we first set as the bandwidth parameter that value obtained by the cross-validation approach. Should the density have negative regions, we then set a grid formed by 50 points between the range $[h_{cv};\ 2 \cdot h_{RoT}]$, and choose that minimum value of h that yields to a well-behaved density (smooth and positive in all its domain).

A.3 Adding Generalized Pareto tails

As mentioned previously, with the kernel and spline techniques we are only capable to estimate the central part of the distribution where available observations lay, having a missing probability at the extremes of the density. Once we have the extracted RNDs, in order to append tails we require to have a missing amount of probability in the tail

to be fitted of at least 0.1%. Should we have a lesser amount of missing probability, no estimation of the tails is required since almost all the density is explained by the observed data.

In case tails are needed, we follow Birru and Figlewski (2012) and use the GPD to approximate the tails of our estimated distributions. In order to do so, we first define one extreme point for each tail called $X_{\alpha_{0R}}$ and $X_{\alpha_{0L}}$ which leave α_{0R} and α_{0L} probability in the right and left tail respectively. In case one or both α_{0R} and α_{0L} are smaller than 1%, we will manually set such α values to be 1%.

We also set an inner second point for each tail called $X_{\alpha_{1R}}$ and $X_{\alpha_{1L}}$, leaving α_{1R} and α_{1L} probability in their respective tails. We define α_{1R} and α_{1L} as

$$\begin{aligned} \alpha_{1R} &= \alpha_{0R} - p \\ \alpha_{1L} &= \alpha_{0L} + p \end{aligned} \tag{A.4}$$

being p some amount of probability. In our case p is set to be 1% probability.

In order to find the GPD parameters, some matching conditions need to be satisfied. We denote the extracted RND and cumulative probability function by $f(\ldots)$ and $F(\ldots)$, respectively. First, we require that the amount of probability contained in each of the GPD tails is the same as the amount contained in the estimated RND tails. And second, we force the new GPD density to pass through the exact $f(X_{\alpha_{0R}})$ $(f(X_{\alpha_{0L}}))$ and $f(X_{\alpha_{1R}})$ $(f(X_{\alpha_{1L}}))$ points, thus matching the shape of the estimated RNDs. That is, both distributions match at the following points,

$$\begin{aligned} F(X_{\alpha_{0L}}) &= F^{GPD}(X_{\alpha_{0L}}) \qquad & F(X_{\alpha_{0R}}) &= F^{GPD}(X_{\alpha_{0R}}) \\ f(X_{\alpha_{0L}}) &= f^{GPD}(X_{\alpha_{0L}}) \qquad & f(X_{\alpha_{0R}}) &= f^{GPD}(X_{\alpha_{0R}}) \\ f(X_{\alpha_{1L}}) &= f^{GPD}(X_{\alpha_{1L}}) \qquad & f(X_{\alpha_{1R}}) &= f^{GPD}(X_{\alpha_{1R}}) \end{aligned} \tag{A.5}$$

However, between $X_{\alpha_{0R}}$ and $X_{\alpha_{1R}}$, as well as between $X_{\alpha_{0L}}$ and $X_{\alpha_{1L}}$, both the estimated RND and the fitted GPD are overlapping, having different values for each strike price contained within this overlapping zone. In order to approximate the distribution of this overlapping zone we define a weighting function which will give different weights to the strike prices based on their distance to $X_{\alpha_{0R}}$, $X_{\alpha_{0L}}$, $X_{\alpha_{1R}}$ and $X_{\alpha_{1L}}$,

$$w = \frac{f\left(X_{\alpha_{0R}}\right) - f\left(X_i\right)}{f\left(X_{\alpha_{0R}}\right) - f\left(X_{\alpha_{1R}}\right)} \tag{A.6}$$

for those i observations which lay within $X_{\alpha_{1R}}$ and $X_{\alpha_{0R}}$. By doing this we avoid abrupt jumps next to the matching points so to reach a smooth transition between both distributions. The smoothed density values for each i data point is then calculated by,

$$f_{X_i}^{new} = w_i f_{X_i} + \left(1 - w_i\right) f_{X_i}^{GPD}$$

The equivalent equations for the left overlapping zone are,

$$w = \frac{f\left(X_{\alpha_{1L}}\right) - f\left(X_i\right)}{f\left(X_{\alpha_{1L}}\right) - f\left(X_{\alpha_{0L}}\right)} \tag{A.7}$$

and

$$f_{X_i}^{new} = \left(1 - w_i\right) f_{X_i} + w_i f_{X_i}^{GPD}$$

Figure 1.1 shows the RND calculated on the S&P 500 for a time horizon of 30 days on the 17 December 2009. In this figure we can appreciate the main body of the distribution (central solid line), which in this case has been calculated using kernel technique; the extreme solid lines which represent the pareto tails which have been appended in each case; and finally the figure depicts with a dotted line what we call the overlapping zone, that is the region between α_0 and α_1 which has been approximated using a weighting scheme as per equations (A.6) and (A.7).

Appendix B

Why so different? Understanding the behavior of risk aversion in developed economies

B.1 Correlation matrix between macroeconomic variables

When regressing the risk aversion series against the set of macroeconomic variables chosen, we could be facing a problem of collinearity. This is, we might be including in the analysis highly correlated variables which will be explaining some of the same variance, and therefore their statistical significance in the model will be reduced. In order to avoid collinearity in our model defined in expression (3.16), we calculate the correlations between the macroeconomic variables for each of the markets considered. Correlations are presented in the following table B.1, where we can see that the correlations between the pairs of variables are fairly low, therefore rejecting the inclusion of redundant variables.

PANEL A - Correlation matrix for the S&P 500

	vix	infl	ipi	unemp	epui	cci	us_eur	y_us	ir	slope
vix	1.0000									
infl	-0.0345	1.0000								
ipi	-0.3333	-0.1924	1.0000							
unemp	0.4634	-0.0088	-0.3529	1.0000						
epui	0.0220	0.1298	-0.1389	0.0636	1.0000					
cci	-0.0863	-0.0405	0.0168	-0.1488	-0.2082	1.0000				
us_eur	-0.2108	0.2394	0.0071	0.0527	-0.0284	-0.1457	1.0000			
y_us	-0.3299	-0.0944	0.0676	-0.0738	-0.1995	0.2774	-0.2506	1.0000		
ir	-0.2102	-0.0512	0.1441	-0.0188	-0.1516	0.0862	-0.1024	0.4694	1.0000	
slope	0.1344	-0.0030	-0.0020	0.0466	-0.0531	-0.0156	-0.0274	0.0148	0.3138	1.0000

PANEL B - Correlation matrix for the EuroStoxx 50

	vix	infl	ipi	unemp	epui	cci	us_eur	y_eur	ir	slope
vix	1.0000									
infl	-0.2484	1.0000								
ipi	-0.3923	0.2046	1.0000							
unemp	0.6652	-0.2725	-0.3708	1.0000						
epui	0.0898	0.0680	0.0511	0.0288	1.0000					
cci	-0.3845	0.0041	0.3946	-0.3077	-0.1562	1.0000				
us_eur	-0.2108	0.1631	0.0709	-0.1336	-0.0498	0.2199	1.0000			
y_eur	-0.4431	0.1426	0.1432	-0.1055	-0.2249	0.2970	0.6070	1.0000		
ir	-0.3496	0.1872	0.1890	-0.2455	-0.1949	0.2883	0.3037	0.5190	1.0000	
slope	0.3634	-0.0926	-0.1443	0.2382	0.0581	-0.2159	-0.2084	-0.2012	0.1659	1.0000

PANEL C - Correlation matrix for the Nikkei 225

	vix	infl	ipi	unemp	epui	cci	y_eur	y_us	ir	slope
vix	1.0000									
infl	-0.0195	1.0000								
ipi	-0.2432	-0.0702	1.0000							
unemp	0.1918	0.0376	-0.0739	1.0000						
epui	0.0455	0.0637	0.0324	-0.0974	1.0000					
cci	0.1010	-0.0788	0.2672	0.1733	-0.0527	1.0000				
y_eur	-0.4431	0.0604	0.0874	0.0061	-0.2163	0.0035	1.0000			
y_us	-0.3299	-0.0210	0.1074	-0.0154	-0.1610	0.1399	0.6064	1.0000		
ir	-0.1404	0.0130	0.1193	-0.1274	-0.0253	0.0099	0.2137	0.2647	1.0000	
slope	0.0240	-0.1115	0.0513	-0.0261	-0.2195	0.0592	0.1828	0.2669	0.7214	1.0000

Table B.1: **Correlation matrix between macroeconomic variables.** The table contains the correlation matrices between the macroeconomic variables considered in this study for each of the markets considered. Panel A shows the correlation matrix for the variables corresponding to the US market (S&P 500 index), panel B contains the correlation matrix of those macroeconomic variables corresponding to the Eurozone market (EuroStoxx 50 index) and finally panel C shows the correlation matrix for those macroeconomic variables corresponding to the Japanese market (Nikkei 225 index).

Bibliography

Almeida, C., Ardison, K., Garcia, R., Vicente, J., 2017. Nonparametric tail risk, stock returns and the macroeconomy. Journal of Financial Econometrics 15 (3), 333–376.

Alonso, F., Blanco, R., Rubio, G., 2005. Testing the forecasting performance of ibex 35 option-implied risk-neutral densities., working paper No. 0505, Banco de España.

Alonso, F., Blanco, R., Rubio, G., 2006. Option-implied preferences adjustments, density forecasts, and the equity risk premium.

Anagnou, I., Bedendo, M., Hodges, S., Tompkins, R., 2002. The relationship between implied and realised probability density functions, working paper, University of Warwick and the University of Technology, Vienna.

Anagnou, I., Bedendo, M., Hodges, S., Tompkins, R., 2005. Forecasting accuracy of implied and garch-based probability density functions. Review of Futures Markets 11, 41–66.

Aït-Sahalia, Y., Fan, J., Li, Y., 2013. The leverage effect puzzle: Disentangling sources of bias at high frequency. Journal of Financial Economics 109, 224–249.

Aït-Sahalia, Y., Lo, A. W., April 1998. Nonparametric estimation of state-price densities implicit in financial asset prices. The Journal of Finance 53, 499–547.

Aït-Sahalia, Y., Lo, A. W., 2000. Nonparametric risk management and implied risk aversion. Journal of Econometrics 94, 9–51.

Bahra, B., 1997. Implied risk-neutral probability density functions from option prices: Theory and application., working paper, Bank of England.

Baker, S. R., Bloom, N., Davis, S. J., November 2016. Measuring economic policy uncertainty. The Quarterly Journal of Economics 131 (4), 1593–1636.

Banz, R., Miller, M., 1978. Prices for state-contingent claims: Some estimates and applications. Journal of Business 51 (4), 653–672.

Bartunek, K., Chowdhury, M., February 1997. Implied risk aversion parameter from option prices. Financial Review 32 (1), 107–124.

Bedoui, R., Hamdi, H., 2015. Option-implied risk aversion estimation. The Journal of Economic Asymmetries 12, 142–152.

Berkowitz, J., 2001. Testing density forecasts with applications to risk management. Journal of Business and Economic Statistics 19, 465–474.

Birru, J., Figlewski, S., 2012. Anatomy of a meltdown: The risk neutral density for the s&p500 in the fall of 2008. Journal of Financial Markets 15, 151–180.

Black, F., Scholes, M., May-June 1973. The pricing of options and corporate liabilities. The Journal of Political Economy 81 (3), 637–654.

Bliss, R. R., Panigirtzoglou, N., 2002. Testing the stability of implied probability density functions. Journal of Banking and Finance 26, 381–422.

Bliss, R. R., Panigirtzoglou, N., 2004. Option-implied risk aversion estimates. Journal of Finance 59, 407–446.

Bollerslev, T., 1986a. Generalised autoregressive conditional heteroskedasticity. Journal of Econometrics 31, 307–327.

Bollerslev, T., 1986b. Generalized autoregressive conditional heteroskedasticity. Journal of Econometrics 31 (3), 307–327.

Bollerslev, T., Zhou, H., 2006. Volatility puzzles: a simple framework for gauging return-volatility transmissions. Journal of econometrics 131 (1-2), 123–160.

Bookstaber, R. M., McDonald, J. B., 1987. A general distribution for describing security price returns. Journal of Business 60 (3).

Breeden, D. T., Litzenberger, R. H., October 1978. Price of state-contingent claims implicit in option prices. Journal of Business 51 (4), 621–651.

Brooks, C., 2008. Introductory econometrics for finance. Cambridge University Press.

Bu, R., Hadri, K., 2007. Estimating option implied risk-neutral densities using spline and hypergeometric functions. Econometrics Journal 10 (2), 216–244.

Campa, J., Chang, K., Reider, R., February 1998. Implied exchange rate distributions: Evidence from otc option markets. Journal of International Money and Finance 17 (1), 117–160.

Carnero, M. A., Peña, D., Ruiz, E., 2007. Effects of outliers on the identification and estimation of garch models. Journal of Time Series Analysis 28, 471–497.

Carnero, M. A., Peña, D., Ruiz, E., 2012. Estimating garch volatility in the presence of outliers. Economic Letters 114, 86–90.

Constantinides, G. M., 1982. Intertemporal asset pricing with heterogeneous consumers and without demand aggregation. Journal of Business 55, 253–268.

Coutant, S., 2000. Time-varying implied risk aversion in option prices using hermite polynomials, working paper, Banque de France.

Craig, B., Glatzer, E., Keller, J., Scheicher, M., 2003. The forecasting performance of the german stock option densities, discussion Paper 17, Studies of Economic Research Centre, Deutsche Bundesbank.

Cramer, H., 1928. On the composition of elementary errors. Scandinavian Actuarial Journal, 13–74.

Dickey, D. A., Fuller, W. A., 1979. Distribution of the estimators for autoregressive time series with a unit root. Journal of the American Statistical Association 74, 427–431.

Engle, R., Kroner, K. F., 1995. Multivariate simultaneous generalized arch. Econometric theory 11 (01), 122–150.

Engle, R. F., Ng, V. K., Rothschild, M., July/August 1990. Asset pricing with a factor arch covariance structure : Empirical estimates for treasury bills. Journal of Econometrics 45 (1/2), 213–237.

Eun, C. S., Shim, S., June 1989. International transmission of stock market movements. The Journal of Financial and Quantitative Analysis 24 (2), 241–256.

Ewing, B. T., Malik, F., 2005. Re-examining the asymmetric predictability of conditional variances: the role of sudden changes in variance. Journal of banking and finance 29 (10), 2655–2673.

Figlewski, S., 2008. Estimating the implied risk neutral density for the U.S. market portfolio. Chapter in *Volatility and Time Series Econometrics: Essays in Honor of Robert F. Engle*. Oxford University Press.

Glosten, L. R., Jagannathan, R., Runkle, D. E., December 1993. On the relation between the expected value and the volatility of the nominal excess return on stocks. The Journal of Finance 48 (5), 1779–1801.

Granger, J., 1969. Investigating causal relationships by econometric models and cross-spectral analysis. Econometrica 37, 424–438.

Hannan, E. J., Quinn, B. G., 1979. The determination of the order of an autoregression. Journal of the Royal Statistical Society 41, 190–195.

Hashmi, A. R., Tay, A., 2012. Handbook of volatility models and their applications. John Wiley & Sons, Ch. Mean, volatility, and skewness spillovers in equity markets, pp. 127–145.

Hassan, S. A., Malik, F., July 2007. Multivariate garch modeling of sector volatility transmission. The Quarterly Review of Economics and Finance 47 (3), 470–480.

Hong, Y., Liu, Y., Wang, S., June 2009. Granger causality in risk and detection of extreme risk spillover between financial markets. Journal of econometrics 150 (2), 271–287.

Härdle, W., 1990. Applied Nonparametric Regression. Cambridge University Press.

Jackwerth, J., Rubinstein, M., 1996. Recovering probability distributions from option prices. Journal of Finance 51 (5), 1611–1631.

Jackwerth, J. C., 2000. Recovering risk aversion from option prices and realized returns. The Review of Financial Studies 13 (2), 433–451.

Jondeau, E., Rockinger, M., 2000. Reading the smile: the message conveyed by methods which infer risk neutral densities. Journal of International Money and Finance 19 (6), 885–915.

Kearney, C., Patton, A., 2000. Multivariate garch modeling exchange rate volatility transmission in the european monetary system. The financial review 35, 29–48.

Kenourgios, D., July 2014. On financial contagion and implied market volatility. International Review of Financial Analysis 34, 21–30.

Kilian, L., Lutkepohl, H., 2017. Structural vector autoregressive analysis. Cambridge University Press.

Künsch, H. R., 1989. The jackknife and the bootstrap for general stationary observations. The Annals of Statistics 17 (3), 1217–1241.

Leiss, M., Nax, H. H., 2018. Option-implied objective measures of market risk. Journal of Banking and Finance 88, 241–249.

Liu, X., Shackleton, M. B., Taylor, S. J., Xu, X., 2007. Closed-form transformations from risk-neutral to real-world distributions. Journal of Banking and Finance, 1501–1520.

Longstaff, F. A., Pan, J., Pedersen, L. H., Singleton, K. J., April 2011. How sovereign is sovereign risk? American Economic Journal: Macroeconomics 3 (2), 75–103.

Lucas, R., 1978. Asset prices in an exchange economy. Econometrica 46, 1429–1446.

Lynch, D., Panigirtzoglou, N., 2008. Summary statistics of option-implied probability density functions and their properties., working paper No. 345, Bank of England.

Madan, D. B., Carr, P. P., Chang, E. C., 1998. The variance gamma process and option prices. European Finance Review, 79–105.

Malz, A., 1997. Estimating the probability distribution of the future exchange rate from option prices. Journal of Derivatives 5 (2), 18–36.

Massacci, D., 2017. Tail risk dynamics in stock returns: Links to the macroeconomy and global markets connectedness. Management Science 63 (9), 3072–3089.

Nadaraya, E. A., 1964. On estimating regression. Theory of Probability and its Applications 10, 186–190.

Nikkinen, J., Sahlström, P., 2004. International transmission of uncertainty implicit in stock index option prices. Global finance journal 15 (1), 1–15.

Pan, J., Singleton, K. J., October 2008. Default and recovery implicit in the term structure of sovereign cds spreads. The Journal of Finance 63 (5).

Panigirtzoglou, N., Skiadopoulos, G., 2004. A new approach to modeling the dynamics of implied distributions: Theory and evidence from the s&p500 options. Journal of Banking and Finance 28, 1499–1520.

Perignon, C., Villa, C., December 2002. Extracting information from option markets: smiles, state-price densities and risk aversion. European Financial Management 8 (4), 495–513.

Pesaran, M., Shin, Y., 1998. Generalized impulse response analysis in linear multivariate models. Economics Letters 58, 17–29.

Poon, S.-H., Granger, C., 2005. Practical issues in forecasting volatility. Financial Analysts journal 41 (2), 478–539.

Poon, S.-H., Granger, C. W. J., June 2003. Forecasting volatility in financial markets: a review. Journal of economic literature 41 (2), 478–539.

Rosenberg, J. V., Engle, R. F., 2002. Empirical pricing kernels. Journal of Financial Economics 64, 341–372.

Rubinstein, M., July 1994. Implied binomial trees. Journal of Finance 49 (3), 771–818.

Schwert, G., December 1989. Why does the stock market volatility change over time? Journal of Finance 44 (5), 1115–1153.

Seillier-Moiseiwisch, F., Dawid, P., 1993. On testing the validity of sequential probability forecasts. Journal of the American Statistical Association 88, 355–359.

Silverman, B. W., 1986. Density Estimation for Statistics and Data Analysis. Vol. 26. Chapman & Hall, London.

Siropoulos, C., Fassas, A., October 2013. Dynamic relations of uncertainty expectations: a conditional assessment of implied volatility indices. Review of Derivatives Research 16 (3), 233–266.

Söderlind, P., Sevensson, L., October 1997. New techniques to extract market expectations from financial instruments. Journal of Monetary Economics 40 (2), 383–429.

Taylor, S. J., 1986. Forecasting the volatility of currency exchange rates. International Journal of Forecasting 3, 159–170.

Taylor, S. J., 2005. Asset Price Dynamics, Volatility, and Prediction. Princeton University Press.

Thakolsri, S., Sethapramote, Y., Jiranyakul, K., 2016. Implied volatility transmissions between thai and selected advanced stock markets. SAGE Open 6 (3).

von Mises, 1931. Wahrscheinlichkeitsrechnung. Wien, Leipzig.

Wang, Y.-H., Yen, K.-C., 2017. The information content of option-implied tail risk on the future returns of the underlying asset. Journal of Futures Market DOI: 10.1002/fut.21887.

Watson, G. S., 1964. Smooth regression analysis. Shankya Series A 26, 359–372.

Whaley, R. E., Spring 2009. Understanding the vix. The Journal of Portfolio Management 35 (3), 98–105.

Yang, Z., Zhou, Y., February 2017. Quantitative easing and volatility spillovers across countries and asset classes. Management Science 63 (2), 333–354.